



Assessing risks to adults and preschool children posed by PM_{2.5}-bound polycyclic aromatic hydrocarbons (PAHs) during a biomass burning episode in Northern Thailand



Siwatt Pongpiachan ^{a,*}, Danai Tipmanee ^{b,c}, Chukkapong Khumsup ^d, Itthipon Kittikoon ^d, Phoosak Hirunyatrakul ^d

^a NIDA Center for Research & Development of Disaster Prevention & Management, School of Social and Environmental Development, National Institute of Development Administration (NIDA), 118 Moo 3, Sereethai Road, Klong-Chan, Bangkok 10240, Thailand

^b International Postgraduate Program in Environmental Management, Graduate School, Chulalongkorn University, Bangkok, Thailand

^c Center of Excellence for Environmental and Hazardous Waste Management (EHWM), Chulalongkorn University, Bangkok, Thailand

^d Bara Scientific Co., Ltd., 968 Rama 4 Silom Bangrak, Bangkok 10500, Thailand

HIGHLIGHTS

- Biomass burning impacts on PM_{2.5}-bound PAHs were investigated in Northern Thailand.
- Diagnostic ratios/PCA plots show that biomass combustion is NOT a major PAH source.
- Northern Thailand residents have a lower cancer risk than residents of world cities.
- Direct ingestion is the major exposure pathway of PM_{2.5}-bound PAHs.

ARTICLE INFO

Article history:

Received 29 August 2014

Received in revised form 3 December 2014

Accepted 7 December 2014

Available online xxxx

Section Editor: Xuexi Tie

Keywords:

Forest fire

PAHs

Northern Thailand

PM_{2.5}

Risk assessment

ABSTRACT

To investigate the potential cancer risk resulting from biomass burning, polycyclic aromatic hydrocarbons (PAHs) bound to fine particles (PM_{2.5}) were assessed in nine administrative northern provinces (NNP) of Thailand, before (N-I) and after (N-II) a haze episode. The average values of Σ3,4-ring PAHs and B[a]P_{Equivalent} concentrations in world urban cities were significantly ($p < 0.05$) much higher than those in samples collected from northern provinces during both sampling periods. Application of diagnostic binary ratios of PAHs underlined the predominant contribution of vehicular exhaust to PM_{2.5}-bound PAH levels in NNP areas, even in the middle of the agricultural waste burning period. The proximity of N-I and N-II values in three-dimensional (3D) principal component analysis (PCA) plots also supports this conclusion. Although the excess cancer risk in NNP areas is much lower than those of other urban area and industrialized cities, there are nevertheless some concerns relating to adverse health impacts on preschool children due to non-dietary exposure to PAHs in home environments.

© 2014 Elsevier B.V. All rights reserved.

1. Introduction

Various studies have investigated the fate and behavior of particulate polycyclic aromatic hydrocarbons (PAHs) in urban areas, including Taiwan (Fang et al., 2005; Tsai et al., 2002; Yang et al., 2006), China (Bi et al., 2002; Tan et al., 2006; Wang et al., 2006), Hong Kong (Guo et al., 2003), Singapore (Karthikeyan et al., 2006), Thailand (Pongpiachan, 2013a,b; Pongpiachan et al., 2013a), Belgium (Ravindra et al., 2006), Germany (Schnelle-Kreis et al., 2005), Sweden (Wingfors et al., 2001), Italy (Caricchia et al., 1999), Greece (Mantis et al., 2005; Vasilakos et al.,

2007), England (Pongpiachan, 2006), the Czech Republic (Ciganek et al., 2004), the United States (Dachs et al., 2002; Park et al., 2001; Poor et al., 2004), Brazil (Dallarosa et al., 2005a,b), Algeria (Yassaa et al., 2001a,b), and Australia (Bartkow et al., 2004; Lim et al., 2005). PAHs, which are categorized as a group of persistent organic pollutants (POPs), are characteristically composed of two to eight benzene rings and can be released from both anthropogenic and natural emission sources (Ravindra et al., 2006; Slezakova et al., 2013). A significant number of studies have provided evidence for the link between the genotoxic effects of PAHs (e.g., cancer, endocrine disruption, and reproductive and developmental effects) and adverse human health impacts over the past decades (Liao et al., 2011; Matsui, 2008; Wickramasinghe et al., 2012). Despite numerous reports discussing atmospheric concentrations of particulate PAHs around the

* Corresponding author.

E-mail address: pongpijun@gmail.com (S. Pongpiachan).

world, knowledge of their chemical characteristics in the tropical atmosphere during haze episodes is severely limited.

Previous studies have highlighted the worsening of air pollution in northern Thailand over recent years, due to the effects of wildfires, unintentional burning of biomass, and burning of agricultural waste, coupled with transboundary haze pollution from the Republic of the Union of Myanmar (RUM), the Lao People's Democratic Republic (LPDR), and eastern Cambodia (Huang et al., 2013; Oanh and Leelasakultum, 2011; Pengchai et al., 2009; Shi et al., 2014a,b). While forest fires and the burning of agricultural waste appear to play an important role in air quality deterioration during cold periods, traffic emissions, local seasonal heating from residential housing, and industrial and fugitive sources also contribute to PAH emissions (Amodio et al., 2013; Mu et al., 2014; Riva et al., 2011; Slezakova et al., 2013; Wei et al., 2012).

Notwithstanding the documentation of the significant effects of PAHs and the variety of potential local sources outlined above, there has been no study to date focusing on either the chemical composition or ecological risk assessment of PM_{2.5}-bound PAHs in Northern Thailand. The primary aim of this research is therefore *i*) to compare the chemical composition of PAH contents in PM_{2.5} before and after a haze episode, and *ii*) to conduct a health risk assessment of inhabitants exposed to PM_{2.5}-bound PAHs in nine administrative provinces within northern Thailand.

2. Materials and methods

2.1. Description of PM_{2.5} observation sites

Northern Thailand differs noticeably from other parts of the Kingdom of Thailand, both in terms of geography and climate. The nine administrative northern provinces are geographically characterized by various mountainous belts, which continue from the Shan Hills in neighboring RUM and LPDR and have the climatic features of a tropical savanna. Collection of PM_{2.5} was conducted daily for seven consecutive days (over 24 h, from 9:00 am to 9:00 am of the following day) on pre-baked (550 °C for 12 h), quartz-fiber filters (QFFs; Whatman 47 mm; article no., 28418542 (US reference)), using MiniVol™ portable air samplers (Airmetrics) with a flow rate of 5 L min⁻¹ through a particle size separator (impactor) and subsequently through a 47-mm filter. A more extensive description of the PM_{2.5} sampling method is given in "EPA Quality Assurance Guidance Document: Method Compendium, Field Standard Operating Procedures for the PM_{2.5} Performance Evaluation Program, United States Environmental Protection Agency Office of Air Quality Planning and Standards" (U.S. EPA, 2002). The weight measurement of PM_{2.5} rigorously adhered to the procedures outlined in the EPA Quality Assurance Document: Method Compendium, PM_{2.5} Mass Weighing Laboratory Standard Operating Procedures for the Performance Evaluation Program, United States Environmental Protection Agency Office of Air Quality Planning and Standards (U.S. EPA, 1998a), and employed micro balances (Mettler Toledo, New Classic MF, MS205DU, Switzerland).

Sampling was conducted during two periods. Period I was before the "haze episode", during the cold season of 2012 (i.e., from 7 to 22 December), while period II was in March 2013 (i.e., from 4 to 19 March). During both periods, sampling was conducted at nine monitoring stations, as follows: Chiang-Rai Province Observation Site (CROS; The Eight Hotel; E: 593783, N: 2258302), Chiang-Mai Province Observation Site (CMOS; Yipparat School; E: 498805, N: 2077713), Nan Province Observation Site (NPOS; Thewarat Hotel; E: 687123, N: 2077209), Phayao Province Observation Site (PYOS; Arunothai Coffee House Homestay; E: 594420, N: 2119215), Mae Hong Son Province Observation Site (MHOS; Mae Hong Son Provincial Forestry Office; E: 391834, N: 2134869), Phrae Province Observation Site (PHOS; Nana Charoenmuang Hotel; E: 620935, N: 2006155), Lampang Province Observation Site (LMOS; Maemoh Training Center; E: 568200, N: 2020017), Lamphun Province Observation Site (LPOS; Lamphun Provincial Administration Organization

Stadium; E: 500441, N: 2052987), and Uttaradit Province Observation Site (UTOS; OUM Hotel; E: 615923, N: 1948269) (Fig. 1). There were no impediments to air flow in the vicinity of the MiniVol™ portable air samplers, which were deliberately situated to be accessible to winds from all directions.

2.1.1. Period I (Nine Northern Provinces-I (N-I); sampling before the haze episode)

Air sampling at group 1 observation sites (CROS, PYOS, and NPOS), group 2 observation sites (LMOS, PHOS, and UTOS), and group-3 observation sites (MHOS, CMOS, and LPOS) was performed synchronously in 2012, every day from 28 November to 4 December, from 7 to 13 December, and from 16 to 22 December, respectively.

2.1.2. Period II (Nine Northern Provinces-II (N-II); sampling after the haze episode)

Monitoring at group 1 sampling sites (CROS, PYOS, and NPOS), group 2 sampling sites (LMOS, PHOS, and UTOS), and group-3 sampling sites (MHOS, CMOS, and LPOS) was conducted synchronously in 2013, every day from 23 February to 2 March, from 4 to 11 March, and from 13 to 20 March, respectively.

2.2. Polycyclic aromatic hydrocarbons (PAHs)

Half of each QFF was extracted with dichloromethane (Fisher Scientific, HPLC grade) using Soxhlet Extraction. The QFFs were spiked with a known amount of deuterated internal standards (including d₁₀-fluorene and d₁₂-perylene) prior to extraction. The organic extract was vacuum-concentrated and evaporated by nitrogen stream to a state of almost complete dryness. Prior to the fractionation process, dried samples were re-dissolved in hexane and then evaporated with nitrogen again, until a final volume of 2 mL was reached. The hexane extract was fractionated by flash chromatography with silica gel using various solvents with increasing polarity. Details of the PAH fractionation methodology can be found in Pongpiachan et al. (2013b) and Tipmanee et al. (2012). The PAH fraction was eluted with 15 mL of 4:6 (v/v) toluene: hexane. The fraction was concentrated with a nitrogen stream until it was almost dry and then eluted with cyclohexane and evaporated under a gentle nitrogen stream until a final volume of 100 µL was achieved.

2.2.1. Chemicals and solvents

All solvents were of HPLC grade and were purchased from Fisher Scientific. A mix of standard solutions of 13 native PAHs [Norwegian Standard (NS 9815: S-4008-100-T): phenanthrene (Phe), anthracene (An), fluoranthene (Fluo), pyrene (Pyr), benz[a]anthracene (B[a]A), chrysene (Chry), benzo[b]fluoranthene (B[b]F), benzo[k]fluoranthene (B[k]F), benzo[a]pyrene (B[a]P), benzo[e]pyrene (B[e]P), indeno[1,2,3-c,d]pyrene (Ind), dibenz[a,h]anthracene (D[a,h]A), and benzo[g,h,i]perylene (B[g,h,i]P)], and a mix of recovery internal standard (IS) PAHs [d₁₂-perylene (d₁₂-Per) and d₁₀-fluorene (d₁₀-Fl)] were purchased from Chiron AS (Stiklestadveien 1, N-7041 Trondheim, Norway). Standard stock solutions of deuterated and native PAHs were prepared in nonane. Working solutions were obtained through appropriate dilution in cyclohexane. Analyses of PAHs were conducted with a gas chromatograph coupled to a mass spectrometer. All 13 PAHs were isolated on a 60-m length × 0.25-mm i.d. capillary column coated with a film of 0.25-m thickness (phase composition: cross-linked/surface bonded 5% phenyl, 95% methylpolysiloxane with Agilent JW Scientific DB-5 GC columns). Helium (99.999%) was used as carrier gas at a constant column flow rate of 1.0 mL min⁻¹ and with a pressure pulse of 25 psi for a duration of 0.50 min. All sample injections (1 µL) were introduced using a universal injector in splitless mode, and standards were introduced using a 10-µL Hamilton syringe. The GC oven temperature was set as follows: 1 min at 40 °C, heated at 8 °C min⁻¹ to 300 °C, and held for 45 min. A Shimadzu GCMS-QP2010 Ultra system was used, consisting

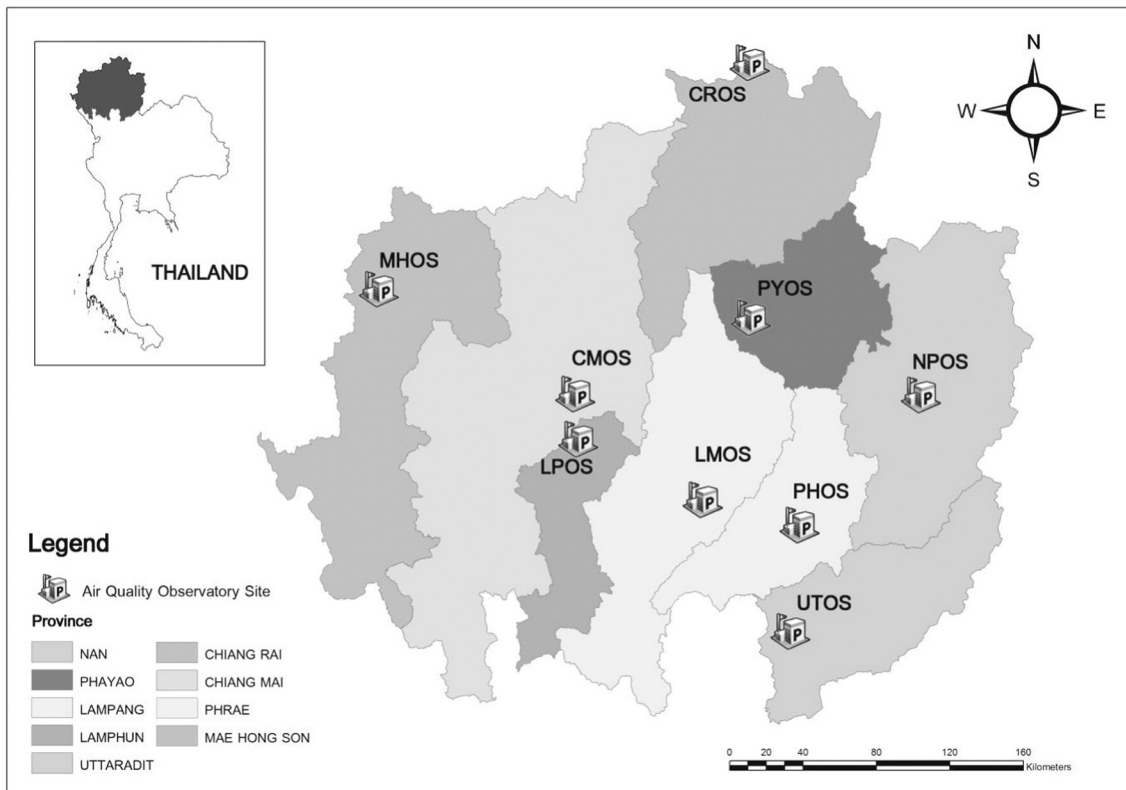


Fig. 1. Air quality observation sites in nine administrative provinces of northern Thailand.

of a high-speed performance system with ASSP function (i.e., achieving maximum scan speed of $20,000 \mu\text{s}^{-1}$), and having ultra-fast data acquisition speed for comprehensive two-dimensional gas chromatography ($\text{GC} \times \text{GC}$). A more comprehensive explanation of the GC/MS method is given in earlier references (Pongpiachan et al., 2011) and will not be discussed here. Both precision and accuracy were tested by employing standard reference material (SRM 1941b) provided by the National Institute of Standard and Technology (NIST). The precision of the procedure was calculated based on relative standard deviation of duplicate samples, and the latter was less than 10%. All sample concentrations were calculated using standardized relative response factors (RRFs) run with each batch (Pongpiachan et al., 2009, 2011).

2.3. Health risk assessment of PAHs

2.3.1. Calculation of excess cancer risk

There are several methods to estimate the excess cancer risk associated with $\text{PM}_{2.5}$ -bounded PAHs (Bandowe et al., 2014; Jia et al., 2011; Ramírez et al., 2011). In this study, the extensively used techniques provided by the Office of Environmental Health Hazard Assessment (OEHHA) of the California Environmental Protection Agency (CalEPA) were applied to estimate the lifetime excess cancer risk from inhalation (ECR) of $\text{PM}_{2.5}$ -bounded PAHs in ambient air of northern Thailand (Jia et al., 2011; OEHHA, 2003; Ramírez et al., 2011). The $B[a]\text{P}_{\text{eq}}$ is computed from the individual $\text{PM}_{2.5}$ -bounded content in each sample and the toxicity equivalency factor (TEF) of individual target compounds by using Eq. (1).

$$\sum B[a]\text{P}_{\text{eq}} = \sum_{i=1}^{n=1} (C_i \times TEF_i) \quad (1)$$

Here, C_i and TEF_i are acronyms for the concentrations of the i th PAH congener and toxic equivalency factor of the i th PAH congener, respectively. Because the toxicity of a single PAH congener can differ by degrees of magnitude, it is essential to show the toxicity of PAHs in terms of their most toxic form, $B[a]\text{P}$. By employing TEF values, which were provided by Nisbet and LaGoy (1992), the toxicity of a combination of PAH congeners can be evaluated in a single number, generally referred to as $B[a]\text{P}$ equivalence ($B[a]\text{P}_{\text{eq}}$). $B[a]\text{P}$ equivalence is a specific number resulting from the product of the concentrations and individual TEF values of each PAH, as described in Eq. (1). In Eq. (2), the acronyms for PAH congeners represent their concentrations and the $B[a]\text{P}_{\text{eq}}$ based on the estimation of Nisbet and LaGoy (1992).

$$B[a]\text{P}_{\text{eq}} = 0.001(\text{Phe} + \text{Fluo} + \text{Pyr}) + 0.01(\text{An} + B[g,h,i]\text{P} + \text{Chry}) + 0.1(B[a]\text{A} + B[b]\text{F} + B[k]\text{F} + \text{Ind}) + B[a]\text{P} + D[a,h]\text{A} \quad (2)$$

ECR is defined as the product of $\sum B[a]\text{P}_{\text{eq}}$ and $UR_{B[a]\text{P}}$ using Eq. (3), where $UR_{B[a]\text{P}}$ (unit risk) represents the number of people at risk of contracting cancer from inhalation at a $B[a]\text{P}$ equivalent concentration of 1 ng m^{-3} within a lifetime of 70 years (Bandowe et al., 2014).

$$ECR = \sum B[a]\text{P}_{\text{eq}} \times UR_{B[a]\text{P}} \quad (3)$$

The authors used two values of $UR_{B[a]\text{P}}$ as provided by the World Health Organization (WHO) (8.7×10^{-5}) and CalEPA (1.1×10^{-6}) for this study (OEHHA, 1994; WHO, 2000). In addition, the abbreviations of $\Sigma 178\text{PAH3-B}[a]\text{P}_{\text{eq}}$, $\Sigma 202\text{PAH4-B}[a]\text{P}_{\text{eq}}$, $\Sigma 228\text{PAH4-B}[a]\text{P}_{\text{eq}}$, $\Sigma 252\text{PAH5-B}[a]\text{P}_{\text{eq}}$, and $\Sigma 276,278\text{PAH6-B}[a]\text{P}_{\text{eq}}$ stand for the sum of $\text{Phe} + \text{An}$, $\text{Fluo} + \text{Pyr}$, $\text{B}[a]\text{A} + \text{Chry}$, $\text{B}[b+k]\text{F} + \text{B}[a]\text{P}$, and $\text{Ind} + \text{D}[a,h]\text{A} + \text{B}[g,h,i]\text{P}$, respectively.

2.3.2. Risk assessment of $\text{PM}_{2.5}$ -bound PAH intake in preschool children

The cancer risk associated with non-dietary ingestion of PAHs in $\text{PM}_{2.5}$ was evaluated for preschool children living in nine administrative

provinces of northern Thailand, using Eq. (4) (Maertens et al., 2008; U.S. EPA, 1997),

$$\text{Cancer risk} = \sum_{i=1}^n \left(\frac{(B[a]P_{eq_i}) \times IR \times EF \times SF \times AF}{BW} \times CF \right) \quad (4)$$

where $B[a]P_{eq}$ represents the toxicity equivalent concentrations according to the methods described by Nisbet and LaGoy (1992) (Eq. (2)). In this case, C_i represents the concentration (mg kg^{-1}) of each carcinogenic PAH in $\text{PM}_{2.5}$. Two ingestion rates (IR) of indoor $\text{PM}_{2.5}$ (mg day^{-1}) were used in this study: 50 and 100 mg day^{-1} (Maertens et al., 2008). EF, SF, AF, and BW represent the exposure factor (i.e., 7 h per day for five years from birth up to the fifth birthday of a preschool child (Maertens et al., 2008)), slope factor (i.e., an oral slope factor for $B[a]P$ of 7.3 $\text{mg kg}^{-1} \text{day}^{-1}$ (U.S. EPA, 2005)), adjustment factor (i.e., an exposure occurrence during early life stages of preschool children with the adjustment factor of 5.8 (Maertens et al., 2008)), and body weight (i.e., an average body weight of 15 kg for preschool children (U.S. EPA, 1997)), respectively. Finally, CF stands for the conversion factor (10^{-6}). All statistical analyses (i.e., t-test, analysis of variance (ANOVA), principal component analysis (PCA)) were carried out using the software SPSS (version 13).

3. Results & discussion

3.1. Impacts of haze episode on $\text{PM}_{2.5}$ -bound PAH contents

Table 1 presents the average mass concentrations of particulate PAHs (pPAHs, reported in pg m^{-3}) of $\text{PM}_{2.5}$ samples collected during N-I (i.e., the average values of CROS, PYOS, NPOS, LMOS, PHOS, UTOS, MHOS, CMOS, and LPOS before the haze episode), during N-II (i.e., the average values obtained from the same sampling stations after the haze episode), and from world cities (WCs) (see Table S1), with their corresponding standard deviations. It is apparent that PAH congeners measured in the present study have relatively low values when compared to values obtained from other studies around the world (Table 1). Several factors, such as the unique tropical wet and dry climate (Köppen Aw, characterized by hot and rainy weather) and the

low industrial emissions in the northern provinces, might have influenced the comparatively low PAH congener levels observed during N-I and N-II. Compared to N-I (i.e., non-burning period), the magnitude of $\Sigma 3,4\text{-ring PAHs}$ in WCs was higher by a factor of 7.6, and that of $B[a]P_{Nisbet-LaGoy}$ was higher by a factor of approximately 105. These results indicate that the emission source strength of light molecular weight PAHs in northern Thailand is much lower than that of other world cities.

Previous studies have indicated that vehicular traffic is the main source of $\text{PM}_{2.5}$ -bound PAHs in urban cities (Martellini et al., 2012; Slezakova et al., 2011, 2013). These findings are consistent with a recent study showing relatively low emission of $\text{PM}_{2.5}$ -bound PAHs from biomass burnings in comparison with those of paper and plastic waste combustion (Park et al., 2013), suggesting possible minor impacts of haze episodes on variation in the levels of fine particulate PAHs. Another combustion chamber study also revealed the comparatively high contribution of low-molecular-weight (LMW) PAHs in $\text{PM}_{2.5}$ released from dry leaf and whole stalk biomass burning (Hall et al., 2012). Gasoline vehicle exhaust, on the other hand, contained more high-molecular-weight (HMW) PAHs (Miguel et al., 1998). Therefore, the more abundant $\Sigma 5,6\text{-ring PAHs}$ during N-I is probably the result of gasoline vehicles passing through the monitoring stations rather than agricultural waste burnings. Compared to the level of $\Sigma 5,6\text{-ring PAHs}$ during N-I, the level during N-II was higher by a factor of 1.4, and that of WCs (see Table S1) was higher than N-I and N-II by a factor of 8.2 and 13.8, respectively. These results highlight the importance of vehicular exhaust as the major source of $\text{PM}_{2.5}$ -bound PAHs on a global scale, with this possibly surpassing many other emission sources, including burning of agricultural waste and forest fires. Because no significant differences were observed between values obtained during N-I and N-II (Table 1), it appears rational to conclude that the haze episode played a minor role in influencing atmospheric contents of $\text{PM}_{2.5}$ -bound PAHs in the northern provinces of Thailand.

3.2. Binary diagnostic ratios

PAHs can be released into air, water, and soil from imperfect combustion of hydrocarbon fuels and/or biomass (pyrogenic sources), from oil spills and other petrochemical products (petrogenic sources), or from the post-depositional transformation of biogenic precursors

Table 1
Statistical descriptions of PAHs [pg m^{-3}] in $\text{PM}_{2.5}$ collected from nine administrative provinces before (N-I) and during (N-II) a biomass-burning episode, compared with the average of world cities.

PAH congener	N-I (n = 9)	N-II (n = 9)	t-Test (p < 0.05) (N-I vs. N-II)	WCs (n = 39)	ANOVA-test (p < 0.05) (N-I vs. N-II vs. WCs)
Ph	182 ± 355	185 ± 465	N.S.	1484 ± 3477	N.S.
An	57 ± 68	18 ± 15	N.S.	396 ± 1073	N.S.
Fluo	84 ± 184	81 ± 191	N.S.	1948 ± 2395	S.
Pyr	182 ± 467	260 ± 696	N.S.	2867 ± 2845	S.
B[a]A	461 ± 1372	337 ± 990	N.S.	1088 ± 1220	N.S.
Chry	333 ± 986	478 ± 1387	N.S.	2140 ± 2618	N.S.
B[b + k]F	13 ± 25	83 ± 142	N.S.	5363 ± 8476	S.
B[e]P	1767 ± 3246	967 ± 1855	N.S.	686 ± 1555	N.S.
B[a]P	17 ± 27	7 ± 22	N.S.	1794 ± 2389	S.
Ind	5 ± 14	7 ± 21	N.S.	2975 ± 5096	N.S.
D[a,h]A	N.D.	N.D.	N.D.	909 ± 1292	N.D.
B[g,h,i]P	7 ± 20	8 ± 24	N.S.	3057 ± 4777	S.
$B[a]P_{equivalent}$					
$B[a]P_{Nisbet-LaGoy}$	70 ± 144	55 ± 112	N.S.	7345 ± 8812	S.
$\Sigma 3,4\text{-ring PAHs}$	1299 ± 3432	1359 ± 3744	N.S.	9923 ± 13,628	S.
$\Sigma 5,6\text{-ring PAHs}$	1809 ± 3332	1072 ± 2064	N.S.	14,784 ± 23,585	N.S.
Ind/B[g,h,i]P	0.71 ± 2.86	0.88 ± 3.71	N.S.	0.97 ± 2.26	N.S.
B[a]P/B[e]P	0.0096 ± 0.023	0.0072 ± 0.027	N.S.	2.62 ± 6.88	N.S.
B[g,h,i]P/B[e]P	0.0040 ± 0.013	0.0083 ± 0.029	N.S.	4.46 ± 12.3	N.S.
$\Sigma 3,4\text{-}/5,6\text{-rings PAHs}$	0.72 ± 2.31	1.27 ± 4.26	N.S.	0.67 ± 1.41	N.S.

(diagenetic sources). Numerous molecular diagnostic ratios of PAHs have been employed as distinctive chemical proxies to identify potential emission sources of PAHs in environmental samples (Pongpiachan, 2014; Yunker et al., 2002, 2011). In this study, Fluo/(Fluo + Pyr), An/(An + Phe), Ind/(Ind + B[g,h,i]P), and B[a]A/(B[a]A + Chry) were applied to discriminate between petrogenic and pyrolytic sources (Zhang et al., 2006). Fluo/(Fluo + Pyr) and An/(An + Phe) are generally employed to characterize PAHs from petrogenic and pyrogenic sources. In cases where the diagnostic ratio of An/(An + Phe) is less than 0.1, a petrogenic source is indicated, while a ratio greater than 0.1 points towards a pyrogenic source. When Fluo/(Fluo + Pyr) is in the range of 0.4 to 0.5, liquid fossil fuel combustion is suggested, while a ratio larger than 0.5 indicates biomass and coal combustion (Yunker et al., 2002). If Ind/(Ind + B[g,h,i]P) and B[a]A/(B[a]A + Chry) are larger than 0.5, there would appear to be a significant influence of coal, grass, and wood (Yunker et al., 2002). However, if B[a]A/(B[a]A + Chry) and Ind/(Ind + B[g,h,i]P) are in the range of 0.2 to 0.35 or 0.2 to 0.5, the impacts of

petroleum combustion (e.g., vehicular exhaust and crude oil combustion) would be a more significant factor.

As illustrated in Fig. 2, the ratios of Fluo/(Fluo + Pyr), An/(An + Phe), Ind/(Ind + B[g,h,i]P), and B[a]A/(B[a]A + Chry) in aerosols collected from numerous cities around the world (see Table S1) were plotted and compared with those obtained during N-I and N-II. The indicated ratios of Ind/(Ind + B[g,h,i]P) and B[a]A/(B[a]A + Chry) are from Asian cities predominantly situated within zones of biomass, coal, and petroleum combustion. Interestingly, only one European city is located within the zone of biomass and coal combustion, while the majority of European cities (i.e., Antwerp, Augsburg, Gothenburg, Naples, Athens, Brno, and Birmingham), North American States (i.e., Baltimore, Texas, and Florida), and Australian cities (i.e., Melbourne, Brisbane, and Springwood) are situated in a zone of petroleum combustion (see Table S1). The ratios of Fluo/(Fluo + Pyr) and An/(An + Phe) were similar to those of Ind/(Ind + B[g,h,i]P) and B[a]A/(B[a]A + Chry), indicating that most Asian cities were influenced by coal and biomass burning. In

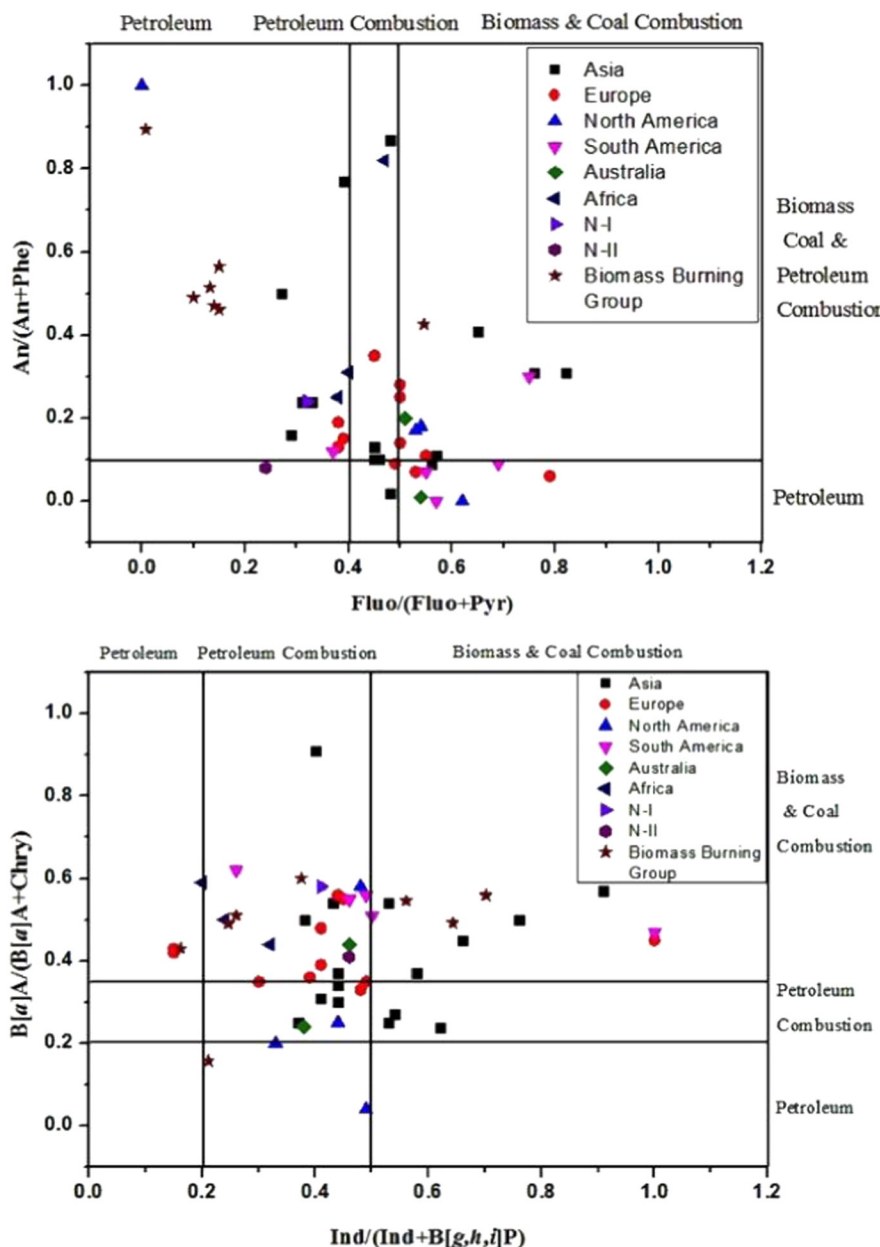


Fig. 2. Diagnostic binary ratios of PM_{2.5}-bound PAHs in NNP, in comparison with those of WCs (see Table S1).

addition, the ratios of Fluo/(Fluo + Pyr) and An/(An + Phe) in different types of biomass burning aerosols (i.e., rice straw burning, sugar cane burning, paddy residue burning, biofuels burning, wheat residue burning, open burning of bonfire, and Para rubber tree burning) from previous studies were mainly located adjacent to those of Asia, N-I and N-II. Similar results were also observed by using the ratios of Ind/(Ind + B[ghi]P) and B[a]A/(B[a]A + Chry). These results point to the importance of "biomass-burning" as one of the main contributors of PAHs in Northern Thailand. It is also worth mentioning that the majority of N-I and N-II plots were positioned within the zone of petroleum and petroleum combustion for both isomer ratio categories. This highlights the prominence of traffic emissions as a source of PM_{2.5}-bound PAHs in the northern provinces of Thailand, even during haze episodes.

3.3. Three-dimensional (3D) plots of PCA

Principal component analysis (PCA) was performed to investigate the impacts of agricultural waste and/or biomass burning on chemical characteristics of PM_{2.5}-bound PAHs collected from the northern provinces of Thailand and compare with other world cities (see Fig. 3 and Table S1). In the current study, three principal components (PC1, PC2 and PC3) were classified with the assistance of varimax rotation based on PAH loading and accounted for 65.5%, 20.3% and 14.2%, respectively, which together explained 100% of the total variance. The clearest features in all categories (Fig. 3) are as follows: (i) 3D plots of TTI1, CNU2, TSC and SNU deviate significantly from those of other Asian cities with the relatively high dispersion of 3D plots attributed to greater complexities of emission source strengths (i.e., both natural and anthropogenic

emissions) observed in Taiwan, China and Singapore; (ii) there are very clear similar sources in air samples from Europe, North America and South America; (iii) 3D plots of Australian cities were similar to those of Europe, North America and South America, except in the case of AMU, suggesting that human activities (e.g., vehicular exhaust and industrial emissions) might be significant sources of particulate PAHs in urban cities; and (iv) 3D plots of N-I and N-II deviate slightly from each other and are located adjacent to those of some European, American and Australian cities. A substantial dissimilarity in 3D plots among individual countries was predominantly due to energy consumption, economic growth, and vegetation cover. In many Asian countries, such as India, China, and Indonesia, more than half of the total PAH emissions come from indoor biomass burning (Shen et al., 2013). Similar findings were also reported in some developed countries, such as the United States, where certified woodstoves were mainly used in rural households (U.S. EPA, 1998b).

Previous studies have shown that in comparison with emissions of fossil fuels, biomass burning contributes large emissions of fine particles enriched with PAHs (Environmental Health Criteria 202, 1998; Hytoenen et al., 2006; Jokiniemi et al., 2006). For instance, particle number size distributions of rice-, wheat- and corn-burned particles demonstrated a noticeable accumulation mode with peaks at 0.10 μm, 0.15 μm and 0.15 μm, with PAH emission factors of 5.26 mg kg⁻¹, 1.37 mg kg⁻¹ and 1.74 mg kg⁻¹, respectively (Zhang et al., 2011). Consequently, one can expect comparatively high PM_{2.5}-bound PAHs during agricultural waste burning periods (i.e., N-II). A recent study using regression models and a technology split method from 69 major sources estimated for a period from 1960 to 2030 reveals

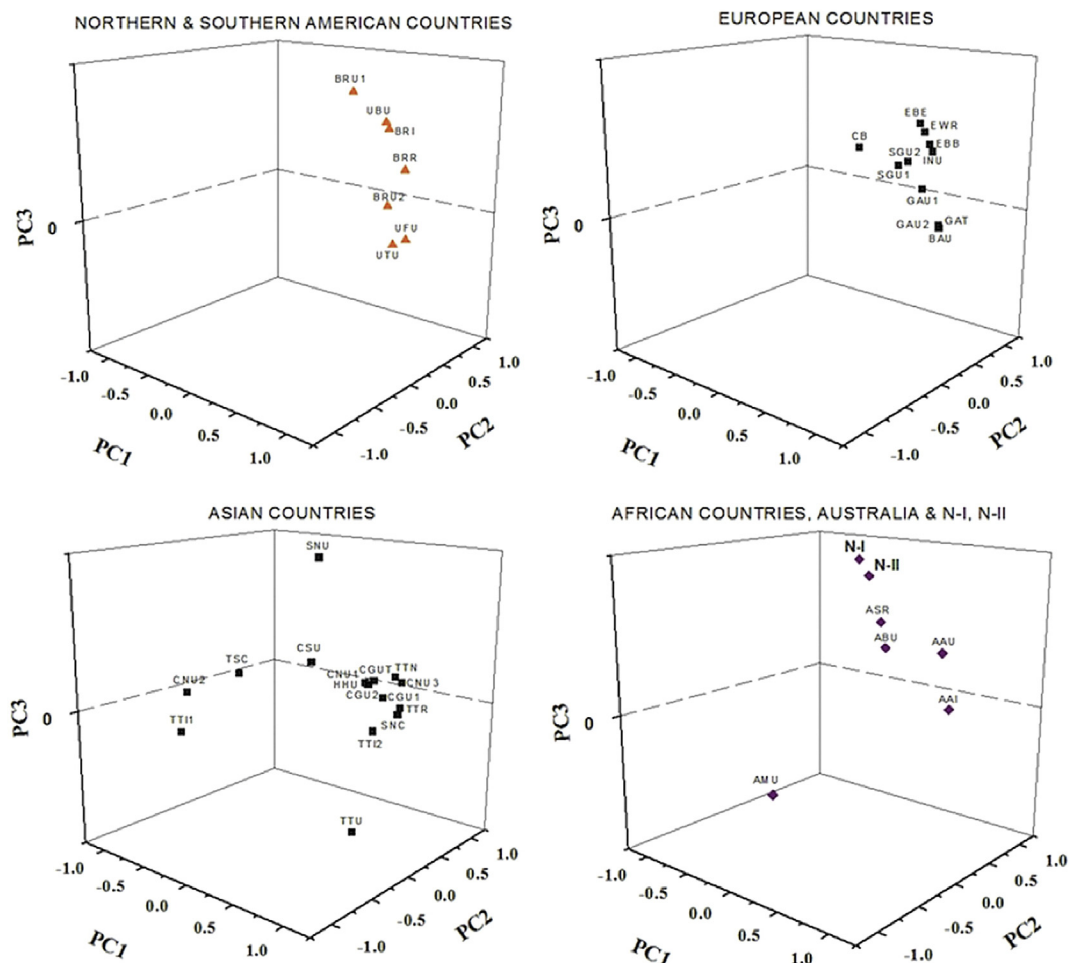


Fig. 3. 3D PCA plots of N-I and N-II, in comparison with those of other WCs (see Table S1).

that residential/commercial biomass burning (60.5%) coupled with open-field biomass burning (agricultural waste burning, deforestation, and wildfire, 13.6%) are two major sources of 16 PAHs (i.e., Nap (naphthalene), Ac (acenaphthylene), Ace (acenaphthene), Fl (fluorene), Phe, An, Fluo, Pyr, B[a]A, Chry, B[b]F, B[k]F, B[a]P, D[a,h]A, Ind, and B[g,h,i]P) (Shen et al., 2013). Interestingly, petroleum consumption by on-road motor vehicles only explains 12.8% of PAH emissions.

In spite of low contributions of traffic exhaust on PAH emissions around the world, the 3D plots of N-I and N-II are situated adjacent to each other, emphasizing that biomass burning contributes only slightly to PM_{2.5}-bound PAH concentrations. There are several reasons responsible for this discrepancy. First, the estimation of Shen et al. (2013) was not intended to focus only on PM_{2.5}-bound PAHs. There will be an uncertainty associated with the prediction due to the calculation of both "gaseous" and "particulate" PAHs. Second, emission factors of PM_{2.5}-bound PAHs are largely dependent on vegetation types, and thus, the biomass burnings in Northern Thailand might have lower contributions in comparison with those of previous studies (Hall et al., 2012; Zhang et al., 2011). Third, vehicular traffic emissions are the main contributors of PM_{2.5}-bound PAHs, as previously mentioned in Sections 3.1–3.2. Overall, the adjacency of 3D plots of N-I and N-II highlights the importance of vehicular exhaust in Northern Thailand, irrespective of haze episodes.

3.4. Health risk assessment

The B[a]P_{eq} concentrations of the individual PAHs, the sum of the 12 priority PAHs using Nisbet and LaGoy's calculation (\sum PAH12-B[a]P_{eq}), the sum of the three MW 178 PAHs (\sum 178PAH3-B[a]P_{eq}), the sum of the four MW 202 PAHs (\sum 202PAH4-B[a]P_{eq}), the sum of the four MW 228 PAHs (\sum 228PAH4-B[a]P_{eq}), the sum of the five MW 252 PAHs (\sum 252PAH5-B[a]P_{eq}), and the sum of the six MW 276,278 PAHs (\sum 276,278PAH6-B[a]P_{eq}) before and after the haze episode are given in Table 2. The average \sum B[a]P_{eq} for both monitoring periods was 63 ± 181 pg m⁻³ and was higher in N-I than in N-II. These values were comparable to values of PM_{2.5}-bound \sum B[a]P_{eq} of 45 pg m⁻³, 50 pg m⁻³, and 64 pg m⁻³ previously reported for Florida (USA), Georgia (USA), and Mississippi (USA) (Zheng et al., 2002), respectively, but much lower than the average value of WCs (see Table 1 and Table S1). The average \sum PAH12 decreased from detected values of 1341 ± 1800 pg m⁻³ and 1464 ± 1914 pg m⁻³ to 70 ± 144 pg m⁻³ and 55 ± 112 pg m⁻³ for N-I and N-II, respectively, after conversion to their B[a]P_{eq} concentration. Similarly, the average \sum PAH12 of WCs was reduced from measured values of $24,021 \pm 12,784$ pg m⁻³ to 7345 ± 8812 pg m⁻³, after conversion to their B[a]P_{eq} concentration. This value exceeded the European Union's annual average B[a]P_{eq} standard (1 ng m⁻³) (European Commission, 2001) but was lower than those of China's State Environmental Protection Agency's (1996) daily B[a]P_{eq} standard (10 ng m⁻³). In addition, neither \sum PAH12-B[a]P_{eq} values of N-I nor N-II exceeded the European Union and China's State Environmental Protection Agency's standards.

The average ECR- \sum PAH12-B[a]P_{eq} of Northern Thailand for a lifetime of 70 years ranged from 6.1×10^{-8} (N-II-CalEPA) to 6.0×10^{-6} (N-I-WHO), as illustrated in Table 2. As a consequence, an estimated mean excess for a lifetime of 70 years of 0.076 per million people (CalEPA) or 6.0 per million people cancer cases (WHO) of the adult residents of N-I will be attributable to respiration of PM_{2.5}-bound 12 PAHs. These values were comparable to those of N-II calculated using the CalEPA method (0.061 per million people) and WHO method (4.8 per million people), highlighting that the biomass-burning source may play a rather minor role in cancer risk. It is worth mentioning that ECR values of WCs have produced much higher results than those estimated for N-I and N-II. Lower ECR values in Northern Thailand cities are likely associated with lower industrial emissions and vehicular exhausts, lower domestic heating due to overall warm weather pattern, but higher precipitation in comparison with those of other world cities.

Table 2
Estimated excess inhalation cancer risk attributed to measured concentrations of PM_{2.5} bounded PAHs of N-I, N-II, and WCs (see Table S1). Two types of excess cancer risk were calculated according to the UR-B[a]P of the WHO (8.7×10^{-5} per ng m⁻³) and CalEPA (1.1×10^{-6} per ng m⁻³) procedures.

	Excess cancer risk per million people (based on UR-B[a]P of CalEPA)						Excess cancer risk per million people (based on UR-B[a]P of WHO)					
	N-I			N-II			N-I			N-II		
	(n = 9)	Aver	St. dev.	(n = 9)	Aver	St. dev.	(n = 9)	Aver	St. dev.	(n = 9)	Aver	St. dev.
Ph-B[a]P _{eq}	2.002E-10	3.905E-10	2.035E-10	5.115E-10	1.632E-09	3.825E-09	1.583E-08	3.089E-08	1.610E-08	4.046E-08	1.291E-07	3.023E-07
An-B[a]P _{eq}	6.272E-10	7.480E-10	1.980E-10	1.650E-10	4.256E-09	1.180E-08	4.955E-08	5.916E-08	1.566E-08	1.303E-08	3.445E-07	9.333E-07
Fluo-B[a]P _{eq}	9.240E-11	2.024E-10	8.910E-11	2.101E-10	2.143E-09	2.635E-09	7.308E-09	1.601E-08	7.047E-09	1.662E-08	1.695E-07	2.084E-07
Pyr-B[a]P _{eq}	2.002E-10	5.137E-10	2.860E-10	7.656E-10	3.154E-09	3.130E-09	1.583E-08	4.063E-08	2.262E-08	6.055E-08	2.494E-07	2.475E-07
B[a]A-B[a]P _{eq}	5.071E-08	1.509E-07	3.707E-08	1.089E-07	1.197E-07	1.342E-07	4.011E-06	1.194E-05	2.932E-06	8.613E-06	9.466E-06	1.061E-05
Chry-B[a]P _{eq}	3.663E-09	1.085E-08	5.258E-09	5.152E-08	2.354E-08	2.880E-08	2.897E-07	8.578E-07	4.159E-07	1.207E-06	1.862E-06	2.278E-06
B[b] + k[B[a]P] _{eq}	1.430E-09	2.750E-09	9.130E-09	1.562E-08	5.899E-07	9.324E-07	1.131E-07	2.175E-07	7.221E-07	1.235E-06	4.666E-05	7.374E-05
B[a]P-B[a]P _{eq}	1.870E-08	2.970E-08	7.700E-09	2.420E-08	1.973E-06	2.628E-06	1.479E-06	2.349E-06	6.090E-06	1.914E-06	1.561E-04	2.079E-04
Ind-B[a]P _{eq}	5.500E-10	1.540E-09	7.700E-10	2.310E-09	3.273E-07	5.606E-07	4.350E-07	1.218E-06	6.090E-08	1.827E-07	2.588E-05	4.434E-05
N.D.	N.D.	N.D.	N.D.	N.D.	9.999E-07	1.421E-06	N.D.	N.D.	N.D.	N.D.	7.908E-05	1.124E-04
B[g,h]P-B[a]P _{eq}	7.700E-11	2.200E-10	8.800E-11	2.640E-10	3.363E-08	5.255E-08	6.090E-09	1.740E-08	6.960E-09	2.088E-08	2.660E-06	4.156E-06
B[a]P-B[a]P _{eq}	7.625E-08	1.978E-07	6.079E-08	1.682E-07	4.079E-06	6.031E-06	1.565E-05	4.808E-06	1.330E-05	4.571E-04	3.226E-04	
B[a]P-B[a]P _{eq}	8.272E-10	1.139E-09	4.015E-10	6.765E-10	5.988E-09	1.563E-08	6.542E-08	9.005E-08	3.176E-08	5.351E-08	4.736E-07	1.236E-06
S202PAH3-B[a]P _{eq}	2.926E-10	7.161E-10	3.751E-10	9.757E-10	5.297E-09	5.764E-09	2.314E-08	5.664E-08	2.967E-08	7.717E-08	4.189E-07	4.559E-07
S228PAH4-B[a]P _{eq}	5.437E-08	1.618E-07	4.233E-08	1.242E-07	1.432E-07	1.630E-07	4.300E-06	1.279E-05	3.348E-06	9.820E-06	1.133E-05	1.289E-05
S252PAH5-B[a]P _{eq}	2.013E-08	3.242E-08	1.683E-08	3.982E-08	2.563E-06	3.560E-06	1.592E-06	2.567E-06	1.331E-06	3.149E-06	2.027E-04	2.816E-04
S276,278PAH6-B[a]P _{eq}	6.270E-10	1.760E-09	8.580E-10	2.574E-09	1.361E-06	2.034E-06	4.955E-06	1.392E-07	6.786E-08	2.036E-07	1.076E-04	1.609E-04

Table 3
Cancer risks associated with non-dietary ingestion of PAHs in house dust for preschool children, as estimated using Eq. (4) (U.S. EPA, 1997; Maertens et al., 2008).

Ingestion rate [mg day ⁻¹]	N-I						N-II						WCs					
	(n = 9)			(n = 9)			(n = 9)			(n = 39)			(n = 39)			(n = 39)		
	50	50	100	50	50	100	100	100	100	50	50	100	Aver	St. dev.	Aver	St. dev.	Aver	St. dev.
Cancer risk ^{Nisbet-Lagoy}	2.305E-03	6.774E-03	4.610E-03	1.355E-02	6.037E-04	1.456E-03	1.207E-03	2.912E-03	7.256E-01	8.707E-01	1.451E+00	1.741E+00						

The average ECR- \sum PAH12-B[a]P_{eq} in WCs were approximately 53 times and 67 times higher than those estimated for N-I and N-II, respectively. This study also indicated higher percentage contributions of ECR- \sum 228PAH4-B[a]P_{eq} of N-I (71%) and N-II (70%), which are much higher than those of WCs (3.5%). Five- to six-ring PAHs seems to be responsible for excess cancer risks in urban area and other industrialized cities, with percentage contributions of 62% and 35% for ECR- \sum 252PAH5-B[a]P_{eq} and ECR- \sum 276,278PAH6-B[a]P_{eq}, respectively.

In this study, non-dietary exposure is defined as human exposure to PM_{2.5}-bound PAHs via both household air and dust (Wilford et al., 2005). Table 3 displays excess cancer risks associated with house dust exposure from N-I, N-II and WCs, ranging from 6.0×10^{-4} (N-II with ingestion rate of 50 mg day⁻¹) to 1.5 (WCs with ingestion rate of 100 mg day⁻¹), depending on ingestion rate (IR). The mean cancer risks of Northern Thailand cities were 1.5×10^{-3} and 2.9×10^{-3} for ingestion rates of 50 mg day⁻¹ and 100 mg day⁻¹, respectively. The cancer risks in WCs for both ingestion rates were notably higher than those derived for Northern Thailand cities. Although the cancer risks of N-I and N-II were much lower than those in WCs, with average values of the former ranging from 10^{-4} to 10^{-3} (i.e., one cancer incidence case per million), they can still be considered to be unacceptable (Maertens et al., 2008). These values are comparable to those of foundry workers (9.06×10^{-4} and 1.09×10^{-3}) in Taiwan (Liu et al., 2010) but are higher than those predicted as occupational exposure for sinter metal workers (3.18×10^{-5} and 4.98×10^{-5}) (Lin et al., 2008; Chiang et al., 2009) and the Canadian maximum acceptable level of risk (1×10^{-5}) (Maertens et al., 2008). The current study therefore indicates some cause for concern in relation to adverse health impacts related to exposure to PM_{2.5}-bound PAHs in preschool children via non-dietary exposure in the home environment.

4. Conclusions

No statistically significant differences in PM_{2.5}-bound PAHs were observed before and after the haze episode, highlighting the impacts of vehicular exhaust as regular sources of fine particulate PAHs in Northern Thailand. Although observed PM_{2.5}-bound PAHs and B[a]P_{eq} levels were considerably lower in NNP than those recorded in WCs, there are some concerns associated with exposure to PM_{2.5}-bound PAHs in preschool children via non-dietary exposure in the home environment. The cancer risk related to exposure through inhalation appears to be minor, while direct ingestion could potentially be a significant pathway for children due to their hand-to-mouth activities, indicating that this exposure route should not be underestimated.

Supplementary data to this article can be found online at <http://dx.doi.org/10.1016/j.scitotenv.2014.12.019>.

Acknowledgments

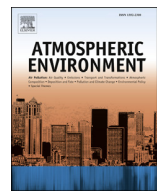
This project was financed by the National Institute of Development Administration (NIDA) Research Center. The authors acknowledge Assist. Prof. Dr. Torpong Kreetachart from the School of Energy and Environment (SEEN), University of Phayao, for his contribution to laboratory work. The authors are grateful for the kind support of the Pollution Control Department, Ministry of Natural Resources and Environment, which provided meteorological data. Ms. Chomsri Choochuary, Ms. Jittiphan Chonchalar, Ms. Panatda Kanchai, and Ms. Tidarat Ponpiboon are acknowledged for their assistance with field samplings.

References

- Amadio, M., Andriani, E., Dambruoso, P.R., de Gennaro, G., Di Gilio, A., Intini, M., Palmisani, J., Tutino, M., 2013. A monitoring strategy to assess the fugitive emission from a steel plant. *Atmos. Environ.* 79, 455–461.
- Bandow, B.A.M., Meusel, H., Huang, R.J., Ho, K., Cao, J., Hoffmann, T., Wilcke, W., 2014. PM_{2.5}-bound oxygenated PAHs, nitro-PAHs and parent-PAHs from the atmosphere of a

- Chinese megacity: seasonal variation, sources and cancer risk assessment. *Sci. Total Environ.* 473–474, 77–87.
- Bartkow, M.E., Huckins, J.N., Müller, J.F., 2004. Field-based evaluation of semipermeable membrane devices (SPMDs) as passive air samplers of polyaromatic hydrocarbons (PAHs). *Atmos. Environ.* 38 (35), 5983–5990.
- Bi, X., Sheng, G., Peng, P., Zhang, Z., Fu, J., 2002. Extractable organic matter in PM₁₀ from LiWan district of Guangzhou City, PR China. *Sci. Total Environ.* 300 (1–3), 213–228.
- Caricchia, A.M., Chiavarini, S., Pezza, M., 1999. Polycyclic aromatic hydrocarbons in the urban atmospheric particulate matter in the city of Naples (Italy). *Atmos. Environ.* 33, 3731–3738.
- Chiang, K.C., Chio, C.P., Chiang, Y.H., Liao, C.M., 2009. Assessing hazardous risks of human exposure to temple airborne polycyclic aromatic hydrocarbons. *J. Hazard. Mater.* 166, 676–685.
- China State Environmental Protection Agency, 1996. Ambient air quality standard. Available: <http://www.sepa.gov.cn/image20010518/5298.pdf> (accessed 25 January 2010).
- Ciganek, M., Necá, J., Adamec, V., Janousek, J., Machala, M., 2004. A combined chemical and bioassay analysis of traffic-emitted polycyclic aromatic hydrocarbons. *Sci. Total Environ.* 334–335, 141–148.
- Dachs, J., Glenn IV, T.R., Gigliotti, C.L., Brunciak, P., Totten, L.A., Nelson, E.D., Franz, T.P., Eisenreich, S.J., 2002. Processes driving the short-term variability of polycyclic aromatic hydrocarbons in the Baltimore and northern Chesapeake Bay atmosphere, USA. *Atmos. Environ.* 36 (14), 2281–2295.
- Dallarosa, J.B., Teixeira, E.C., Pires, M., Fachel, J., 2005a. Study of the profile of polycyclic aromatic hydrocarbons in atmospheric particles (PM₁₀) using multivariate methods. *Atmos. Environ.* 39 (35), 6587–6596.
- Dallarosa, J.B., Mônego, J.G., Teixeira, E.C., Stefens, J.L., Wiegand, F., 2005b. Polycyclic aromatic hydrocarbons in atmospheric particles in the metropolitan area of Porto Alegre, Brazil. *Atmos. Environ.* 39 (9), 1609–1625.
- Environmental Health Criteria 202, 1998. International Programme on Chemical Safety. United Nations Environmental Programme. International Labor Organization, World Health Organization.
- European Commission, 2001. Air quality standards. Available: <http://ec.europa.eu/environment/air/quality/standards.htm> (accessed 25 January 2010).
- Fang, G.C., Wu, Y.S., Chen, J.C., Fu, P.P.C., Chang, C.N., Ho, T.T., Chen, M.H., 2005. Characteristic study of polycyclic aromatic hydrocarbons for fine and coarse particulates at Pastureland near Industrial Park sampling site of central Taiwan. *Chemosphere* 60 (3), 427–433.
- Guo, H., Lee, S.C., Ho, K.F., Wang, X.M., Zou, S.C., 2003. Particle-associated polycyclic aromatic hydrocarbons in urban air of Hong Kong. *Atmos. Environ.* 37 (38), 5307–5317.
- Hall, D., Wu, C.Y., Hsu, Y.M., Stormer, J., Engling, G., Caputo, K., et al., 2012. PAHs, carbonyls, VOCs and PM_{2.5} emission factors for pre-harvest burning of Florida sugarcane. *Atmos. Environ.* 55, 164–172.
- Huang, K., Fu, J.S., Hsu, N.C., Gao, Y., Dong, X., Tsay, S.C., Lam, Y.F., 2013. Impact assessment of biomass burning on air quality in Southeast and East Asia during BASE-ASIA. *Atmos. Environ.* 78, 291–302.
- Hytoinen, K., Tissari, J., Yli-Pirilä, P., Jokiniemi, J., 2006. PAH emissions from a masonry heater in small scale wood combustion. *Proc. 7th International Aerosol Conference*, Sep. 10–15, St. Paul, Minnesota, USA, pp. 245–246.
- Jia, Y., Stone, D., Wang, W., Schrlau, J., Tao, S., Simonich, S.L.M., 2011. Estimated reduction in cancer risk due to PAH exposures if source control measures during the 2008 Beijing Olympics were sustained. *Environ. Health Perspect.* 119, 815–820.
- Jokiniemi, J., Lyranenen, J., Tapper, U., 2006. Fine particle characterization by electron microscopy in a small scale masonry heater during poor and good combustion condition. *Proc. 7th International Aerosol Conference*, Sep. 10–15, St. Paul, Minnesota, USA, pp. 244–245.
- Karthikeyan, S., Balasubramanian, R., See, S.W., 2006. Optimization and validation of a low temperature microwave-assisted extraction method for analysis of polycyclic aromatic hydrocarbons in airborne particulate matter. *Talanta* 69 (1), 79–86.
- Liao, M.C., Chio, P.C., Chen, Y.W., Ju, R.Y., Li, H.W., Cheng, H.Y., Liao, C.H.V., Chen, C.S., Ling, P.M., 2011. Lung cancer risk in relation to traffic-related nano/ultrafine particle-bound PAHs exposure: a preliminary probabilistic assessment. *J. Hazard. Mater.* 190 (1–3), 150–158.
- Lim, M.C.H., Ayoko, G.A., Morawska, L., 2005. Characterization of elemental and polycyclic aromatic hydrocarbon compositions of urban air in Brisbane. *Atmos. Environ.* 39 (3), 463–476.
- Lin, Y.C., Lee, S.J., Chang-Chien, G.P., Tsai, P.J., 2008. Characterization of PAHs exposure in workplace atmospheres of a sinter plant and health-risk assessment for sinter workers. *J. Hazard. Mater.* 158, 636–643.
- Liu, H.H., Yang, H.H., Chou, C.D., Lin, M.H., Chen, H.L., 2010. Risk assessment of gaseous/particulate phase PAH exposure in foundry industry. *J. Hazard. Mater.* 181, 105–111.
- Maertens, R.M., Yang, X.F., Zhu, J.P., Gagne, R.W., Douglas, G.R., White, P.A., 2008. Mutagenic and carcinogenic hazards of settled house dust I: polycyclic aromatic hydrocarbon content and excess lifetime cancer risk from preschool exposure. *Environ. Sci. Technol.* 42, 1747–1753.
- Mantis, J., Chaloulakou, A., Samara, C., 2005. PM₁₀-bound polycyclic aromatic hydrocarbons (PAHs) in the Greater Area of Athens, Greece. *Chemosphere* 59 (5), 593–604.
- Martellini, T., Giannoni, M., Lepri, L., Katsoyiannis, A., Alessandra, Cincinelli A., 2012. One year intensive PM_{2.5} bound polycyclic aromatic hydrocarbons monitoring in the area of Tuscany, Italy. Concentrations, source understanding and implications. *Environ. Pollut.* 164, 252–258.
- Matsui, S., 2008. Endocrine disruptors. *Encyclopedia of Ecology*, pp. 1259–1260.
- Miguel, A.H., Kirchstetter, T.W., Harley, R.A., Hering, S.V., 1998. On-road emissions of particulate polycyclic aromatic hydrocarbons and black carbon soot from gasoline and diesel vehicles. *Environ. Sci. Technol.* 32, 450–455.
- Mu, L., Peng, L., Liu, X., Song, C., Bai, H., Zhang, J., Hu, D., He, Q., Li, F., 2014. Characteristics of polycyclic aromatic hydrocarbons and their gas/particle partitioning from fugitive emissions in coke plants. *Atmos. Environ.* 83, 202–210.
- Nisbet, I.C.T., LaGoy, P.K., 1992. Toxic equivalency factors (TEFs) for polycyclic aromatic hydrocarbons (PAHs). *Regul. Toxicol. Pharmacol.* 16, 290–300.
- Oanh, K.N.T., Leelasakultum, K., 2011. Analysis of meteorology and emission in haze episode prevalence over mountain-bounded region for early warning. *Sci. Total Environ.* 409 (11), 2261–2271.
- OEHHA, 1994. Benzo[a]pyrene as a Toxic Air Contaminant. California Environmental Protection Agency, Berkeley, California, USA (<http://www.arb.ca.gov/toxics/id/summary/bap.pdf>) accessed March 19, 2013).
- OEHHA (Office of Environmental Hazards Assessments), 2003. Air Toxics Hot Spots Program Risk Assessment Guidelines. California Environmental Protection Agency, Oakland, California, USA (http://oehha.ca.gov/air/hot_spots/pdf/HRAfinalnoapp.pdf) accessed March 19, 2013).
- Park, J.S., Wade, T.L., Sweet, S., 2001. Atmospheric distribution of polycyclic aromatic hydrocarbons and deposition to Galveston Bay, Texas, USA. *Atmos. Environ.* 35 (19), 3241–3249.
- Park, Y.K., Kim, W., Jo, Y.M., 2013. Releases of harmful air pollutants from open burning of domestic municipal solid wastes in a metropolitan area of Korea. *Aerosol Air Qual. Res.* 13, 1365–1372.
- Pengchai, P., Chantara, S., Sopajaree, K., Wangkarn, S., Tengcharoenkul, U., Rayanakorn, M., 2009. Seasonal variation, risk assessment and source estimation of PM₁₀ and PM₁₀-Bound PAHs in the ambient air of Chiang Mai and Lamphun, Thailand. *Environ. Monit. Assess.* 154, 197–218.
- Pongpiachan, S., 2006. Source Apportionment of Semi-volatile Organic Compounds in Urban and Rural Air. (PhD thesis). University of Birmingham, Birmingham.
- Pongpiachan, S., 2013a. Vertical distribution and potential risk of particulate polycyclic aromatic hydrocarbons in high buildings of Bangkok, Thailand. *Asian Pac. J. Cancer Prev.* 14 (3), 1865–1877.
- Pongpiachan, S., 2013b. Diurnal variation, vertical distribution and source apportionment of carcinogenic polycyclic aromatic hydrocarbons (PAHs) in Chiang-Mai, Thailand. *Asian Pac. J. Cancer Prev.* 14 (3), 1851–1863.
- Pongpiachan, S., 2014. Application of binary diagnostic ratios of polycyclic aromatic hydrocarbons for identification of tsunami 2004 backwash sediments in Khao Lak, Thailand. *Sci. World J.* <http://dx.doi.org/10.1155/2014/485068> (Article ID 485068, 14 pages).
- Pongpiachan, S., Bualert, S., Sompongchaiyakul, P., Kositanont, C., 2009. Factors affecting sensitivity and stability of polycyclic aromatic hydrocarbons. *Anal. Lett.* 42 (13), 2106–2130.
- Pongpiachan, S., Hirunyatrakul, P., Kittikoon, I., Khumsup, C., 2011. Parameters influencing on sensitivities of polycyclic aromatic hydrocarbons measured by Shimadzu GCMS-QP2010 Ultra Gas Chromatography/Book 3. Intech Open Access Publisher 978-953-51-0298-4. <http://dx.doi.org/10.5772/32234>.
- Pongpiachan, S., Choochay, C., Hattayrone, M., Kositanont, C., 2013a. Temporal and spatial distribution of particulate carcinogens and mutagens in Bangkok, Thailand. *Asian Pac. J. Cancer Prev.* 14 (3), 1879–1887.
- Pongpiachan, S., Tipmanee, D., Deelaman, W., Muprasit, J., Feldens, P., Schwarzer, K., 2013b. Risk assessment of the presence of polycyclic aromatic hydrocarbons (PAHs) in coastal areas of Thailand affected by the 2004 tsunami. *Mar. Pollut. Bull.* 76, 370–378.
- Poor, N., Tremblay, R., Kay, H., Bhethanabotla, V., Swartz, E., Luther, M., Campbell, S., 2004. Atmospheric concentrations and dry deposition rates of polycyclic aromatic hydrocarbons (PAHs) for Tampa Bay, Florida, USA. *Atmos. Environ.* 38 (35), 6005–6015.
- Ramírez, N., Cuadras, A., Rovira, E., Marcé, R.M., Borrell, F., 2011. Risk assessment related to atmospheric polycyclic aromatic hydrocarbons in gas and particle phases near industrial sites. *Environ. Health Perspect.* 119, 1110–1116.
- Ravindra, K., Bencs, L., Wauters, E., Hoog, J.D., Deutsch, F., Roekens, E., Bleux, N., Berghmans, P., Grieven, R.V., 2006. Seasonal and site-specific variation in vapour and aerosol phase PAHs over Flanders (Belgium) and their relation with anthropogenic activities. *Atmos. Environ.* 40 (4), 771–785.
- Riva, G., Pedretti, E.F., Toscano, G., Duca, D., Pizzi, A., 2011. Determination of polycyclic aromatic hydrocarbons in domestic pellet stove emissions. *Biomass Bioenergy* 35 (10), 4261–4267.
- Schnelle-Kreis, J., Sklorz, M., Peters, A., Cyrys, J., Zimmermann, R., 2005. Analysis of particle-associated semi-volatile aromatic and aliphatic hydrocarbons in urban particulate matter on a daily basis. *Atmos. Environ.* 39 (40), 7702–7714.
- Shen, H., Huang, Y., Wang, R., Zhu, D., Li, W., Shen, G., et al., 2013. Global atmospheric emissions of polycyclic aromatic hydrocarbons from 1960 to 2008 and future predictions. *Environ. Sci. Technol.* 47, 6415–6424.
- Shi, G.L., Liu, G.R., Tian, Y.Z., Zhou, X.Y., Peng, X., Feng, Y.C., 2014a. Chemical characteristic and toxicity assessment of particle associated PAHs for the short-term anthropogenic activity event: during the Chinese new year's festival in 2013. *Sci. Total Environ.* 482–483, 8–14.
- Shi, Y., Sasai, T., Yamaguchi, Y., 2014b. Spatio-temporal evaluation of carbon emissions from biomass burning in Southeast Asia during the period 2001–2010. *Ecol. Model.* 272, 98–115.
- Slezakova, K., Castro, D., Begonha, A., Delerue-Matos, C., Alvim-Ferraz, M.C., Morais, S., Pereira, M.C., 2011. Air pollution from traffic emissions in Oporto, Portugal: health and environmental implications. *Microchem. J.* 99 (1), 51–59.
- Slezakova, K., Castro, D., Delerue-Matos, C., Alvim-Ferraz, M.C., Morais, S., Pereira, M.C., 2013. Impact of vehicular traffic emissions on particulate-bound PAHs: levels and associated health risks. *Atmos. Environ.* 127, 141–147.
- Tan, J.H., Bi, X.H., Duan, J.C., Rahn, K.A., Sheng, G.Y., Fu, J.M., 2006. Seasonal variation of particulate polycyclic aromatic hydrocarbons associated with PM₁₀ in Guangzhou, China. *Atmos. Environ.* 80 (4), 250–262.

- Tipmanee, D., Deelaman, W., Pongpiachan, S., Schwarzer, K., Sompongchaiyakul, P., 2012. Using polycyclic aromatic hydrocarbons (PAHs) as a chemical proxy to indicate tsunami 2004 backwash in Khao Lak coastal area, Thailand. *Nat. Hazards Earth Syst. Sci.* 12, 1441–1451.
- Tsai, P.J., Shieh, H.Y., Lee, W.J., Lai, S.O., 2002. Characterization of PAHs in the atmosphere of carbon black manufacturing workplaces. *J. Hazard. Mater.* 91 (1–3), 25–42.
- U.S. EPA, 1997. Exposure factors handbook. EPA/600/P-95/002Fa, b, c. U.S. Environmental Protection Agency, Office of Research and Development, Washington, DC.
- U.S. EPA, 1998a. Locating and Estimating Air Emissions From Sources of Polycyclic Organic Matter. EPA, Washington, DC.
- U.S. EPA, 1998b. EPA quality assurance document: method compendium. PM_{2.5} Mass Weighing Laboratory Standard Operating Procedures for the Performance Evaluation Program. United States Environmental Protection Agency Office of Air Quality Planning and Standards (October 1998).
- U.S. EPA, 2002. EPA quality assurance guidance document: method compendium. Field Standard Operating Procedures for the PM_{2.5} Performance Evaluation Program. United States Environmental Protection Agency Office of Air Quality Planning and Standards (Revision No. 2, March 2002).
- U.S. EPA, 2005. Guidelines for carcinogen risk assessment. EPA/630/P-03/001B. U.S. Environmental Protection Agency, Washington, DC.
- Vasilakos, Ch., Levi, N., Maggos, Th., Hatzianestis, J., Michopoulos, J., Helmis, C., 2007. Gas-particle concentration and characterization of sources of PAHs in the atmosphere of a suburban area in Athens, Greece. *J. Hazard. Mater.* 140 (1–2), 45–51.
- Wang, G., Huang, L., Zhao, X., Niu, H., Dai, Z., 2006. Aliphatic and polycyclic aromatic hydrocarbons of atmospheric aerosols in five locations of Nanjing urban area, China. *Atmos. Res.* 81 (1), 54–66.
- Wei, S., Huang, B., Liu, M., Bi, X., Ren, Z., Sheng, G., Fu, J., 2012. Characterization of PM_{2.5}-bound nitrated and oxygenated PAHs in two industrial sites of South China. *Atmos. Res.* 109–110, 76–83.
- WHO, 2000. Air Quality Guidelines for Europe. WHO Regional Office for Europe, Copenhagen, Denmark (http://www.euro.who.int/_data/assets/pdf_file/0005/74732/E71922.pdf accessed March 19, 2013).
- Wickramasinghe, P.A., Karunaratne, P.G.G.D., Sivakanesan, R., 2012. PM₁₀-bound polycyclic aromatic hydrocarbons: biological indicators, lung cancer risk of realistic receptors and 'source-exposure-effect relationship' under different source scenarios. *Chemosphere* 87 (11), 1381–1387.
- Wilford, B., Shoeib, M., Harner, T., Zhu, J., Jones, K., 2005. Polybrominated diphenyl ethers in indoor dust in Ottawa, Canada: implications for sources and exposure. *Environ. Sci. Technol.* 39, 7027–7035.
- Wingfors, H., Sjödin, Å., Haglund, P., Brorström-Lundén, E., 2001. Characterisation and determination of profiles of polycyclic aromatic hydrocarbons in a traffic tunnel in Gothenburg, Sweden. *Atmos. Environ.* 35 (36), 6361–6369.
- Yang, H.H., Tsai, C.H., Chao, M.R., Su, Y.L., Chien, S.M., 2006. Source identification and size distribution of atmospheric polycyclic aromatic hydrocarbons during rice straw burning period. *Atmos. Environ.* 40 (7), 1266–1274.
- Yassaa, N., Meklati, B.Y., Cecinato, A., 2001a. Chemical characteristics of organic aerosols in Algiers city area: influence of a fat manufacture plant. *Atmos. Environ.* 35 (34), 6003–6013.
- Yassaa, N., Meklati, B.Y., Cecinato, A., Marino, F., 2001b. Chemical characteristics of organic aerosol in Bab-Ezzouar (Algiers). Contribution of bituminous product manufacture. *Chemosphere* 45 (3), 315–322.
- Yunker, M.B., Macdonald, R.W., Vingarzan, R., Mitchell, R.H., Goyette, D., Sylvestre, S., 2002. PAHs in the Fraser River basin: a critical appraisal of PAH ratios as indicators of PAH source and composition. *Org. Geochem.* 33 (4), 489–515.
- Yunker, M.B., Macdonald, R.W., Snowdon, L.R., Fowler, B.R., 2011. Alkane and PAH biomarkers as tracers of terrigenous organic carbon in Arctic Ocean sediments. *Org. Geochem.* 42 (9), 1109–1146.
- Zhang, H.B., Luo, Y.M., Wong, M.H., Zhao, Q.G., Zhang, G.L., 2006. Distributions and concentrations of PAHs in Hong Kong soils. *Environ. Pollut.* 141, 107–114.
- Zhang, H., Hu, D., Chen, J., Ye, X., Wang, S.X., Hao, J.M., Wang, L., Zhang, R., An, Z., 2011. Particle size distribution and polycyclic aromatic hydrocarbons emissions from agricultural crop residue burning. *Environ. Sci. Technol.* 45 (13), 5477–5482.
- Zheng, M., Cass, G.R., Schauer, J.J., Edgerton, E.S., 2002. Source apportionment of PM_{2.5} in the southeastern United States using solvent-extractable organic compounds as tracers. *Environ. Sci. Technol.* 36 (11), 2361–2371.



Enhanced PM₁₀ bounded PAHs from shipping emissions

S. Pongpiachan ^{a,*}, M. Hattayanone ^b, C. Choochuay ^a, R. Mekmok ^c, N. Wuttijak ^c, A. Ketratanakul ^c

^a NIDA Center for Research & Development of Disaster Prevention & Management, School of Social and Environmental Development, National Institute of Development Administration (NIDA), 118 Moo 3, Sereethai Road, Klong-Chan, Bangkapi, Bangkok 10240, Thailand

^b Faculty of Humanities and Social Sciences, Songkhla Rajabhat University, Songkhla 90000, Thailand

^c IRPC PCL 555/2 Energy Complex, Building B, 7th Floor, Vibhavadi Rangsit Rd., Chatuchak, Bangkok 10900, Thailand

HIGHLIGHTS

- Impacts of shipping emissions on atmospheric contents of PM₁₀ bounded PAHs and MI were investigated.
- Shipping emissions significantly increase the genotoxicity of PM₁₀.
- Coal combustion and diesel emissions are two principle sources of PAHs during both shipping and non-shipping periods.
- During the non-shipping period, coal combustion from nearby power plant is the major source of PAHs.

ARTICLE INFO

Article history:

Received 19 June 2014

Received in revised form

19 February 2015

Accepted 26 February 2015

Available online 27 February 2015

Keywords:

Industrial estate

Mutagenicity

Polycyclic aromatic compounds

Vehicle emissions

Thailand

ABSTRACT

Earlier studies have highlighted the importance of maritime transport as a main contributor of air pollutants in port area. The authors intended to investigate the effects of shipping emissions on the enhancement of PM₁₀ bounded polycyclic aromatic hydrocarbons (PAHs) and mutagenic substances in an industrial area of Rayong province, Thailand. Daily PM₁₀ speciation data across two air quality observatory sites in Thailand during 2010–2013 were collected. Diagnostic binary ratios of PAH congeners, analysis of variances (ANOVA), and principal component analysis (PCA) were employed to evaluate the enhanced genotoxicity of PM₁₀ during the docking period. Significant increase of PAHs and mutagenic index (MI) of PM₁₀ were observed during the docking period in both sampling sites. Although stationary sources like coal combustions from power plants and vehicular exhausts from motorway can play a great role in enhancing PAH concentrations, regulating shipping emissions from diesel engine in the port area like Rayong is predominantly crucial.

© 2015 Elsevier Ltd. All rights reserved.

1. Introduction

The Map Ta Phut Industrial Estate (MIE) is the world's eighth largest petrochemical industrial park and one of the largest steel, oil refinery, and petrochemical factory complexes in Southeast Asia. The MIE, located in the town of Map Ta Phut in Rayong Province, is part of the Eastern Seaboard of Thailand (EST), which is an emerging economic region that plays a key role in Thailand's economy. A major advantage for the MIE is that it owns Map Ta Phut Industrial Port, which serves more than 5000 ships per year. As with many other anthropogenic activities, industrial estates and ports have been identified as principal contributors of various

environmental pollutants. Polycyclic aromatic hydrocarbons (PAHs), especially benzo[a]pyrene (B[a]P), have been widely recognized as a group of persistent organic pollutants responsible for cancer, endocrine disruption, and reproductive and developmental defects (Hoyer, 2001; Matsui, 2008). Because of their potential carcinogenic and mutagenic characteristics, numerous studies have investigated PAHs and found strong associations between meteorological parameters and the atmospheric content of PAHs (Marcosa et al., 2010; Massei et al., 2003; Pongpiachan et al., 2009a). In addition to the many studies associated with the atmospheric fate of PAHs, several efforts have also been made to assess the mutagenicity of ambient aerosols in response to particular concerns related to adverse health effects (de Andrade et al., 2011; Pongpiachan et al., 2013a; Vu et al., 2012). Among the various types of potential emission sources, traffic exhausts, energy

* Corresponding author.

E-mail address: pongpijun@gmail.com (S. Pongpiachan).

production and industrial emissions are generally considered the two principal contributors of carcinogens and mutagens to the urban atmospheric environment (Coronas et al., 2009; Dong et al., 2013; Pongpiachan, 2013a,b; Pongpiachan et al., 2013a; Villalobos-Pietrini et al., 2006).

Numerous studies have indicated a direct link between deteriorating air quality and shipping emissions (e.g., Contini et al., 2011; Fauser et al., 2013; Gregoris et al., 2014; Zhao et al., 2013). A list of potential pollutants from ship emissions is comprehensive and can be found in the emission inventory guidelines for road traffic and ships (EMEP/CORINAIR, 2007). However, despite several extensive studies focusing on the chemical characterization of air pollutants, there has been no report of either carcinogenic or mutagenic substances derived from shipping emissions. During the past decades, various interests have been focusing over negative impacts of PM₁₀-bounded PAHs on human health associated with cancer, endocrine disruption, reproductive and developmental effects (Hoyer, 2001; Matsui, 2008; Wickramasinghe et al., 2012). Unfortunately, at present, there is only one publication related to the mutagenicity of ambient particles in a petrochemical industrial area (Coronas et al., 2008). Although various studies have raised concerns over the adverse health effects of ambient air pollution in relation to industrial activities, no study focusing on the correlation between the mutagenicity and carcinogenicity of PM₁₀ in the EST has been published. In order to draw any definite conclusions regarding the principal sources of carcinogens and mutagens in the EST, it is therefore crucial to conduct long-term monitoring at both roadside and seaport sites. This study aims to investigate whether there are any significant enhancements to particulate PAHs and the mutagenicity of PM₁₀ during the docking period at observatory sites adjacent to the IRPC seaport. The impacts of traffic emissions and other industrial activities on the variation of PAHs and the Mutagenic Index (MI) were also analyzed with great caution.

2. Experimental methodology

2.1. Sampling sites

Air samples were collected at Pluakgate Temple Observatory Station (PTOS) ($12^{\circ}39'41.70''N$, $101^{\circ}18'53.62''E$) and the IRPC Complex Zone Observatory Station (ICZ) ($12^{\circ}39'10.46''N$, $101^{\circ}18'7.66''E$). PTOS is located within a petrochemical industrial area of Tumbol Cherrgnern, Muang District, Rayong Province, which is located approximately 1.2 km northeast of the IRPC Refineries (Fig. 1). The ICZ station ($12^{\circ}39'10.46''N$, $101^{\circ}18'7.66''E$) was selected because of its proximity to the IRPC seaport (i.e., a distance of approximately 1.4 km), meaning that it could be taken as representative of a mixture of shipping and industrial emissions (Fig. 1). The IRPC seaport is located in the same area as its refinery in Rayong Province. It offers a number of facilities and dock services for clients, including tugboats, piloting services, lighters, fresh water and fuel, weigh scales, container yards, warehouses, and machines and equipment for the transshipment of goods. The PTOS and ICZ sites were approximately 2-km apart within each cluster and regularly used as accidental gas leakage warning stations and trace gas monitoring sites to expand the annual database for the Pollution Control Department of Thailand. Both observatory sites are located almost 18 km to the southeast of the MIE.

2.2. Filter sample collection and meteorological data

Tisch high-volume air samplers (TE 6070; Tisch Environmental Inc., OH, USA) were employed to achieve unmanned 24-h samplings for PM₁₀. Total ambient PM₁₀ samples from both observatory sites were collected on 75 days from February 1–10, 2010

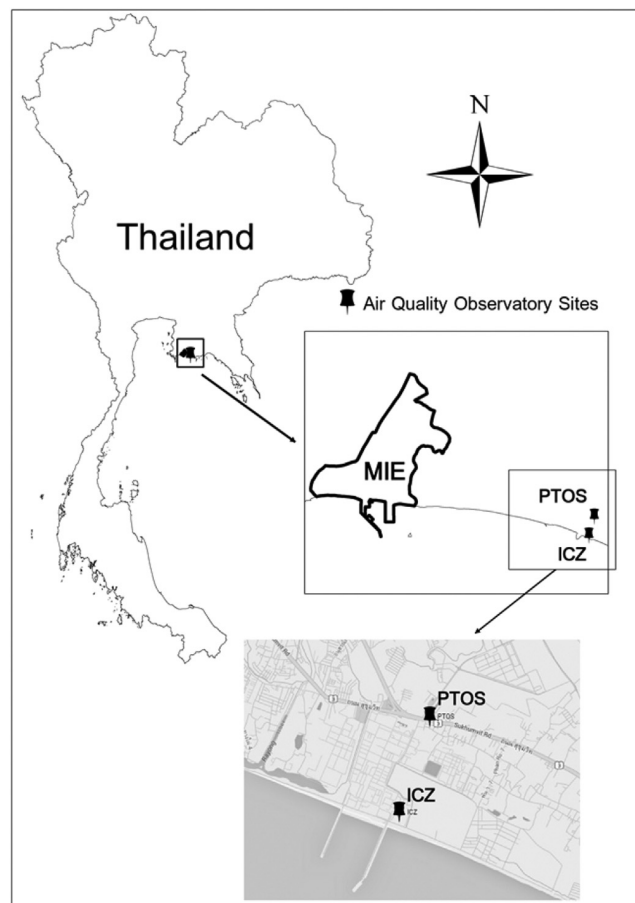


Fig. 1. Locations of air sample observatory sites used in this study: PTOS - Pluakgate Temple Observatory Station; ICZ - IRPC Complex Zone Observatory Station.

($n = 10$), April 19–28, 2011 ($n = 10$), March 5–14, 2012 ($n = 10$), October 27–31, 2012 ($n = 5$), March 22–31, 2013 ($n = 10$), and June 7 to July 6, 2013 ($n = 30$). PM₁₀ samples were collected simultaneously at both sites for 24 h every day from 09:00 a.m. to 09:00 a.m. on the following day. During the sampling period, the Tisch high-volume air samplers were employed with a flow rate of $1.132 \text{ m}^3 \text{ min}^{-1}$. The sample airflow rate was calibrated for conditions of standard temperature and pressure. A more comprehensive explanation of the air sampling method is given in the “Compendium Method IO-2.2. Sampling of Ambient Air for PM₁₀ using an Andersen Dichotomous Sampler” (US EPA, 1999). Airborne particles were collected on a Whatman™ 1851-865 Grade QM-A Quartz Microfiber Filter Sheet for Air Sampling, Size: $20 \times 25 \text{ cm}$, Pore Size: $2.2 \mu\text{m}$ (QMF), which had been heated to 450°C for 4.5 h to remove any organic material.

2.3. Chemicals analysis of PAHs

Standard PAHs (a mixture of the 15 PAHs listed in the Norwegian Standard (NS 9815: S-4008-100-T); each $100 \mu\text{g mL}^{-1}$ in toluene: unit: $1 \times 1 \text{ mL}$) and a mix of recovery Internal Standard PAHs (d_{12} -perylene (d_{12} -Per), d_{10} -fluorene (d_{10} -Fl); each $100 \mu\text{g mL}^{-1}$ in xylene: unit: $1 \times 1 \text{ mL}$) were supplied by Chiron AS (Stiklestadveine 1, N-7041 Trondheim, Norway). All organic solvents (i.e., DCM and Hexane) were HPLC-grade, purchased from Fisher Scientific. Standard stock solutions of $4 \mu\text{g mL}^{-1}$ of deuterated PAHs (used as internal standards) and $100 \mu\text{g mL}^{-1}$ of native PAHs were prepared in

nonane. Working solutions were obtained by appropriate dilution in *n*-cyclohexane. All solutions were stored in amber-colored vials at –20 °C. Silica gel (0.040–0.063 mm) was purchased from Merck and all materials used (e.g., silica gel, glass, and cotton wool) were Soxhlet-extracted with DCM for 24 h and kept dry (in a desiccator) until use. The fractionation/cleanup and blow-down processes followed the method reported by Gogou et al. (1996). All samples were analyzed for PAHs using a Shimadzu GCMS-QP2010 Ultra Gas system coupled with 60-m long × 0.25 mm i.d. capillary column coated with a 0.25-μm film thickness (Agilent JW Scientific DB-5 GC columns) (Pongpiachan et al., 2009b; Pongpiachan et al., 2012).

2.4. Mutagenicity assay

Mutagenicity assays were performed in accordance with the pre-incubation technique (Yahagi et al., 1997) using the *Salmonella*, *typhimurium* strains TA98 and TA100. Mutagenicity of the organic extracts was assessed by the *Salmonella*/microsome assay with the standard plate incorporation method, called the “Ames Test” (Ames et al., 1975). The procedure consists of adding the buffer or S-9 mix, histidine-dependent bacteria (about 10⁸), and test chemical to 2 mL of top agar containing biotin and a trace amount of histidine (0.05 mM each). In each of the assays, positive and negative controls were conducted. The positive controls in the absence of metabolic activator (-S9) were 2-aminofluorine (2-AF) for both TA98 and TA100 strains. Each determination was made in triplicate and at least two independent experiments performed to confirm the results. The impacts of shipping emissions on mutagenicity of PM₁₀ were investigated with the assistance of a computation of MI. This MI was employed to evaluate the enhancement of mutagenicity, above background levels at both observatory sites, due to shipping emissions within that area, as described in Eq. (1).

$$MI = \frac{\text{Number of Colonies in Sample}}{\text{Number of Colonies in Negative Control}} \quad (1)$$

3. Results

Table 1 summarizes the concentrations of the selected 15 PAHs measured in the 150 samples taken at PTOS and ICZ during the docking and non-docking periods. The statistical description of PAH congeners at each observatory site shows a wide range of PAH mass

concentrations. The average ΣPAH concentrations were significantly higher during the docking periods at both observatory sites, highlighting the influence of shipping emissions on the level of air quality in the study area. The most abundant aromatic ring groups at both observatory sites during the docking period were four-ring PAHs, three-ring PAHs, five-ring PAHs, and six-ring PAHs, which contributed 82%, 11%, 6%, and 2%, respectively. In accordance with the results measured at both sampling sites, the five- and six-ring PAHs were found in the PM₁₀, contributing 41% and 23%, respectively, whilst the three- and four-ring PAHs contributed only 8% and 27%, respectively. The comparatively high percentage contributions of five- and six-ring PAHs indicates that the emission source is a high-temperature process, such as the combustion of fuels in engines (Tobiszewski and Namiesnik, 2012). During the non-docking period, the average B[a]P concentrations at PTOS and ICZ were approximately 88 and 8 times lower, respectively, than the value of the guideline limit of annual B[a]P concentration (i.e., 1 ng m^{−3} or 1000 pg m^{−3}), as proposed by the World Health Organization. However, the average values of PTOS_{Docking Period} and ICZ_{Docking Period} were almost eight times higher than the value of 250 pg m^{−3}, proposed by the UK Expert Panel of Air Quality Standard (UK EPAQS, 1999). These facts underline the need for controlling shipping emissions in order to reduce the risks associated with such exposure to carcinogens in this area. **Table 2** shows average MI values higher than one using the standard Ames Test TA98 strain without the addition of the S9 mixture. For samples collected during the docking period and tested in the absence of S9, the MI values were significantly higher than during the non-docking period for both stations. Furthermore, the samples collected during the docking periods that were tested with TA100 without the addition of the S9 mixture, showed higher MI values than those observed during the non-docking periods for both sampling sites. As illustrated in **Table 3**, the binary ratios of PAHS_{Docking Period}/PAHS_{Non-Docking Period} of both observatory sites were higher than one. Significant enhancements of Phe, Fluo, Pyr, 11H-B[a]F, 11H-B[b]F, B[a]A, Chry, B[e]P, B[a]P, and Ind were also observed during the docking period for both sampling sites. The results clearly indicate that shipping emissions play a primary role as a temporary source of both mutagenic and carcinogenic activities of PM₁₀. In addition, there were no significant differences of PAHs between the two observatory sites for both monitoring periods. This indicates that contributions from stationary sources at the two sites did not display significant variation, highlighting both the homogeneity of the air masses within the study area and the robustness of the

Table 1

Statistical description of PAH concentrations [pg m^{−3}] measured at PTOS and ICZ during the docking and non-docking periods.

	Docking period (n = 35)		Non-docking period (n = 40)		Docking period (n = 35)		Non-docking period (n = 40)	
	PTOS		PTOS		ICZ		ICZ	
	Average	Std. dev.	Average	Std. dev.	Average	Std. dev.	Average	Std. dev.
Phe	1.20E+04	1.97E+04	2.70E+01	3.17E+01	1.16E+04	1.39E+04	3.19E+01	4.44E+01
An	1.01E+03	2.39E+03	1.52E+01	2.08E+01	2.51E+03	5.96E+03	1.88E+01	2.48E+01
Fluo	4.76E+03	7.91E+03	1.12E+01	1.36E+01	4.27E+03	4.60E+03	1.23E+01	2.22E+01
Pyr	9.59E+03	1.72E+04	1.10E+01	1.49E+01	1.11E+04	1.40E+04	1.41E+01	3.04E+01
11H-B[a]F	1.58E+04	2.88E+04	1.79E+00	7.42E+00	1.93E+04	2.53E+04	1.41E+00	6.10E+00
11H-B[b]F	7.30E+03	1.33E+04	1.45E+01	4.81E+01	6.87E+03	1.16E+04	9.20E+00	3.42E+01
B[a]A	3.28E+04	5.52E+04	3.25E+01	6.23E+01	4.29E+04	5.87E+04	2.29E+01	3.93E+01
Chry	2.60E+04	4.37E+04	8.81E+01	1.99E+02	2.84E+04	3.77E+04	8.00E+01	1.62E+02
B[b+k]F	1.09E+03	2.64E+03	5.51E+01	7.05E+01	6.90E+02	1.05E+03	1.84E+02	7.54E+02
B[e]P	4.15E+03	6.38E+03	3.67E+01	6.34E+01	3.60E+03	7.50E+03	3.11E+01	6.34E+01
B[a]P	2.06E+03	3.19E+03	1.14E+01	2.25E+01	2.19E+03	3.82E+03	1.30E+02	7.10E+02
Ind	1.11E+03	1.22E+03	4.47E+01	6.08E+01	3.68E+03	7.55E+03	6.63E+01	2.01E+02
D[a,h]A	3.71E+02	2.05E+03	8.59E+00	2.91E+01	2.36E+02	9.48E+02	N.D.	N.D.
B[g,h,i]P	8.12E+01	4.16E+02	4.94E+01	9.12E+01	7.98E+00	3.45E+01	9.30E+01	2.46E+02
ΣPAHs	1.18E+05	1.79E+05	3.12E+02	4.62E+02	1.37E+05	1.73E+05	6.95E+02	1.89E+03

Table 2

Statistical descriptions of MI as assessed by TA98 and TA100.

Site Period	PTOS		PTOS		t-Test ($p < 0.01$)	ICZ		ICZ		t-Test ($p < 0.01$)
	Docking (n = 35)	Non-docking (n = 40)	Average	Std. dev.		Average	Std. dev.	Average	Std. dev.	
MI	Average	Std. dev.	Average	Std. dev.	($p < 0.01$)	Average	Std. dev.	Average	Std. dev.	($p < 0.01$)
TA98 (-S9)	1.42E+00	1.72E-01	1.24E+00	1.16E-01	S	1.46E+00	1.63E-01	1.20E+00	1.42E+00	S
TA100 (-S9)	1.39E+00	9.50E-02	1.23E+00	5.40E-02	S	1.30E+00	6.40E-02	1.24E+00	1.39E+00	S

Table 3

Binary diagnostic ratios of PAHs measured during the docking and non-docking periods at PTOS and ICZ.

	Docking/Non-docking		Docking/Non-docking		Docking vs. Non-docking		Docking vs. Non-docking		Docking		Non-docking
	PTOS		ICZ		PTOS		ICZ		PTOS-ICZ		PTOS-ICZ
	Average	Std. dev.	Average	Std. dev.	t-Test ($p < 0.005$)		t-Test ($p < 0.005$)		t-Test ($p < 0.005$)		t-Test ($p < 0.005$)
Phe	4.43E+02	6.21E+02	3.65E+02	3.12E+02	S		S		NS		NS
An	6.62E+01	1.15E+02	1.33E+02	2.41E+02	NS		NS		NS		NS
Fluo	4.24E+02	5.81E+02	3.47E+02	2.07E+02	S		S		NS		NS
Pyr	8.74E+02	1.16E+03	7.84E+02	4.59E+02	S		S		NS		NS
11H-B[a]F	8.83E+03	3.89E+03	1.37E+04	4.14E+03	S		S		NS		NS
11H-B[b]F	5.05E+02	2.75E+02	7.47E+02	3.39E+02	S		S		NS		NS
B[a]A	1.01E+03	8.86E+02	1.88E+03	1.49E+03	S		S		NS		NS
Chry	2.95E+02	2.20E+02	3.56E+02	2.33E+02	S		S		NS		NS
B[b+k]F	1.97E+01	3.75E+01	3.74E+00	1.40E+00	NS		NS		NS		NS
B[e]P	1.13E+02	1.01E+02	1.16E+02	1.18E+02	S		S		NS		NS
B[a]P	1.80E+02	1.42E+02	1.69E+01	5.38E+00	S		S		NS		NS
Ind	2.48E+01	2.01E+01	5.55E+01	3.76E+01	S		S		NS		NS
D[a,h]A	4.32E+01	7.05E+01	N.D.	N.D.	NS		NS		NS		NS
B[g,h,i]P	1.64E+00	4.57E+00	8.58E-02	1.40E-01	NS		NS		NS		NS
Σ PAHs	3.78E+02	3.87E+02	1.98E+02	9.14E+01	S		S		NS		NS

chemical analysis. If shipping is major contributor of PAHs, stationary sources may not be discernible. Neither the spatial variability of other stationary sources nor any particular meteorological conditions appear to play a major role in governing PAH concentrations at both monitoring sites.

The toxicity equivalent concentration (TEQ) equation is widely used for estimating the risk of exposure to PAHs and it can be calculated as follows (Pongpiachan et al., 2013b; Yang et al., 2007; Yu et al., 2008):

$$TEQ = \sum_i [C_i \times TEF_i] \quad (2)$$

where C_i and TEF_i are acronyms for the levels of each PAH congener and the toxic equivalency factors, respectively. As the toxicity of each PAH congener might differ broadly by orders of magnitude, it is important to show the toxicity of PAHs as a form of the most toxic congener of PAHs, B[a]P. By employing the TEF, the comprehensive toxicity of a matrix of PAHs can be represented in a single value, namely the TEQ. As illustrated in Eq. (2), the TEQ is a summation of the concentration and individual TEF values of each PAH congener. Equations (3)–(5) were calculated for TEQ based on Nisbet and Lagoy (1992), U.S. EPA (1993), and Cecinato (1997), respectively. In these calculations, the acronyms for the PAH compounds represent their concentrations.

$$\begin{aligned} TEQ_{Nisbet \text{ and } Lagoy} = & 0.001(Phe + Fluo + Pyr) \\ & + 0.01(An + B[g,h,i]P + Chry) \\ & + 0.1(B[a]A + B[b]F + B[k]F + Ind) \\ & + B[a]P + D[a,h]A \end{aligned} \quad (3)$$

$$\begin{aligned} TEQ_{US-EPA} = & 0.06(B[a]A) + 0.07(B[b]F + B[k]F) + B[a]P \\ & + 0.08(Ind) + 0.6(D[a,h]A) \end{aligned} \quad (4)$$

$$\begin{aligned} TEQ_{Cecinato} = & 0.01(Chry) + 0.1(B[a]A + B[b]F + B[k]F + Ind) \\ & + B[a]P + D[a,h]A \end{aligned} \quad (5)$$

An initial one-way ANOVA test showed significant differences in the TEQ values computed using the three methods, as previously mentioned. The average of the TEQ_{Nisbet} and $Lagoy$ values was significantly higher than the TEQ_{US-EPA} and $TEQ_{Cecinato}$ values, as displayed in Table 4. A relationship of TEQ values between the two different sampling periods was evaluated, as exhibited in Table 4. TEQ values observed during the docking periods were significantly higher than during the non-docking period for both sampling sites. The most reasonable elucidation for this might be the relatively high contribution of HMW PAHs in both PTOS_{Docking Period} and ICZ_{Docking Period} samples, which have high TEF values. The ICZ_{Docking Period} samples show the highest TEQ values, as calculated by the Nisbet and Lagoy ($7.49E+03 \pm 1.20E+04 \text{ pg m}^{-3}$), Cecinato ($7.44E+03 \pm 1.19E+04 \text{ pg m}^{-3}$), and U.S. EPA models ($5.25E+03 \pm 8.59E+03 \text{ pg m}^{-3}$). This could be due to a relatively high percentage contribution by the six-ring aromatic groups of PAHs (i.e., B[g,h,i]P and Ind), which are predominantly caused by the combustion of diesel fuel by cargo ships during the docking period.

4. Discussion

Binary ratios of PAHs have been frequently applied as diagnostic tools to identify PAH emission sources, classify samples by position, and evaluate the significance of pyrolysis and petroleum-derived

Table 4

TEQ values [pg m^{-3}] as assessed by three different methods: Nisbet and Lagov, U.S. EPA, and Cecinato using PAH values measured at PTOS and ICZ for both docking and non-docking periods.

	PTOS		PTOS		ICZ		ICZ	
	Docking period ($n = 35$)		Non-docking period ($n = 40$)		Docking period ($n = 35$)		Non-docking period ($n = 40$)	
	Average	Std. dev.	Average	Std. dev.	Average	Std. dev.	Average	Std. dev.
TEQ-Nisbet and Lagov	6.23E+03	1.17E+04	3.50E+01	7.40E+01	7.49E+03	1.20E+04	1.59E+02	8.14E+02
TEQ-US-EPA	4.41E+03	8.02E+03	2.60E+01	5.30E+01	5.25E+03	8.59E+03	1.49E+02	7.81E+02
TEQ-Cecinato	6.19E+03	1.16E+04	3.40E+01	7.30E+01	7.44E+03	1.19E+04	1.58E+02	8.11E+02

PAHs (Guo et al., 2003; Mantis et al., 2005; Yunker et al., 2002). Table 5 includes characteristic diagnostic ratios cited from previous works, coupled with the PAH diagnostic ratio values computed for the PM_{10} studied. The diagnostic ratios calculated between the PM_{10} -bound PAHs in this study indicate that both sites were influenced by numerous potential sources with some unique features. Firstly, the binary ratios of $\text{Ind}/(\text{Ind} + \text{B}[g,h,i]\text{P})$, $\text{Fluo}/(\text{Fluo} + \text{Pyr})$, $\text{An}/(\text{An} + \text{Phe})$, and $\text{B}[a]\text{A}/(\text{B}[a]\text{A} + \text{Chry})$ observed during the non-docking period ranged from 0.42 (ICZ) to 0.47 (PTOS), 0.47 (ICZ) to 0.51 (PTOS), 0.36 (PTOS) to 0.37 (ICZ), and 0.22 (ICZ) to 0.27 (PTOS), respectively. The binary ratios of $\text{Ind}/(\text{Ind} + \text{B}[g,h,i]\text{P})$, $\text{B}[a]\text{P}/\text{B}[g,h,i]\text{P}$, and $\text{B}[a]\text{A}/(\text{B}[a]\text{A} + \text{Chry})$ were mostly higher during the docking period than during the non-docking period at both sites (Table 5). The above ratios for the non-docking period are in accordance with those previously reported for diesel engines. The $\text{An}/(\text{An} + \text{Phe})$ ratios for PTOS_{Non-Docking Period} (0.36) and ICZ_{Non-Docking Period} (0.37) show values similar to diesel engine emissions (i.e., 0.35), whereas the $\text{Fluo}/(\text{Fluo} + \text{Pyr})$ ratios of PTOS_{Non-Docking Period} (0.51) and ICZ_{Non-Docking Period} (0.47)

are in good agreement with diesel engine emissions (i.e., >0.5) (Guo et al., 2003; Ravindra et al., 2006, 2008). This indicates that traffic emissions from diesel trucks and other vehicles were the main contributors to PAHs at both sampling sites during the non-docking period. In this study, the ratios of $\text{B}[a]\text{P}/\text{B}[g,h,i]\text{P}$ and $\text{B}[a]\text{A}/(\text{B}[a]\text{A} + \text{Chry})$ ranged from 0.23 (PTOS_{Non-Docking period}) to 275 (ICZ_{Docking Period}), and 0.22 (ICZ_{Non-Docking period}) to 0.60 (ICZ_{Docking period}), respectively (Table 5). These two binary ratios are approaching those reported for coal/coke combustion, suggesting that coal combustion might have played an important role during both sampling periods (Ravindra et al., 2008; Tang et al., 2005). In addition, the ratios of $\text{Ind}/(\text{Ind} + \text{B}[g,h,i]\text{P})$, $\text{B}[a]\text{P}/\text{B}[g,h,i]\text{P}$, and $\text{Fluo}/(\text{Fluo} + \text{Pyr})$ also reveal that coal combustion might be the predominant source of PAHs during the non-docking period. This can be attributed to IRPC's combined heat and power plant, which was operational by mid-2011, producing 220 MW of electricity and 450 tons hr^{-1} of steam for IRPC's integrated petrochemical complex in Rayong Province. The power plant can be operated by either natural gas or coal through steam-powered turbines.

Table 5

Binary diagnostic ratios of PAHs obtained from this study in comparison with those of other reports.

Diagnostic ratio	$\text{Ind}/(\text{Ind} + \text{B}[g,h,i]\text{P})$	$\text{B}[a]\text{P}/\text{B}[g,h,i]\text{P}$	$\text{Fluo}/(\text{Fluo} + \text{Pyr})$	$\text{An}/(\text{An} + \text{Phe})$	$\text{B}[a]\text{A}/(\text{B}[a]\text{A} + \text{Chry})$
PTOS _{Non-Docking period}	0.47	0.23	0.51	0.36	0.27
PTOS _{Docking period}	0.93	25	0.33	0.08	0.56
ICZ _{Non-Docking period}	0.42	1.39	0.47	0.37	0.22
ICZ _{Docking period}	1.0	275	0.28	0.18	0.60
Gasoline engine	0.18 ^a	0.5–0.6 ^b	<0.5 ^c	0.50 ^d	0.49 ^e
Diesel engine	0.35–0.7 ^f	0.3–0.4 ^g	>0.5 ^c	0.35 ^d	0.68 ^e
Coal/coke	0.33 ^h	>1.25 ^b	0.53 ⁱ	—	0.50 ^h
Coal burning	0.56 ^f	0.9–6.6 ^j	0.57 ^k	0.24 ^d	0.46 ^k
Wood combustion	0.62 ^l	—	0.51 ^k	0.16 ^k	0.43 ^m
Natural gas combustion	0.32 ^k	—	0.49 ^k	0.12 ^k	0.39 ^k
CF (cooking fumes) ⁿ	0.40	1.33	0.69	0.48	0.43
ETS (environmental tobacco smoke) ⁿ	0.52	1.89	0.77	0.39	0.30
Pyrogenic	—	—	—	>0.1 ^o	—
Petrogenic	<0.2	—	<0.4 ^p	<0.1 ^o	<0.2
Traffic	—	<0.6 ^q	—	—	—
Non-traffic	—	>0.6 ^r	—	—	—

—: Not Reported.

^a Wang et al., 2008; Del et al., 2005.

^b Ravindra et al., 2008.

^c Ravindra et al., 2008; Ravindra et al., 2006.

^d Guo et al., 2003.

^e Khalili et al., 1995; Vasilakos et al., 2007.

^f Wang et al., 2008; Del et al., 2005; Ravindra et al., 2008, 2006; Vasilakos et al., 2007; Saarnio et al., 2008.

^g Bourotte et al., 2005.

^h Tang et al., 2005.

ⁱ Saarnio et al., 2008.

^j Akyüz and Çabuk, 2008.

^k Galarneau, 2008.

^l Del et al., 2005; Ravindra et al., 2008; Akyüz and Çabuk, 2008; Mantis et al., 2005.

^m Akyüz and Çabuk, 2008; Mantis et al., 2005.

ⁿ Zhang et al., 2009.

^o Pies et al., 2008.

^p Yunker et al., 2002.

^q Pandey et al., 1999.

^r Zhang et al., 2008.

Table 6

Principal components (PC) pattern for Varimax rotated components applied to PM₁₀-bound PAHs and MI from ICZ and PTOS during the docking and non-docking periods. Any values that higher than 0.5 will be highlighted as bold.

	Docking period			Non-docking period		
	PC1	PC2	PC3	PC1	PC2	PC3
MI-TA98	0.138	-0.006	0.694	-0.053	-0.343	0.402
MI-TA100	-0.041	-0.023	0.708	-0.117	-0.312	0.619
Phe	0.906	0.119	0.049	0.011	0.408	0.793
An	0.412	0.037	-0.059	-0.143	0.429	-0.203
Fluo	0.916	0.025	-0.020	-0.007	0.415	0.801
Pyr	0.950	0.112	0.069	-0.017	0.290	0.860
11H-B[a]F	0.955	0.179	0.084	0.073	0.697	0.065
11H-B[b]F	0.720	-0.030	0.054	0.080	0.786	0.021
B[a]A	0.949	0.205	0.099	0.055	0.845	0.131
Chry	0.958	0.158	0.081	0.068	0.797	0.021
B[b+k]F	-0.186	0.610	-0.598	0.981	-0.102	-0.001
B[e]P	0.275	0.690	0.139	0.246	-0.369	0.451
B[a]P	0.243	0.899	-0.162	0.969	-0.098	-0.053
Ind	0.383	0.671	0.224	0.965	0.006	0.117
D[a,h]A	-0.184	0.552	-0.571	0.031	-0.206	0.360
B[g,h,i]P	0.095	-0.215	-0.353	0.920	0.214	-0.083
ΣPAHs	0.968	0.230	0.073	0.979	0.157	0.010

It is also worth mentioning that the liquid and chemical terminal of the IRPC port handles annual throughput of 15 million tons and serves more than 2000 vessels per year. Furthermore, the majority of ships handled employ dual-fuel mode (hybrid system) engines because of their fuel flexibility. Multi-fuel engines utilize a “cruise mode” combustion process when operating on crude oils. When a vessel approaches port, the engine operation transfers from crude oil to diesel and thus, it utilizes the conventional diesel process. The comparatively high B[a]P/B[g,h,i]P ratios observed during the docking period suggest that the principal source of PAHs is non-traffic. Interestingly, the relatively low Fluo/(Fluo + Pyr) and An/(An + Phe) ratios highlight the importance of petrogenic sources during the docking period. Based on the diagnostic binary ratios calculated, it was determined that the PAH compounds at the two sampling sites during the two different periods were contributed by mixed sources of pyrogenic combustion and petrogenic sources.

Despite using a single binary ratio, using PCA as the multivariate analytical tool can reduce a set of original variables (measured PAHs and MI content in PM₁₀ samples) and extract a small number of latent factors (principal components, PCs) for the analysis of the relationships among the observed variables. Data submitted for the analysis were arranged in a matrix, where each column corresponded to one parameter and each row represented the number of samples. These data matrixes were evaluated through PCA, which allowed the summarized data to be analyzed further. As illustrated in Table 6, the PC patterns for Varimax rotated components of two observatory sites during the docking period are composed of three components, which account for 45.6%, 16.0%, and 8.2% for the total of variances of PC1, PC2, and PC3, respectively. The contributions of PC1 and PC2 explain 62% of the total variance, and that of PC1 (45.6% of the variation) is almost six times higher than PC3 (8.2%). PC1 comprises exclusively PAHs (3,4), because they show strong positive correlation coefficients. It is well known that diesel exhausts are major sources of LMW PAHs and thus, the strong correlation coefficients of Phe, Fluo, Pyr, and Chry observed in PC1 can be attributed to shipping emissions during the docking period (Abrantes et al., 2004; Tavares et al., 2004). The positive correlation coefficients for B[b+k]F ($R = 0.610$), B[e]P ($R = 0.690$), B[a]P ($R = 0.899$), and Ind ($R = 0.671$) imply that coal fly ash from nearby power plants is probably the main source found in PC2, because HMW PAHs are often found in particles derived from incomplete combustion of coal (Masala et al., 2012). There are also moderate

loadings of MI-TA98 (-S9) as well as MI-TA100 (-S9) observed in PC3 for both sampling periods. This can be attributed to the generation of mutagenic compounds from industrial boilers, as previously mentioned by several studies (e.g., Addink and Altwicker, 2004; Duo and Leclerc, 2007; Ishikawa et al., 1997). The strong positive loadings of B[b+k]F ($R = 0.981$), B[a]P ($R = 0.969$), Ind ($R = 0.965$), and B[g,h,i]P ($R = 0.920$) observed in PC1 (28.4%) during the non-docking period suggest that coal combustion might play an important role as a stationary source of PAHs. The positive loadings of 11H-B[a]F ($R = 0.697$), 11H-B[b]F ($R = 0.786$), B[a]A ($R = 0.845$), and Chry ($R = 0.797$) measured in PC2 (21.8%) reflect the uniqueness of the emission sources, possibly due to the complexity of industrial activities within the study area.

5. Conclusions

In conclusion, the application of PAH binary ratios coupled with PCA highlights the significance of controlling shipping emissions from diesel oil combustion in areas like the IRPC seaport. Even though reliable results of the contributions of sources of PAHs has not been achieved, it seems rational to conclude that coal combustion in nearby power plants was the principal contributor of PM₁₀-bound PAHs within the study area, particularly during periods without shipping transport activities. In addition, it appears reasonable to ascribe comparatively high levels of coal combustion and diesel emissions as the two principle sources of PAHs during both sampling periods.

Acknowledgments

This work was performed with the approval of the National Institute of Development Administration (NIDA) and financial support from IRPC. The authors acknowledge the staff of the Faculty of Environmental Management, Prince of Songkla University, and Bara Scientific Co., Ltd. for their contributions to the laboratory work.

References

- Abrantes, R.D., Assunção, J.V.D., Pesquero, C.R., 2004. Emission of polycyclic aromatic hydrocarbons from light-duty diesel vehicles exhaust. *Atmos. Environ.* 38 (11), 1631–1640.
- Addink, R., Altwicker, E.R., 2004. Formation of polychlorinated dibenzo-p-dioxins and dibenzofurans on secondary combustor/boiler ash from a rotary kiln burning hazardous waste. *J. Hazard. Mater.* 114 (1–3), 53–57.
- Akyü, z. M., Cabuk, H., 2008. Particle-associated polycyclic aromatic hydrocarbons in the atmospheric environment of Zonguldak, Turkey. *Sci. Total Environ.* 405, 62–70.
- Ames, N., McCann, J., Yamasaki, E., 1975. Methods for detecting carcinogens and mutagens with the *Salmonella*/mammalian-microsome mutagenicity test. *Mutat. Res.* 31, 347–364.
- Bourrotte, C., Forti, M., Taniguchi, S., Bicego, M., Lotufo, P., 2005. A wintertime study of PAHs in fine and coarse aerosols in São Paulo city, Brazil. *Atmos. Environ.* 39, 3799–3811.
- Cecinato, A., 1997. Polynuclear aromatic hydrocarbons (PAH), benz(a)pyrene (BaPy) and nitrated-PAH (NPAH) in suspended particulate matter. *Ann. Chim.* 87, 483–496.
- Contini, D., Gambaro, A., Belosi, F., De Pieri, S., Cairns, W.R.L., Donateo, A., Zanotto, E., Citron, M., 2011. The direct influence of ship traffic on atmospheric PM_{2.5}, PM₁₀ and PAH in Venice. *J. Environ. Manag.* 92 (9), 2119–2129.
- Coronas, M.V., Horn, R.C., Ducatti, A., Rocha, J.V., Vargas, V.M.F., 2008. Mutagenic activity of airborne particulate matter in a petrochemical industrial area. *Mutat. Res.-Gen. Toxicol. Environ.* 650 (2), 196–201.
- Coronas, M.V., Pereira, T.S., Rocha, J.A.V., Lemos, A.T., Fachel, J.M.G., Salvadori, D.M.F., Vargas, V.M.F., 2009. Genetic biomonitoring of an urban population exposed to mutagenic airborne pollutants. *Environ. Int.* 35 (7), 1023–1029.
- de Andrade, S.J., Varella, S.D., Pereira, G.T., Zocolo, G.J., de Marchi, M.R.R., Varanda, E.A.A., 2011. Mutagenic activity of airborne particulate matter (PM10) in a sugarcane farming area (Araraquara city, Southeast Brazil). *Environ. Res.* 111 (4), 545–550.
- Del, R., Sienna, M., Rosazza, N., Prendez, M., 2005. Polycyclic aromatic hydrocarbons and their molecular diagnostic ratios in urban atmospheric respirable particulate matter. *Atmos. Res.* 75, 267–281.

- Dong, J., Cheng, Z., Li, F., 2013. PAHs emission from the pyrolysis of Western Chinese coal. *J. Anal. Appl. Pyrolysis* 104, 502–507.
- Duo, W., Leclerc, D., 2007. Thermodynamic analysis and kinetic modelling of dioxin formation and emissions from power boilers firing salt-laden hog fuel. *Chemosphere* 67 (9), S164–S176.
- EMEP/CORINAIR, 2007. Emission Inventory Guidebook – 2007. European Environment Agency. <http://www.eea.europa.eu/publications/EMEP-CORINAIR5/page016.html>.
- Fauser, P., Sanderson, H., Lofstrøm, P., 2013. Modelling air concentrations and risk of carcinogens and co-carcinogens in Gibraltar and source apportionment of nearby industrial facilities. *Atmos. Poll. Res.* 4 (4), 377–386.
- Galarneau, E., 2008. Source specificity and atmospheric processing of airborne PAHs: implications for source apportionment. *Atmos. Environ.* 42, 8139–8149.
- Gogou, A., Stratigakis, N., Kanakidou, M., Stephanou, E., 1996. Organic aerosol in Eastern Mediterranean: component source reconciliation by using molecular markers and atmospheric back trajectories. *Org. Geochem.* 25, 79–96.
- Gregoris, E., Argiriadis, E., Vecchiato, M., Zambon, S., De Pieri, S., Donatoe, A., Contini, D., Piazza, R., Barbante, C., Gambaro, A., 2014. Gas-particle distributions, sources and health effects of polycyclic aromatic hydrocarbons (PAHs), polychlorinated biphenyls (PCBs) and polychlorinated naphthalenes (PCNs) in Venice. *Sci. Total Environ.* 476–477, 393–405.
- Guo, H., Lee, S.C., Ho, K.F., Wang, X.M., Zou, S.C., 2003. Particle-associated polycyclic aromatic hydrocarbons in urban air of Hong Kong. *Atmos. Environ.* 37, 5307–5317.
- Hoyer, B.P., 2001. Reproductive toxicology: current and future directions. *Biochem. Pharmacol.* 62 (12), 1557–1564.
- Ishikawa, R., Buekens, A., Huang, H., Watanabe, K., 1997. Influence of combustion conditions on dioxin in an industrial-scale fluidized-bed incinerator: experimental study and statistical modeling. *Chemosphere* 35 (3), 465–477.
- Khalili, N.R., Scheff, P.A., Holsen, T.M., 1995. PAH source fingerprints for coke ovens, diesel and gasoline engines, highway tunnels, and wood combustion emissions. *Atmos. Environ.* 29, 533–542.
- Mantis, J., Chaloulakou, A., Samara, C., 2005. PM₁₀-bound polycyclic aromatic hydrocarbons (PAHs) in the greater area of Athens, Greece. *Chemosphere* 59, 593–604.
- Marcosa, M.M., Harrison, M.R., Schuhmacher, M., Domingo, L.J., Pongpiachan, S., 2010. Inferences over the sources and processes affecting polycyclic aromatic hydrocarbons in the atmosphere derived from measured data. *Sci. Total Environ.* 408, 2387–2393.
- Masala, S., Bergvall, C., Westerholm, R., 2012. Determination of benzo[a]pyrene and dibenzopyrenes in a Chinese coal fly ash certified reference material. *Sci. Total Environ.* 432, 97–102.
- Massei, M.A., Ollivon, D., Garban, B., Chevreuil, M., 2003. Polycyclic aromatic hydrocarbons in bulk deposition at a suburban site: assessment by principal component analysis of the influence of meteorological parameters. *Atmos. Environ.* 37 (22), 3135–3146.
- Matsui, S., 2008. Endocrine Disruptors. In: Encyclopedia of Ecology, pp. 1259–1260.
- Nisbet, I.C.T., LaGoy, P.K., 1992. Toxic equivalency factors (TEFs) for polycyclic aromatic hydrocarbons (PAHs). *Regul. Toxicol. Pharmacol.* 16, 290–300.
- Pandey, P.K., Patel, K.S., Lenicek, J., 1999. Polycyclic aromatic hydrocarbons: need for assessment of health risks in India? Study of an urban-industrial location in India. *Environ. Monit. Assess.* 59, 287–319.
- Pies, C., Hoffmann, B., Petrowsky, J., Yang, Y., Ternes, T.A., Hofmann, T., 2008. Characterization and source identification of polycyclic aromatic hydrocarbons (PAHs) in river bank soils. *Chemosphere* 72, 1594–1601.
- Pongpiachan, S., Thamanu, K., Ho, K.F., Lee, S.C., Sompongchaiyakul, P., 2009a. Predictions of gas-particle partitioning coefficients (K_p) of polycyclic aromatic hydrocarbons at various occupational environments of Songkhla province, Thailand. *Southeast Asian J. Trop. Med. Public Health* 40 (6), 1377–1394.
- Pongpiachan, S., Bualert, S., Sompongchaiyakul, P., Kositanont, C., 2009b. Factors affecting sensitivity and stability of polycyclic aromatic hydrocarbons. *Anal. Lett.* 42 (13), 2106–2130.
- Pongpiachan, S., Hirunyatrakul, P., Kittikoon, I., Khumsup, C., 2012. Parameters Influencing on Sensitivities of Polycyclic Aromatic Hydrocarbons Measured by Shimadzu GCMS-qp2010 Ultra Gas. Intech Open Access Publisher, ISBN 978-953-51-0298-4. <http://dx.doi.org/10.5772/32234>.
- Pongpiachan, S., 2013a. Vertical distribution and potential risk of particulate polycyclic aromatic hydrocarbons in high buildings of Bangkok, Thailand. *Asian Pac. J. Cancer Prev.* 14 (3), 1865–1877.
- Pongpiachan, S., 2013b. Diurnal variation, vertical distribution and source apportionment of carcinogenic polycyclic aromatic hydrocarbons (PAHs) in Chiang-Mai, Thailand. *Asian Pac. J. Cancer Prev.* 14 (3), 1851–1863.
- Pongpiachan, S., Choochuay, C., Hattayanone, M., Kositanont, C., 2013a. Temporal and spatial distribution of particulate carcinogens and mutagens in Bangkok, Thailand. *Asian Pac. J. Cancer Prev.* 14 (3), 1879–1887.
- Pongpiachan, S., Tipmanee, D., Deelaman, W., Muprasit, J., Feldens, P., Schwarzer, K., 2013b. Risk assessment of the presence of polycyclic aromatic hydrocarbons (PAHs) in coastal areas of Thailand affected by the 2004 tsunami. *Mar. Pollut. Bull.* 76, 370–378.
- Ravindra, K., Bencs, L., Wauters, E., Dehoog, J., Deutsch, F., Roekens, E., et al., 2006. Seasonal and site-specific variation in vapour and aerosol phase PAHs over Flanders (Belgium) and their relation with anthropogenic activities. *Atmos. Environ.* 40, 771–785.
- Ravindra, K., Sokhi, R., Vangrieken, R., 2008. Atmospheric polycyclic aromatic hydrocarbons: source attribution, emission factors and regulation. *Atmos. Environ.* 42, 2895–2921.
- Saarnio, K., Sillanpaa, M., Hillamo, R., Sandell, E., Pennanen, A., Salonen, R., 2008. Polycyclic aromatic hydrocarbons in size-segregated particulate matter from six urban sites in Europe. *Atmos. Environ.* 42, 9087–9097.
- Tang, N., Hattori, T., Taga, R., Igarashi, K., Yang, X., Tamura, K., et al., 2005. Polycyclic aromatic hydrocarbons and nitropolycyclic aromatic hydrocarbons in urban air particulates and their relationship to emission sources in the Pan-Japan Sea countries. *Atmos. Environ.* 39, 5817–5826.
- Tavares, J.M., Pinto, J.P., Souza, A.L., Scarmínio, I.S., Solci, M.C., 2004. Emission of polycyclic aromatic hydrocarbons from diesel engine in a bus station, Londrina, Brazil. *Atmos. Environ.* 38 (30), 5039–5044.
- Tobiszewski, M., Namiesnik, J., 2012. PAHs diagnostic ratios for the identification of pollution emission sources. *Environ. Pollut.* 162, 110–119.
- UK EPAQS, 1999. Expert Panel on Air Quality Standards. Polycyclic Aromatic Hydrocarbons. Report for the Department of the Environment, Transport and the Regions.
- US EPA, 1993. Provisional Guidance for Quantitative Risk Assessment of Polycyclic Aromatic Hydrocarbons. NC EPA-600/R-93/089. US Environmental Protection Agency, Research Triangle Park.
- US-EPA, 1999. Compendium of Methods for the Determination of Inorganic Compounds in Ambient Air. Compendium Method IO-2.2. Sampling of Ambient Air for PM10 Using an Andersen Dichotomous Sampler. EPA/625/R-96/010a. Available from: <http://www.epa.gov/ttnamti1/files/ambient/inorganic/mthd-2-2.pdf>.
- Vasilakos, C., Levi, N., Maggos, T., Hatzianestis, J., Michopoulos, J., Helmis, C., 2007. Gas-particle concentration and characterization of sources of PAHs in the atmosphere of a suburban area in Athens, Greece. *J. Hazard. Mater.* 140, 45–51.
- Villalobos-Pietrini, R., Amador-Muñoz, O., Waliszewski, S., Hernández-Mena, L., Munive-Colín, Z., Gómez-Arroyo, S., Bravo-Cabrera, J.L., Frías-Villegas, A., 2006. Mutagenicity and polycyclic aromatic hydrocarbons associated with extractable organic matter from airborne particles 10 µm in Southwest Mexico City. *Atmos. Environ.* 40 (30), 5845–5857.
- Vu, B., Alves, C.A., Gonçalves, C., Pio, C., Gonçalves, F., Pereira, R., 2012. Mutagenicity assessment of aerosols in emissions from wood combustion in Portugal. *Environ. Pollut.* 166, 172–181.
- Wang, X., Cheng, H., Xu, X., Zhuang, G., Zhao, C., 2008. A wintertime study of polycyclic aromatic hydrocarbons in PM2.5 and PM2.5–10 in Beijing: assessment of energy structure conversion. *J. Hazard. Mater.* 157, 47–56.
- Wickramasinghe, P.A., Karunaratne, P.G.G.D., Sivakanesan, R., 2012. PM10-bound polycyclic aromatic hydrocarbons: biological indicators, lung cancer risk of realistic receptors and 'source-exposure-effect' relationship under different source scenarios. *Chemosphere* 87, 1381–1387.
- Yahagi, T., Nagano, M., Seino, Y., 1997. Mutagenicities of N-nitrosoamines on *Salmonella*. *Mutat. Res.* 48, 121–130.
- Yang, X., Okada, Y., Tang, N., Matsunaga, S., Tamura, K., Lin, J., Kameda, T., Toriba, A., Hayakawa, K., 2007. Long-range transport of polycyclic aromatic hydrocarbons from China to Japan. *Atmos. Environ.* 41, 2710–2718.
- Yu, Y., Guo, H., Liu, Y., Huang, K., Wang, Z., Zhan, X., 2008. Mixed uncertainty analysis of polycyclic aromatic hydrocarbon inhalation and risk assessment in ambient air of Beijing. *J. Environ. Sci.* 20, 505–512.
- Yunker, M.B., Macdonald, R.W., Vingarzan, R., Mitchell, R.H., Goyette, D., Sylvestre, S., 2002. PAHs in the Fraser River basin: a critical appraisal of PAH ratios as indicators of PAH source and composition. *Org. Geochem.* 33, 489–515.
- Zhang, W., Zhang, S., Wan, C., Yue, D., Ye, Y., Wang, X., 2008. Source diagnostics of polycyclic aromatic hydrocarbons in urban road runoff, dust, rain and canopy throughfall. *Environ. Pollut.* 153, 594–601.
- Zhang, L., Bai, Z., You, Y., Wu, J., Feng, Y., Zhu, T., 2009. Chemical and stable carbon isotopic characterization for PAHs in aerosol emitted from two indoor sources. *Chemosphere* 75, 453–461.
- Zhao, M., Zhang, Y., Ma, W., Fu, Q., Yang, X., Li, C., Zhou, B., Yu, Q., Chen, L., 2013. Characteristics and ship traffic source identification of air pollutants in China's largest port. *Atmos. Environ.* 64, 277–286.



Impacts of micro-emulsion system on polychlorinated dibenzo-p-dioxins (PCDDs) and polychlorinated dibenzofurans (PCDFs) reduction from industrial boilers

S. Pongpiachan ^{a,*}, T. Wiriwutikorn ^b, C. Rungruang ^b, K. Yodden ^b, N. Duangdee ^c, A. Sbrilli ^d, M. Gobbi ^d, C. Centeno ^d

^a NIDA Center for Research & Development of Disaster Prevention & Management, School of Social and Environmental Development, National Institute of Development Administration (NIDA), 118 Moo 3, Serithai Road, Klong-Chan, Bangkok 10240, Thailand

^b Hazardous Substance Division, Waste and Hazardous Substance Management Bureau, Pollution Control Department (PCD), 92 Soi Phahonyothin 7, Phahonyothin Rd., Sam Sen Nai, Phayathai, Bangkok, Thailand

^c Red Bull Distillery Co., Ltd., 15 Moo 14, Vibhavadi Rangsit Road, Chomphon Sub-District, Chatuchak District, Bangkok, Thailand

^d Stockholm Convention Unit, Environmental Management Branch, Wagramerstrasse 5, A-1400 Vienna, Austria

HIGHLIGHTS

- Reductions of PCDD/PCDF emissions from a boiler was observed.
- Micro-emulsion technology also reduces SO₂/CO and NO_x/CO.
- This can be a promising technology for reducing dioxins.

ARTICLE INFO

Article history:

Received 30 October 2015

Received in revised form 31 December 2015

Accepted 3 January 2016

Available online 8 January 2016

Keywords:

Best available techniques (BAT)

Best environmental practices (BEP)

PCDDs/PCDFs

Micro-emulsion

Industrial boiler

ABSTRACT

Previous studies have raised public concerns regarding issues of adverse health impacts on human exposure to PCDDs/PCDFs. Industrial boilers have been criticized as one of the main contributors of PCDDs/PCDFs emissions. To minimize dioxin releases from unintentional production, a study on the best available techniques (BAT) and best environmental practices (BEP) was conducted using a micro-emulsion technology, which was developed for enhancing the combustion efficiency of industrial boilers. In this study, the performance of micro-emulsion technology on reducing PCDDs/PCDFs emissions from an industrial boiler using three types of fuels, 100% heavy fuel oil (100% HFO), 90% HFO coupled with 10% ethanol (90% HFO–10% ethanol), and 90% HFO coupled with 10% water (90% HFO–10% water), were carefully evaluated and statistically analyzed. The use of the ANOVA statistical method for the analysis of variance showed that there were no significant differences associated with the trace gaseous concentrations (e.g., CO, NO_x, and SO₂) among the three types of fuels. Furthermore, an industrial boiler using 90% HFO–10% ethanol tends to show the minimum PCDDs/PCDFs emissions in comparison with other two types of fuels. In addition, significant reductions of TCDDs, PeCDDs, HxCDDs, HpCDDs, TCDFs, PeCDFs, and total PCDDs were observed in an industrial boiler using the combination of HFO and ethanol. Overall, micro-emulsion can be considered a promising clean technology in term of PCDDs/PCDFs reduction.

© 2016 Elsevier Ltd. All rights reserved.

1. Introduction

Persistent organic pollutants (POPs) are toxic organic compounds that negatively impact human health. They have been broadly investigated in various environmental compartments

[19,22,20,21,23,24]. POPs released to the environment can travel through wind and water, so they can and do adversely affect people and wildlife far from their original sources. POPs show comparatively strong environmental persistence and can be subjected to bioaccumulation and biomagnification in different types of living organisms [8,18,26,28]. It is also widely acknowledged that polychlorinated dibenzo-p-dioxins (PCDDs) and polychlorinated dibenzofurans (PCDFs) are carcinogens and mutagens, which are

* Corresponding author. Tel.: +66 2 727 3113; fax: +66 2 732 0276.

E-mail address: pongpijun@gmail.com (S. Pongpiachan).

unintentionally produced from thermal processes [7,11,13]. Fossil fuel fired utilities including stoves, incinerators and boilers are considered as main contributors of PCDDs/PCDFs emissions after open and domestic waste burnings [5,9,27,29]. A regional project, "Demonstration of BAT and BEP in the Fossil fuel-fired Utilities and Industrial Boilers in response to the Stockholm Convention on POPs", officially approved for full implementation by the Global Environmental Facility (GEF) in April 2010, aims to investigate the emissions of PCDDs/PCDFs and other contaminants from representative industrial and power boilers in ESEA (East and South East Asia) countries and implement BAT and BEP measures to reduce their emissions. One important intervention is the enhancement of the combustion efficiency of industrial boilers. Recently, an innovative technology called "micro-emulsion system" was introduced, which is a static mixer composed of the liquid fuel reduced to the micron level that allows in the oxygen necessary for fuel oxidation.

Previous studies have highlighted the importance of water–oil emulsion as an alternative fuel for reducing pollutants from large pilot power plants [2], diesel engines [14], and commercial boilers [6]. Numerous investigations have also focused on the combustion characteristics of heavy oil–water emulsions [4], the formation of water-in-diesel oil nano-emulsions using water/mixed nonionic surfactant/diesel oil systems [3], and the micro-explosion at high temperature of water in oil emulsion droplets during the Leidenfrost effect [16]. As a consequence of the accumulation of knowledge and technology that has been recently developed, micro-emulsion systems are a green-technology that attracts industrial investors that have financial interest in reducing fuel costs as well as decreasing air pollutants from combustion processes. Although several reports underline promising outcomes in reducing air pollutants from boilers by using a micro-emulsion system, there is no credible evidence that this technology can reduce dioxin emissions these boilers. Overall, this study aims to quantify the reduction of dioxins and traditional emissions from industrial boilers as a result of applying the micro-emulsion system.

2. Experimental methodology

2.1. Descriptions of a sampling site

All samples were collected from an industrial boiler at the Red Bull Distillery Factory (RBDF) ($13^{\circ}36'58.97''N$, $100^{\circ}17'00.82''E$).

The RBDF is located within an industrial area of Tumbol Nadee, Muang District, Samutsakorn Province, which is located approximately 38 km southwest of Bangkok. Red Bull Distillery (1988) Co., Ltd. installed modern and highly efficient wastewater treatment plants that are capable of treating 270,000 cubic liters of wastewater per year. The treated water is reused within the premises. Many waste products are also recycled. For instance, the by-product from molasses is used to produce bionic fertilizer, the reconditioned solid whiskey residue is used in place of chemical fertilizer in rice fields and the liquid residue, when treated, will produce methane gas that is used as a supplementary fuel in place of bunker oil to save energy. The RBDF is also the first liquor and alcohol producer in Thailand to receive ISO 9001 GMP and HACCP certification with a policy that is responsible towards society and the environment, including its continuous contribution to the public. In this study, the steam boiler STANDARDKESSEL ITALIANA Condor Classic, which is a pressurized boiler at effectively three smokes passes and a completely wet back, was employed with the assistances of fire tube (Weishaupt RMS 70/1A with 700 HP). Additionally, this steam boiler uses 1500 Fuel Oil 1500 (FOLS#2) C for producing steam 10.300 KG h^{-1} .

2.2. Micro-emulsion system

The principal aims of micro-emulsion system are to generate small fuel droplets, generally 2–100 nm in diameter, of a non-continuous phase mixture of a surfactant and water based fuel; and to eventually lead to a unique opportunity in fuel flexibility and engine performance (i.e., the ability to replace conventional fuel combustion properties coupled with the ability to substitute up to 25% alternative fuels such as alcohol). In this study, the micro-emulsion system (MEC Marine) was selected because of its capability to improve the combustion efficiency by exponentially enhancing the surface availability for the oxidation of the identical fuel (Fig. 1). Since a better combustion of fuel with lower hydrocarbon chains lead to less air pollutant emissions, it was expected that an industrial boiler combined with micro-emulsion system could have lower PCDD/PCDF emissions. In addition, an alcohol-feeding circuit, an additive-feeding circuit for more than 12%, a control panel, and a static mixer were employed for this study, as an extension of the standard machinery assembled on the industrial boiler. It should be noted that electrostatic precipitators (EPS) had been implicated in the formation of PCDD/PCDFs [25]. Therefore, air pollution control system (APC) was terminated during the experiment.

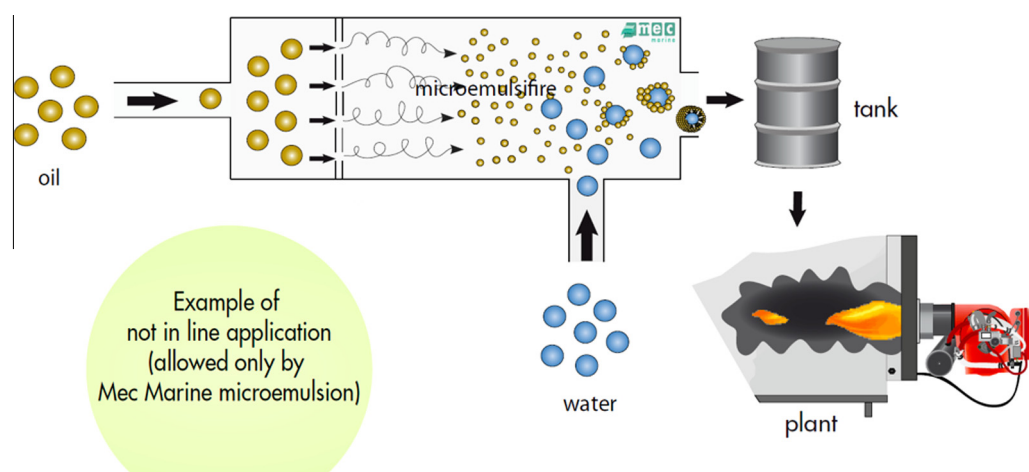


Fig. 1. Schematic diagram of MEC marine micronization processes.

Table 1

Statistical descriptions of trace gaseous species, TSP, and PCDD/PCDFs emitted from three types of fuels.

Fuel type	HFO (n = 3)		HFO + ethanol (n = 3)		HFO + water (n = 3)		ANOVA test (p < 0.05)
	Aver	Stdev	Aver	Stdev	Aver	Stdev	
Sampling period	15/08/12–17/08/12		29/04/15–01/05/15		06/05/15–08/05/15		
SO ₂ (ppm)	178	57.9	335	29.9	413	160	NS
NO _x as NO ₂ (ppm)	107	4.90	208	11.7	252	21.2	S
CO (ppm)	1.73	0.418	33.7	40.2	7.83	2.32	NS
TSP (mg Sm ⁻³)	79.0	26.5	144	52.9	84.0	10.3	NS
Total PCDD/PCDF (ng Sm ⁻³)	0.733	0.519	0.186	0.0318	0.809	1.30	NS
Total I-TEQ (ng I-TEQ Sm ⁻³)	0.00457	0.00486	0.00360	0.000755	0.0170	0.0224	NS
<i>Determination of PCDD/PCDFs (ng Sm⁻³)</i>							
1. Total PCDD/PCDF							
1.1 Total PCDD	0.133	0.0231	0.0113	0.0370	0.697	1.13	
(1) TCDDs	0.0963	0.112	0.0620	0.0269	0.248	0.393	NS
(2) PeCDDs	0.0180	0.00721	0.00700	0.00361	0.160	0.258	NS
(3) HxCDDs	0.0100	0.00173	0.0350	0.00346	0.223	0.299	NS
(4) HpCDDs	0.00867	0.00551	0.00933	0.00321	0.211	0.276	NS
(5) OCDD	<0.025	ND	>0.033	ND	<0.015	ND	S
1.2 Total PCDF	0.600	0.712	0.0727	0.0756	0.112	0.0447	
(1) TCDFs	0.198	0.0332	0.0330	0.00436	0.0423	0.0656	S
(2) PeCDFs	0.0443	0.0265	0.0267	0.00208	0.0557	0.0852	NS
(3) HxCDFs	0.0667	0.0914	0.0103	0.00493	0.0210	ND	NS
(4) HpCDFs	0.130	0.179	0.00800	0.00800	0.0210	ND	NS
(5) OCDF	0.161	0.186	<0.033	ND	<0.021	ND	NS
Total dioxin	0.733	0.519	0.186	0.0318	0.809	1.30	NS
<i>Determination of PCDD/PCDFs (ng Sm⁻³)</i>							
1.3 Total I-TEQ							
(1) 2,3,7,8-TCDD	0.000467	0.0000516	0.000667	0.000175	0.00175	0.00186	NS
(2) 1,2,3,7,8-PeCDD	0.000467	0.0000516	0.000700	0.000514	0.00165	0.00194	NS
(3) 1,2,3,4,7,8-HxCDD	0.000100	ND	0.000433	0.000769	0.000167	0.000103	NS
(4) 1,2,3,6,7,8-HxCDD	0.000100	ND	0.000433	0.000769	0.000233	0.000207	NS
(5) 1,2,3,7,8,9-HxCDD	0.000100	ND	0.000450	0.000761	0.000200	0.000155	NS
(6) 1,2,3,4,6,7,8-HpCDD	0.0000633	0.0000288	0.00133	0.00312	0.0000717	0.0000319	NS
(7) OCDD	0.0000233	0.00000516	0.00652	0.0159	0.0000200	ND	NS
(8) 2,3,7,8-TCDF	0.000233	0.000103	0.000883	0.00168	0.000933	0.00129	NS
(9) 1,2,3,7,8-PeCDF	0.0000967	0.0000585	0.000467	0.000898	0.000383	0.000478	NS
(10) 2,3,4,7,8-PeCDF	0.00120	0.000620	0.00135	0.000423	0.00502	0.00715	NS
(11) 1,2,3,4,7,8-HxCDF	0.000733	0.000907	0.000667	0.00109	0.000433	0.000516	NS
(12) 1,2,3,6,7,8-HxCDF	0.000667	0.000804	0.00100	0.00143	0.000400	0.000465	NS
(13) 2,3,4,6,7,8-HxCDF	0.000383	0.000440	0.000917	0.00146	0.000267	0.000258	NS
(14) 1,2,3,7,8,9-HxCDF	0.000167	0.000103	0.000433	0.000769	0.000100	ND	NS
(15) 1,2,3,4,6,7,8-HpCDF	0.000617	0.000801	0.00145	0.00331	0.0000600	0.0000322	NS
(16) 1,2,3,4,7,8,9-HpCDF	0.000242	0.000242	0.00131	0.00313	0.0000367	0.0000103	NS
(17) OCDF	0.000167	0.000147	0.00652	0.0159	0.0000200	ND	NS

Remarks: S, NS, and ND stand for significance, non-significance, and not determined respectively.

Sm³ = dry standard cubic meter for gas condition means at temperature of 20 °C, pressure of 1 atm and dry basis (United States Region).

I-TEQ (international toxicity equivalence) = the value is calculated by using the toxicity equivalence factors (TEF).

2.3. Sample collection and trace gaseous data

As far as the analysis of PCDD/PCDFs is concerned, the air emission monitoring was based on U.S. EPA Method-23/HRGC-HRMS (High Resolution Gas Chromatography/High Resolution Mass Spectrometry), with 10 h sampling time, while U.S. EPA Method-2/S-Type Pitot Tube was used for the sampling of temperature, pressure, velocity, and flow rate. U.S. EPA Method-4/Condensate Technique and Portable Detector (Portable Flue Gas Analyzer System TESTO 350) were applied for the measurement of moisture content and trace gaseous species (i.e. Oxygen (O₂), Carbon Monoxide (CO), Carbon Dioxide (CO₂), Sulfur Dioxide (SO₂), and Oxide of Nitrogen (NO_x)), respectively. In this study, Apex Isokinetic Source Sampling Systems (AISSS) was selected for extracting a representative flue gas sample from a source to determine dust and fumes emissions in accordance with U.S. EPA 23 Reference Methods. This system was constructed of nozzles, probes and liners, glassware, consoles, modular sample cases, umbilicals, and pumps. AISSS allows the operator to monitor gas velocities, temperatures, pressures and adjust sample flow rates to obtain a representative flue gas sample. The samplings of PCDD/PCDFs were conducted running

the boiler with three different fuel types namely 100% HFO without microemulsion device (100% HFO), 90% HFO coupled with 10% ethanol (90% HFO-10% ethanol), and 90% HFO coupled with 10% water (90% HFO-10% water), both with the Mec Marine microemulsion device installed, at three distinctive monitoring periods, which were 15/08/2012–17/08/2012, 29/04/2015–01/05/2015, and 06/05/2015–08/05/2015, respectively.

2.4. Chemicals analysis of PCDD/PCDFs

All chemical analyses of the PCDD/PCDFs were conducted at SGS environmental laboratories that have ISO 17025 accreditations and demonstrate the effectiveness to properly execute testing methods practices, inspection routines, data validation and employee competences. ISO 17025 is an international standard, which sets the general requirements for the competence of testing and calibration laboratories. In this study, 17 congeners of PCDD/PCDFs were qualitatively and quantitatively analyzed to include the following: 2,3,7,8-TCDD, 1,2,3,7,8-PeCDD, 1,2,3,4,7,8-HxCDD, 1,2,3,6,7,8-HxCDD, 1,2,3,7,8,9-HxCDD, 1,2,3,4,6,7,8-HpCDD, OCDD, 2,3,7,8-TCDF, 1,2,3,7,8-PeCDF, 2,3,4,7,8-PeCDF, 1,2,3,4,7,8-HxCDF,

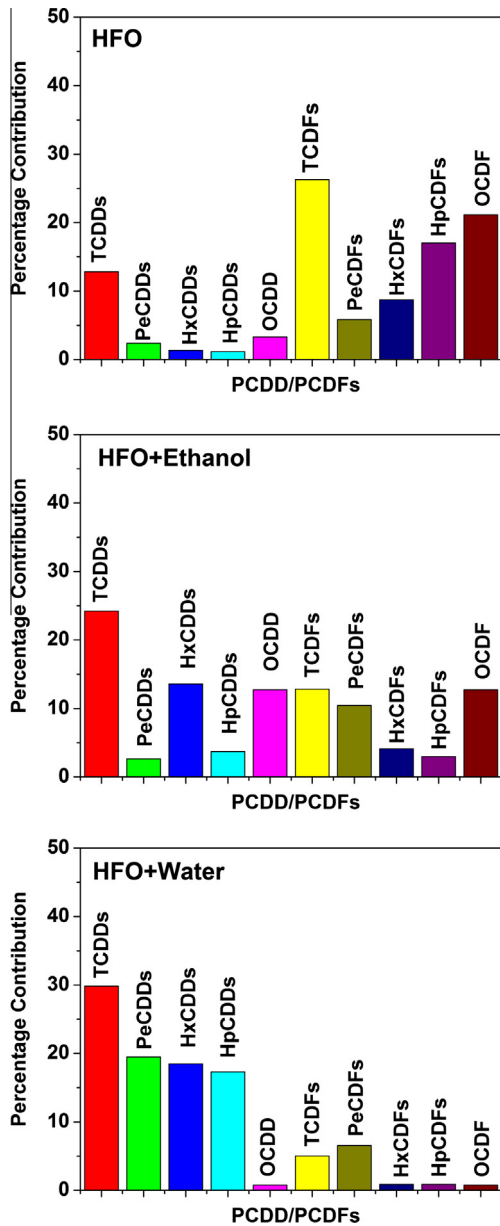


Fig. 2. Percentage contribution of each PCDD/PCDFs congener from three different fuel types.

1,2,3,6,7,8-HxCDF, 2,3,4,6,7,8-HxCDF, 1,2,3,7,8,9-HxCDF, 1,2,3,4,6,7,8-HpCDF, 1,2,3,4,7,8,9-HpCDF, and OCDF. A clear description for dioxin analysis is given in Table S1A as a flowchart. In addition, the QA/QC requirements for exhaust air measurements were as follows: (i) the isokinetic rate must be examined, and the result must be during 90–110%; (ii) the sampling equipment must be checked for leaks and proper calibration; (iii) the sample control using chain of custody (COC) form must be used for sample delivery and control to and within the laboratory; and (iv) field blank to checks to determine any contamination must be conducted. In addition, the QA/QC examinations of the analyses were conducted by calculating blanks and recoveries as clearly described in Table S1B. The average recovery rate of ^{13}C labeled 2,3,7,8-chlorine substituted dioxins was $81.7 \pm 9.38\%$. The precisions and accuracies were assured by using NIST (National Institute of Standards and Technology)-SRM (Standard Reference Material)-1649b urban dust. In addition, two HRGC–HRMS namely Waters Autospec Premier and Waters Autospec Ultima were used in this study.

3. Results

Table 1 summarizes the concentrations of the selected 17 PCDD/PCDF congeners measured in the nine samples with three different conditions taken from an industrial boiler stack at the RBDF, as previously mentioned in Section 2.3. The statistical description of the PCDD/PCDF congeners at each condition shows a wide range of mass concentrations. The average concentrations of the PCDD/PCDF congeners range from $7.00 \times 10^{-3} \pm 3.61 \times 10^{-3}$ ng Sm $^{-3}$ to $2.48 \times 10^{-1} \pm 3.93 \times 10^{-1}$ ng Sm $^{-3}$ for PeCDDs and TCDDs, respectively. Further investigation was conducted by calculating percentage contribution of each congener to its total dioxin concentrations with three different fuel types. The most abundant congeners in the 100% HFO condition were TCDFs ($1.98 \times 10^{-1} \pm 3.32 \times 10^{-2}$ ng Sm $^{-3}$), OCDF ($1.61 \times 10^{-1} \pm 1.86 \times 10^{-1}$ ng Sm $^{-3}$), HpCDFs ($1.30 \times 10^{-1} \pm 1.79 \times 10^{-1}$ ng Sm $^{-3}$), and TCDDs ($9.63 \times 10^{-2} \pm 1.12 \times 10^{-2}$ ng Sm $^{-3}$), with the contribution in the order of 26.3%, 21.2%, 17.0%, and 12.8% (Table 1 and Fig. 2). It is evident that PCDF congeners were almost entirely associated with the 100% HFO condition. On the contrary, the main compositions of dioxin congeners observed in 90% HFO–10% ethanol condition were TCDDs ($6.20 \times 10^{-2} \pm 2.69 \times 10^{-2}$ ng Sm $^{-3}$), HxCDDs ($3.50 \times 10^{-2} \pm 3.46 \times 10^{-3}$ ng Sm $^{-3}$), OCDD ($>3.30 \times 10^{-2}$ ng Sm $^{-3}$), TCDFs ($3.30 \times 10^{-2} \pm 4.36 \times 10^{-3}$ ng Sm $^{-3}$), OCDF ($<3.30 \times 10^{-2}$ ng Sm $^{-3}$), and PeCDFs ($2.67 \times 10^{-2} \pm 2.08 \times 10^{-3}$ ng Sm $^{-3}$) with percentage contributions of 24.2%, 13.6%, 12.8%, 12.8%, and 10.5%, respectively (see Fig. 2). These results were in partly good agreement with those of 90% HFO–10% water condition, which are responsible for the emissions of TCDDs ($2.48 \times 10^{-1} \pm 3.93 \times 10^{-1}$ ng Sm $^{-3}$), PeCDDs ($1.60 \times 10^{-1} \pm 2.58 \times 10^{-1}$ ng Sm $^{-3}$), HxCDDs ($2.23 \times 10^{-1} \pm 2.99 \times 10^{-1}$ ng Sm $^{-3}$), and HpCDDs ($2.11 \times 10^{-1} \pm 2.76 \times 10^{-1}$ ng Sm $^{-3}$) with percentage contributions of 29.8%, 19.5%, 18.5%, and 17.3%, respectively. It is reasonable to conclude that the micro-emulsion system dramatically changed the abundant patterns of PCDD/PCDF congeners. In addition, it is important to clarify that the fuel flow rates had not been measured and thus some uncertainties on exact flow rates still remain. As a consequence, it would be safe to apply the emission factors for the evaluations of PCDD/PCDFs reduction efficiencies using three different types of fuels. The emission factors (EFs) of PCDD/PCDFs calculated by using 100% HFO, 90% HFO–10% ethanol, and 90% HFO–10% water were $1.60 \mu\text{g TEQ TJ}^{-1}$, $0.58 \mu\text{g TEQ TJ}^{-1}$, and $0.50 \mu\text{g TEQ TJ}^{-1}$, respectively. It is also worth mentioning that the emissions per year of PCDD/PCDFs using 100% HFO, 90% HFO–10% ethanol, and 90% HFO–10% water were $129 \mu\text{g TEQ year}^{-1}$, $49.1 \mu\text{g TEQ year}^{-1}$, and $37.8 \mu\text{g TEQ year}^{-1}$, respectively. The environmental benefits of using micro-emulsion system is quite evident based on the comparatively low EFs of PCDD/PCDFs using 90% HFO–10% ethanol and 90% HFO–10% water, highlighting that micro-emulsions are a real promising technology to reduce pollutants.

4. Discussion

Although the micro-emulsion system appears to be responsible for higher percentage contributions to PCDD congeners, the mixture of 90% HFO–10% ethanol shows significantly ($p < 0.05$) lower emission concentrations of TCDDs, PeCDDs, HpCDDs, TCDFs, and PeCDFs due to its comparatively lower hydrocarbon combustions compared with those of 100% HFO (see Table 1).

Several reasons might have been responsible for this finding. Firstly, ethanol used in this study was produced from molasses by fermentation. Generally, molasses have 50–55% concentration of sugar in the form of sucrose. Although molasses could be a chlorine source, previous studies found that the chlorine concentrations in the ethanol samples were below the detection limits of

Table 2

Statistical descriptions of diagnostic binary ratios of trace gaseous species and PCDD/PCDFs emitted from three types of fuels.

Fuel type	HFO (n = 3)		HFO + ethanol (n = 3)		HFO + water (n = 3)		ANOVA test (p < 0.05, p < 0.1)
	Aver	Stdev	Aver	Stdev	Aver	Stdev	
Sampling period	15/08/12–17/08/12		29/04/15–01/05/15		06/05/15–08/05/15		
SO ₂ /CO	102.88	41.60	9.94	11.89	52.70	25.67	S, S
NO _x /CO	61.92	15.20	6.17	7.37	32.17	9.89	S, S
SO ₂ /NO _x	1.66	0.54	1.61	0.17	1.64	0.65	NS, NS
TCDDs/PeCDDs	5.38	2.08	8.65	3.79	1.55	3.13	NS, S
TCDDs/HxCDDs	9.55	1.85	2.10	0.62	1.67	3.42	S, S
TCDDs/HpCDDs	11.08	6.51	6.89	2.56	1.76	3.58	NS, S
TCDDs/OCDD	3.82	0.53	2.17	0.72	11.85	16.96	NS, NS
PeCDDs/HxCDDs	1.78	0.71	0.24	0.08	1.08	2.23	NS, NS
PeCDDs/HpCDDs	2.06	1.41	0.80	0.32	1.14	2.33	NS, NS
PeCDDs/OCDD	0.71	0.27	0.25	0.09	7.65	11.12	NS, NS
HxCDDs/HpCDDs	1.16	0.69	3.28	0.80	1.06	2.20	NS, NS
HxCDDs/OCDD	0.40	0.07	1.03	0.18	7.11	10.68	NS, NS
HpCDDs/OCDD	0.34	0.20	0.32	0.09	6.73	9.93	NS, NS
TCDFs/PeCDFs	4.49	2.53	1.20	0.18	0.75	1.46	NS, S
TCDFs/HxCDFs	2.98	3.68	3.33	1.30	5.16	9.70	NS, NS
TCDFs/HpCDFs	1.53	1.91	4.16	0.61	4.22	7.01	NS, NS
TCDFs/OCDF	1.23	1.29	0.90	0.19	2.00	2.85	NS, NS
PeCDFs/HxCDFs	0.66	0.89	2.76	1.04	6.91	12.72	NS, NS
PeCDFs/HpCDFs	0.34	0.46	3.45	0.36	5.65	9.14	NS, NS
PeCDFs/OCDF	0.27	0.32	0.75	0.14	2.68	3.68	NS, NS
HxCDFs/HpCDFs	0.51	0.90	1.25	0.47	0.82	1.25	NS, NS
HxCDFs/OCDF	0.41	0.67	0.27	0.11	0.39	0.49	NS, NS
HpCDFs/OCDF	0.81	1.30	0.22	0.04	0.47	0.43	NS, NS

Remarks: S and NS stand for significance and non-significance respectively.

the method [1,17]. The best efficiency for reducing dioxin emission by using the mixture of 90% HFO–10% ethanol might probably have been ascribed to the extremely low level of chlorine content in this fuel. Secondly, it is worth mentioning that chlorine has been used for many years in RBDF to treat industrial waters as a part of hygiene control procedure because of its capacity to inactive most pathogenic microorganisms. As a consequence, the formation of PCDD/PCDFs from chlorine content in the mixture of 90% HFO–10% water cannot be neglected. Thirdly, the micro-emulsion system operating condition might have somehow decreased the PCDD/PCDFs emissions and thus enhance the dioxin reducing efficiency. Fourthly, an earlier study indicated that the formation of dioxins depends strongly on the concentration of the precursor molecules [15], which is HFO for this case. Hence the fact that 100% HFO showed the highest PCDD/PCDF emissions was in good agreement with a previous study.

These results highlight the potential of the micro-emulsion system as an alternative technology for cleaner productions. Despite no significant differences observed in the emissions of NO_x and CO produced by three different fuel types, as shown in Table 1, the binary diagnostic ratio of NO_x/CO of 100% HFO significantly ($p < 0.05$) reveals the highest value, indicating more concern for generating nitro-Polycyclic Aromatic Hydrocarbons (nitro-PAHs) with a relatively high NO_x condition (Table 2). Previous studies found formations of nitro-PAHs from the heterogeneous reaction of ambient particle-bound PAHs with N₂O₅/NO₃/NO₂ [30], particularly formed via electrophilic nitration reactions in the presence with NO₂ from such combustion sources as diesel engines [12,10]. Because nitro-PAHs are highly toxic compounds, the fact that NO_x/CO emission ratios from the micro-emulsion system were significantly lower than those of 100% HFO indicates the importance of this clean technology for planning strategies for preventive medicine and sustainable industrial development.

As illustrated in Table 2, the diagnostic binary ratios of TCDDs/HxCDDs observed in 100% HFO were significantly higher than those of the micro-emulsion system. Both TCDDs and PeCDDs have comparatively high toxic equivalency factors (TEF) (i.e., 1 and 0.5 for TCDDs and PeCDDs, respectively), thus these findings have

raised concerns over the use of 100% HFO in industrial boilers. On the contrary, the combustion of the 90% HFO–10% water mixture exhibits the significantly lowest binary ratios of TCDDs/PeCDDs ($p < 0.1$), TCDDs/HxCDDs ($p < 0.05$), TCDDs/HpCDFs ($p < 0.1$), and TCDFs/PeCDFs ($p < 0.1$). These results imply that the HFO-alcohol-water mixture reduces the most toxic dioxin TCDD and decreases NO_x, which will subsequently lead to the formation of nitro-PAHs. It is also important to highlight that the binary ratios of HxCDDs/OCDD, PeCDFs/HxCDFs, PeCDFs/HpCDFs, and PeCDFs/OCDF emitted from the 100% HFO were comparatively lower than the other two types of fuels. However, the TEF values of HxCDDs and PeCDFs were 10 and 20 times lower than those of TCDD, thus the use of 100% HFO raises public health concerns over TCDD emissions.

The correlation coefficients (R -values) of I-TEQ of 17 PCDD/PCDF congeners obtained from the linear regression plots between 100% HFO vs. 90% HFO–10% ethanol, HFO + ethanol vs. HFO + water, and HFO vs. HFO + water were carefully investigated (see Fig. 3). The combination of HFO + ethanol vs. HFO + water showed the highest R -value of 0.900 with $p < 0.0001$, whilst those of HFO vs. HFO + water and HFO vs. HFO + ethanol indicated the lowest R -values of 0.328 ($p < 0.215$) and 0.560 ($p < 0.0229$), respectively. The strong positive correlation of PCDD/PCDF congeners emitted from the combustions of HFO + ethanol and HFO + water highlights the substantial similarities of dioxin distribution patterns from the micro-emulsion system. The fact that both R -values from HFO vs. HFO + water and HFO vs. HFO + ethanol were much lower than those of HFO + ethanol vs. HFO + water underlines discrepancies in the PCDD/PCDF distribution patterns caused by different combustion mechanisms. Consequently, fewer toxic dioxin congeners were produced with the assistances of the micro-emulsion system.

5. Conclusions

This study describes the effects of micro-emulsion system on the reduction of PCDDs and PCDFs from an industrial boiler. The results statistically demonstrated that effects of the addition of

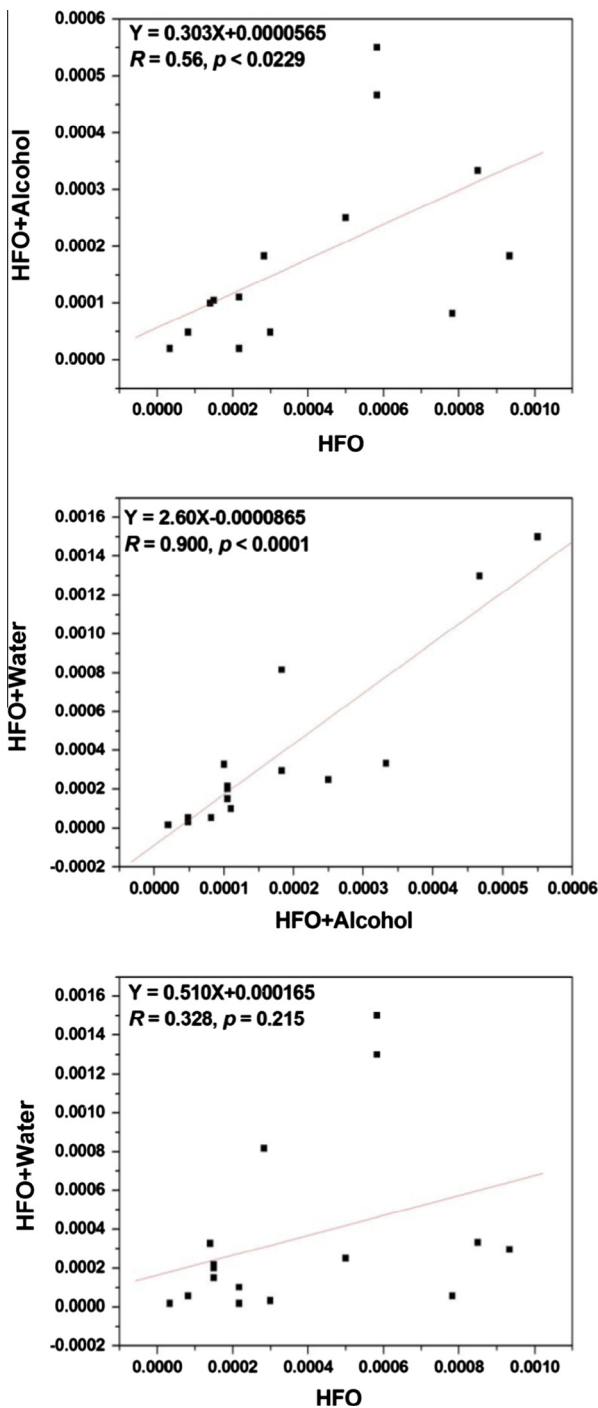


Fig. 3. Slopes, intercepts and correlation coefficients from linear regressions of each PCDD/PCDFs congener from HFO vs. HFO + alcohol, HFO + alcohol vs. HFO + water, and HFO vs. HFO + water.

either ethanol or water to heavy fuel oil changed PCDD/PCDF pattern in flue gases and also traditional gas component characteristics. This study may succeed in the analysis of PCDD/PCDF data of flue gases from an industrial boiler. However, it appears that the results obtained cannot be applied to other cases due to insufficient data regarding to effectiveness of micro-emulsion system in a wide range. In spite of the fact that the total I-TEQ value obtained from HFO + ethanol did not change very well compared to those of HFO-100%, it is rational to conclude that PCDD/PCDF congener can be changed by applying micro-emulsion system. One possible reason of the result is the concentration level of PCDD/PCDF was

extremely low. Overall, it seems reasonable to affirm that the application of micro-emulsion system highlights a potential reduction of PCDD/PCDF emissions from an industrial boiler, particularly in the case of the HFO + ethanol mixture, and that the micro-emulsion system can be a promising best available technology for decreasing PCDD/PCDF emissions from industrial boiler sector.

Acknowledgement

The authors acknowledge GEF (Global Environment Fund) for financial support of this project.

Appendix A. Supplementary material

Supplementary data associated with this article can be found, in the online version, at <http://dx.doi.org/10.1016/j.fuel.2016.01.003>.

References

- [1] Abrantes R, Assunção JV, Pesquero CR, Nóbrega RP, Bruns RE. Comparison of emission of dioxins and furans from gasohol- and ethanol-powered vehicles. *J Air Waste Manage Assoc* 2011;61(12):1344–52.
- [2] Alouis C, L'Insalata A, Fortunato L, Saponaro A, Beretta F. Study of water-oil emulsion combustion in large pilot power plants for fine particle matter emission reduction. *Exp Therm Fluid Sci* 2007;31(5):421–6.
- [3] Al-Sabagh AM, Emara MM, Noor El-Din MR, Aly WR. Formation of water-in-diesel oil nano-emulsions using high energy method and studying some of their surface active properties. *Egypt J Pet* 2011;20(2):17–23.
- [4] Ballester JM, Fueyo N, Dopazo C. Combustion characteristics of heavy oil-water emulsions. *Fuel* 1996;75(6):695–705.
- [5] Chang MB, Lee CH. Dioxin levels in the emissions from municipal waste incinerators in Taiwan. *Chemosphere* 1998;36(11):2483–90.
- [6] Dooher J, Genberg R, Moon S, Gilmarin B, Jakatt S, Skura J, et al. Combustion studies of water/oil emulsion on a commercial boiler using No. 2 oil and low and high sulphur No. 6 oil. *Fuel* 1980;59(12):883–92.
- [7] Everaert K, Baeyens J. The formation and emission of dioxins in large scale thermal processes. *Chemosphere* 2002;46(3):439–48.
- [8] Gui D, Yu R, He X, Tu Q, Chen L, Wu Y. Bioaccumulation and biomagnification of persistent organic pollutants in Indo-Pacific humpback dolphins (*Sousa chinensis*) from the Pearl River Estuary, China. *Chemosphere* 2014;114:106–13.
- [9] Hedman B, Naslund M, Marklund S. Emission of PCDD/F, PCB, and HCB from combustion of firewood and pellets in residential stoves and boilers. *Environ Sci Technol* 2006;40(16):4968–75.
- [10] Inomata S, Fushimi A, Sato K, Fujitani Y, Yamada H. 4-Nitrophenol, 1-nitropyrene, and 9-nitroanthracene emissions in exhaust particles from diesel vehicles with different exhaust gas treatments. *Atmos Environ* 2015;110:93–102.
- [11] Ishikawa R, Buekens A, Huang H, Watanabe K. Influence of combustion conditions on dioxin in an industrial scale fluidised-bed incinerator: experimental study and statistical modeling. *Chemosphere* 1997;35(3):465–77.
- [12] Karavalakis G, Bakeas E, Fontaras G, Stournas S. Effect of biodiesel origin on regulated and particle-bound PAH (polycyclic aromatic hydrocarbon) emissions from a Euro 4 passenger car. *Energy* 2011;36(8):5328–37.
- [13] Kawamoto K. Potential formation of PCDD/Fs and related bromine-substituted compounds from heating processes for ashes. *J Hazard Mater* 2009;168(2–3):641–8.
- [14] Lin CY, Wang KH. Diesel engine performance and emission characteristics using three-phase emulsions as fuel. *Fuel* 2004;83(4–5):537–45.
- [15] Milligan MS, Altwicker ER. Chlorophenol reactions on fly ash: 1. adsorption/desorption equilibria and conversion to polychlorinated dibenz-p-dioxins. *Environ Sci Technol* 1996;30(1):225–9.
- [16] Mura E, Massoli P, Josset C, Loubar K, Bellettre J. Study of the micro-explosion temperature of water in oil emulsion droplets during the Leidenfrost effect. *Exp Therm Fluid Sci* 2012;43:63–70.
- [17] Pereira EA, Tavares MFM, Stevanato A, Cardoso AA. Evaluation of inorganic and organic contaminants in alcohol fuel using capillary electrophoresis. *Quím Nova* 2006;29:66–71.
- [18] Peterson SH, Peterson MG, Debier C, Covaci A, Dírtu AC, Malarvannan G, et al. Deep-ocean foraging northern elephant seals bioaccumulate persistent organic pollutants. *Sci Total Environ* 2015;533:144–55.
- [19] Pongpiachan S. Application of cloud point extraction for the determination of pyrene in natural water. *Southeast Asian J Trop Med Public Health*. 2009;40(2):392–400.
- [20] Pongpiachan S, Choochay C, Hattayanone M, Kositanont C. Temporal and spatial distribution of particulate carcinogens and mutagens in Bangkok, Thailand. *Asian Pac J Cancer Prev* 2013;14(3):1879–87.
- [21] Pongpiachan S, Tipmanee D, Deelaman W, Muprasit J, Feldens P, Schwarzer K. Risk assessment of the presence of polycyclic aromatic hydrocarbons (PAHs) in

- coastal areas of Thailand affected by the 2004 tsunami. *Mar Pollut Bull* 2013;76:370–8.
- [22] Pongpiachan S. A preliminary study of using polycyclic aromatic hydrocarbons as chemical tracers for traceability in soybean products. *Food Control* 2015;47:392–400.
- [23] Pongpiachan S, Hattayanone M, Choochua C, Mekmok R, Wuttijak N, Ketratanakul A. Enhanced PM10 bounded PAHs from shipping emissions. *Atmos Environ* 2015;108:13–9.
- [24] Pongpiachan S, Tipmanee D, Khumsup C, Kittikoon I, Hirunyatrakul P. Assessing risks to adults and preschool children posed by PM2.5-bound polycyclic aromatic hydrocarbons (PAHs) during a biomass burning episode in Northern Thailand. *Sci Total Environ* 2015;508:435–44.
- [25] Ruuskanen J, Vartiainen T, Kojo I, Manninen H, Oksanen J, Frankenheuser M. Formation of polychlorinated dibenz-p-dioxins and dibenzofurans in co-combustion of mixed plastics with coal: exploratory principal component analysis. *Chemosphere* 1994;28(11):1989–99.
- [26] Sonne C, Gustavson K, Letcher RJ, Dietz R. Physiologically-based pharmacokinetic modelling of distribution, bioaccumulation and excretion of POPs in Greenland sledge dogs (*Canis familiaris*). *Environ Res* 2015;142:380–6.
- [27] U.S. EPA., 1997. Locating and estimating air emissions from sources of dioxins and furans. Office of air quality planning and standards, office of air and radiation, U.S. Environmental Protection Agency, Research Triangle Park, North Carolina 27711.
- [28] Weijts L, Briels N, Adams DH, Lepoint G, Das K, Blust R, et al. Bioaccumulation of organohalogenated compounds in sharks and rays from the southeastern USA. *Environ Res* 2015;137:199–207.
- [29] Zhang HJ, Ni YW, Chen JP, Zhang Q. Influence of variation in the operating conditions on PCDD/F distribution in a full-scale MSW incinerator. *Chemosphere* 2008;70(4):721–30.
- [30] Zimmermann K, Jariyasopit N, Simonich SLM, Tao S, Atkinson R, Arey J. Formation of nitro-PAHs from the heterogeneous reaction of ambient particle-bound PAHs with $N_2O_5/NO_3/NO_2$. *Environ Sci Technol* 2013;47(15):8434–42.

SHORT RESEARCH AND DISCUSSION ARTICLE

Assessment of selected metals in the ambient air PM₁₀ in urban sites of Bangkok (Thailand)

Siwatt Pongpiachan¹ · Akihiro Iijima²

Received: 19 July 2015 / Accepted: 24 November 2015
© Springer-Verlag Berlin Heidelberg 2015

Abstract Estimating the atmospheric concentrations of PM₁₀-bounded selected metals in urban air is crucial for evaluating adverse health impacts. In the current study, a combination of measurements and multivariate statistical tools was used to investigate the influence of anthropogenic activities on variations in the contents of 18 metals (i.e., Al, Sc, V, Cr, Mn, Fe, Co, Ni, Cu, Zn, As, Se, Cd, Sb, Ba, La, Ce and Pb) in ambient air. The concentrations of PM₁₀-bounded metals were measured simultaneously at eight air quality observatory sites during a half-year period at heavily trafficked roads and in urban residential zones in Bangkok, Thailand. Although the daily average concentrations of Al, V, Cr, Mn and Fe were almost equivalent to those of other urban cities around the world, the contents of the majority of the selected metals were much lower than the existing ambient air quality guidelines and standard limit values. The sequence of average values of selected metals followed the order of Al>Fe>Zn>Cu>Pb>Mn>Ba>V>Sb>Ni>As>Cr>Cd>Se>Ce>La>Co>Sc. The probability distribution function (PDF) plots showed sharp symmetrical bell-shaped curves in V and Cr, indicating that crustal emissions are the predominant sources of these

two elements in PM₁₀. The comparatively low coefficients of divergence (COD) that were found in the majority of samples highlight that site-specific effects are of minor importance. A principal component analysis (PCA) revealed that 37.74, 13.51 and 11.32 % of the total variances represent crustal emissions, vehicular exhausts and the wear and tear of brakes and tires, respectively.

Keywords Metals · PM₁₀ · Multivariate statistics · Enrichment factor · Bangkok

Introduction

During the past few years, there have been significant concerns over various potential adverse health effects of enhanced PM₁₀ levels in the urban atmosphere, which are mainly associated with anthropogenic activities. One of the many crucial aspects of the PM₁₀ study in ambient air is predominantly related to its mutagenicity and carcinogenicity (Pongpiachan 2013a, b; Pongpiachan et al. 2013, 2015a, b). Another interesting issue is deeply connected to the chemical compositions of metals in PM₁₀. Previous studies have indicated that the majority of metals favourably existed in finer particles because they possess lower densities and a larger surface area per volume unit and organic matter content (Charlesworth et al. 2003; Madrid et al. 2008; Yatkin and Bayram 2008a, b). Several studies have highlighted the adverse health impacts of exposure to ambient metals, such as lead (Rosen 1995), mercury (Ratcliffe et al. 1996), cadmium (Yang et al. 2014), chromium (Berardi et al. 2015), arsenic (Wang et al. 2014a, b) and vanadium (Zwolak 2014).

There is no current comprehensive study focusing on the PM₁₀-bounded heavy metals or a calculation of the enrichment factors in the urban atmosphere of Bangkok.

Responsible editor: Philippe Garrigues

✉ Siwatt Pongpiachan
pongpijun@gmail.com

¹ NIDA Center for Research and Development of Disaster Prevention and Management, School of Social and Environmental Development, National Institute of Development Administration (NIDA), 118 Moo 3, Sereethai Road, Klong-Chan, Bangkapi, Bangkok 10240, Thailand

² Department of Regional Activation, Faculty of Regional Policy, Takasaki City University of Economics, 1300 Kaminamie, Takasaki, Gunma 370-0801, Japan

Meanwhile, the majority of studies have highlighted the health risk assessment of total suspended particles (TSP) collected from a few air quality observatory sites in developed countries, but there is a lack of information on the metals in PM₁₀ collected simultaneously from multiple locations, particularly in Southeast Asian countries, which poses a greater health risk to residents. Consequently, it would be valuable to observe a series of data sources on the representative urban emissions of metals; this information would be crucial for the Pollution Control Department (PCD) to develop relevant air quality standards and for the scientific community to accumulate adequate baseline data for worldwide cities.

The main purpose of this study was to assess both the temporal and spatial distribution characteristics of selected metals in PM₁₀ collected from multiple PCD air quality observatory sites to evaluate their behaviour in Bangkok. In addition, the strength of crustal and non-crustal sources was carefully evaluated by applying the concept of enrichment factors coupled with statistical methods based on Pearson correlation coefficients, hierarchical cluster analysis (HCA) and principal component analysis (PCA) for determining and distinguishing the pollution sources and their contribution. Particulate metals have both natural sources and anthropogenic sources. Since the metal compositions of the two major sources (i.e. anthropogenic and natural sources) overlap, the impact of anthropogenic metals in the environment must be both quantitatively and qualitatively evaluated against a dynamic background of natural metals. This can be conducted by using numerous combinations of statistical techniques. For statistical treatment, multivariate statistical methods such as HCA and PCA are employed for the purpose of source apportionment. In this study, HCA was conducted for the qualitative classification of sources with the agglomerative hierarchical clustering method and the squared euclidean distance. In addition, the standardisation was not conducted for this study since standardisation is not always appropriate prior to the clustering (Milligan and Cooper 1987). PCA was performed with the Varimax rotation (only factors with eigenvalues >1) to quantitatively categorise a large number of emission sources into five principal components (PCs).

Materials and methods

Description of the air quality observatory sites and PM₁₀ sample collection

In this study, eight air quality observatory sites, namely Klongchan National Housing Authority (KHA; 13° 49' 11.761" N 100° 34' 33.190" E), Nonsreewitayakom High

School (NWS; 13° 42' 28.937" N 100° 32' 50.443" E), Singharaj Pitayakhom High School (SPS), Huakwang National Housing Authority (HHA; 13° 46' 41.720" N 100° 34' 06.760" E), Thonburi Power Substation (TPS; 13° 43' 39.205" N 100° 29' 11.776" E), Chokchai 4 Police Box (CPB; 13° 47' 33.474" N 100° 35' 45.879" E), Dindang National Housing Authority (DHA; 13° 46' 59.544" N 100° 32' 25.618" E) and Badindecha High School (BHS; 13° 46' 10.745" N 100° 36' 52.433" E), were carefully chosen for the investigation of selected metals in PM₁₀ (see Fig. 1). It is notable and should be underlined that CPB, DHA and TPS were positioned near traffic routes, while KHA, NWS, HHA, SPS and BHS were located at the residential zones. Therefore, CPB, DHA, TPS and KHA, as well as NWS, HHA, SPS and BHS can be considered representatives of "vehicular exhausts" and "urban residential background", respectively. Air sampling was conducted in 24-h periods at all air quality sites simultaneously once every month from January to June 2008 constructing a database of 48 individual air samples (i.e. 6×8=48). Graseby-Anderson high-volume air samplers TE-6001 were used to achieve unmanned 24-h samplings for PM₁₀. A total of 48 air samples were acquired using high-volume-yielding sample volumes of approximately 1632 m³ for each 24-h sample. PM₁₀ were collected on 20×25-cm Whatman glass fibre filters (GFFs) at a flow rate of approximately 1.133 m³ min⁻¹ (i.e. 40 cfm). A more comprehensive explanation of the air sampling method was given in "Compendium Method IO-2.2. Sampling of ambient air for PM₁₀ using an Andersen Dichotomous Sampler". In addition, all of the information of 11 meteorological parameters was provided by PCD, and the abbreviations, namely Rain, CO, WS, SO₂, O₃, NO₂, T, RH, Rad, WD and P, represent precipitation, carbon monoxide, wind speed, sulphur dioxide, ozone, nitrogen dioxide, ambient temperature, relative humidity, solar radiation, wind direction and atmospheric pressure, respectively.

Analysis of selected metals

Sample preparation and analytical procedure were described in detail in the previous studies (Iijima et al. 2009, 2010). Briefly, sample-loaded filters were placed into PTFE vessels and digested in a mixture of 2 mL of hydrofluoric acid (50 % atomic absorption spectrometry grade; Kanto Chemical Co. Inc.), 3 mL of nitric acid (60 % electronic laboratory grade; Kanto Chemical Co. Inc.) and 1 mL of hydrogen peroxide (30 % atomic absorption spectrometry grade; Kanto Chemical Co. Inc.) in a microwave digestion system (Multiwave; Anton Parr GmbH). The microwave oven was operated under the condition of 700 W for 10 min and 1000 W for a further 10 min. Hydrofluoric acid was evaporated by heating the sample solutions at 200 °C on a hot plate. The digested solutions were further diluted with 0.1 mol L⁻¹ nitric

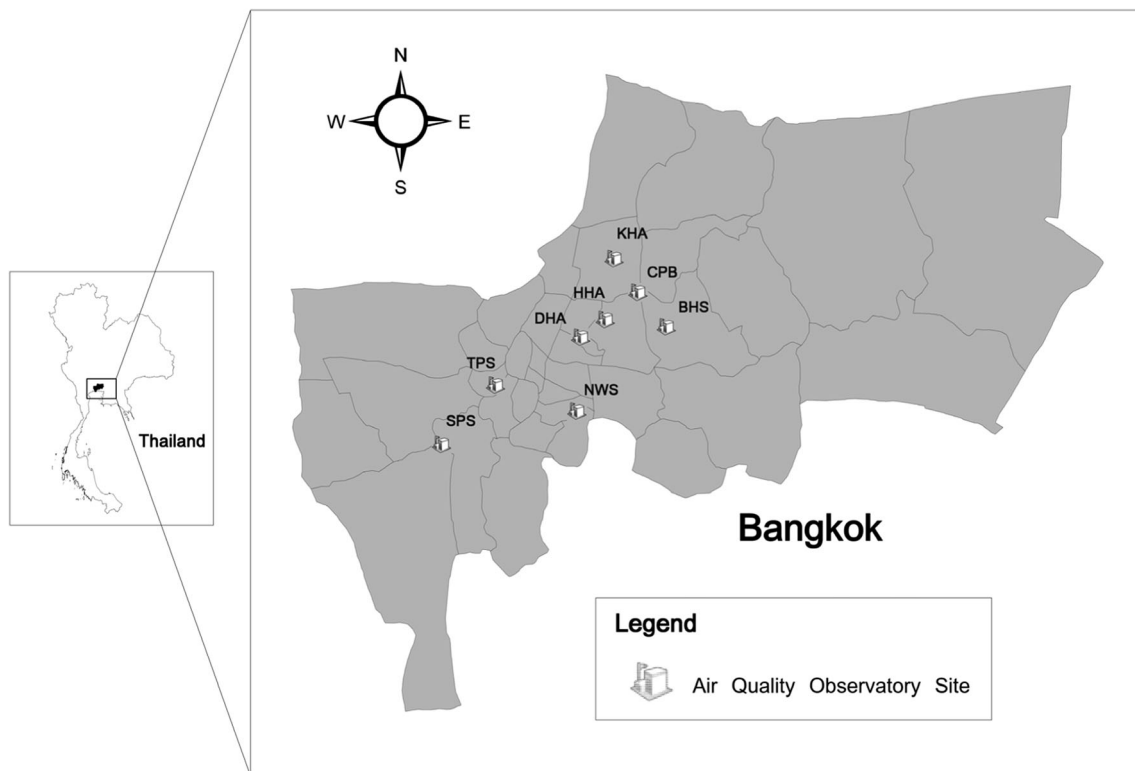


Fig. 1 A map of eight air quality observatory sites in Bangkok

acid (prepared from 60 % nitric acid) and added to obtain a 50-mL sample. The concentrations of Al, Sc, V, Cr, Mn, Co, Ni, Cu, Zn, As, Se, Cd, Sb, Ba, La, Ce and Pb were determined by inductively coupled plasma mass spectrometry (Agilent 7500cx, Agilent Technologies Inc.). All the analytical procedures were validated by using the standard reference material (SRM) 1648 (urban particulate matter) that was prepared by the US National Institute of Standard and Technology (NIST). The analytical results were in good agreement with the certified or reference values.

Statistical analysis

In an attempt to evaluate the fate of trace metals as measured in PM₁₀, an analysis of variance (ANOVA), hierarchical cluster analysis (HCA) and principal component analysis (PCA) with Varimax rotation (v. 13.0 SPSS Inc., Chicago, IL, USA) were performed on the dataset. PCA has been used extensively in receptor modelling to classify the main potential source categories influencing a provided receptor site. This statistical analysis functions on sample-to-sample variations of the normalised atmospheric concentrations. PCA does not straightforwardly gain concentrations of selected metals from numerous potential sources but ascertains a minimum number of common factors whose variance often explains most of the variance in the species.

Results and discussion

Comparison of PM₁₀-bounded selected metal concentrations

The 24-h concentrations of particulate Al, Sc, V, Cr, Mn, Fe, Co, Ni, Cu, Zn, As, Se, Cd, Sb, Ba, La, Ce and Pb are listed in Table 1. In general, all of the concentrations of selected metals were above the detection limit. Atmospheric Al had the highest daily average concentration of $1047 \pm 785 \text{ ng m}^{-3}$, with concentrations ranging between 193 and 2946 ng m^{-3} . Fe was the second most abundant species in the atmosphere, with a daily average concentration of $951 \pm 572 \text{ ng m}^{-3}$. The atmospheric concentrations of Zn ranged between 39 and 930 ng m^{-3} . Cu, Pb and Mn also had comparatively high concentrations in the atmosphere, with daily average levels of 98.6 ± 57.8 , 53.5 ± 50.8 and $35.3 \pm 26.0 \text{ ng m}^{-3}$, respectively. The maximum concentration that was recorded for Cu was 295 ng m^{-3} , while Pb had a maximum level of 253 ng m^{-3} . Sc presented the lowest atmospheric concentrations, reaching an average concentration that was 5817 times lower than that of Al and 5283 times lower than that of Fe. Co presented similarly low concentrations. To globally evaluate the PM₁₀-bounded selected metal concentrations as measured in Bangkok, the statistical descriptions of the 18 selected metals of the present study were compared with a selection of previous studies in similar environments (see Table 1). Despite

Table 1 Statistical description of PM₁₀-bound heavy metals (ng m⁻³)

	Annual standard limit	This study	Spain ^a		Korea ^b		China ^c		Brazil ^d		Italy ^e		Denmark ^f		Sweden ^g				
			Zaragoza		R1	R2	R3	Baoshan	Putuo	Bonsucesso	Botafogo	BD	ID	GG	DB	Odense	Tange	Stockholm	
			Aver	Stdev	Aver	Stdev	Aver	Aver	Stdev	Aver	Stdev	Aver	Stdev	Aver	Stdev	Aver	Aver	Stdev	
Al	1047	785	2690	3180	N.A.	N.A.	3712	2315	3115	3.232	N.A.	N.A.	1132	757	455	940	N.A.	N.A.	
Sc	0.180	0.159	N.A.	N.A.	N.A.	N.A.	N.A.	N.A.	N.A.	N.A.	N.A.	N.A.	N.A.	N.A.	N.A.	N.A.	N.A.	N.A.	
V	1000 ^h	7.09	3.14	6.56	9.17	N.A.	N.A.	N.A.	N.A.	5.87	0.04	1.50	0.01	10	22	17	22	5.0	2.8
Cr	2.5×10 ⁷	5.73	3.27	7.70	4.94	14.1	4.9	10.1	56	0.044	22	0.015	24.1	0.2	0.48	0.01	3.1	3.9	
Mn	150 ^h	35.3	26.0	24.7	16.4	86.0	36.1	52.2	189	0.140	92	0.058	37.7	0.1	12.4	0.2	6.6	9.3	
Fe		951	572	666	396	2574	755	1235	6827	3.910	2660	3.49	2363	29	115	10	298	299	
Co		0.406	0.454	0.128	0.331	N.A.	N.A.	N.A.	N.A.	0.40	0.02	0.091	0.002	0.2	0.3	0.2	0.3	N.A.	
Ni	20 ^h	6.46	6.01	0.833	1.22	16.6	6.8	11.3	32	0.029	11	0.012	3.56	0.07	0.35	0.02	4.6	3.7	
Cu		98.6	57.8	22.8	10.6	205	125	226	41	0.024	22	0.011	57.6	0.2	10.6	0.4	9.9	24	
Zn		236	144	212	220	N.A.	N.A.	N.A.	N.A.	0.415	303	0.177	115	1	46	2	17	35	
As	6 ^h	6.12	4.59	N.A.	N.A.	N.A.	N.A.	N.A.	N.A.	N.A.	N.A.	N.A.	N.A.	N.A.	1.8	1.8	1.3	1.4	
Se		2.66	2.71	N.A.	N.A.	N.A.	N.A.	N.A.	N.A.	N.A.	N.A.	N.A.	N.A.	N.A.	N.A.	N.A.	N.A.	N.A.	
Cd	5 ^{h, i}	4.16	19.8	N.A.	4.6	1.2	5.5	3	0.003	2	0.001	0.54	0.02	0.10	0.05	N.A.	N.A.	0.7	
Sb		6.73	6.14	N.A.	N.A.	N.A.	N.A.	N.A.	N.A.	N.A.	N.A.	N.A.	N.A.	N.A.	3.3	6.7	7.4	19	
Ba		34.6	27.2	33.1	38.8	N.A.	N.A.	N.A.	N.A.	N.A.	N.A.	N.A.	N.A.	N.A.	23	22	25	43	
La		0.683	0.522	N.A.	N.A.	N.A.	N.A.	N.A.	N.A.	N.A.	N.A.	N.A.	N.A.	N.A.	N.A.	N.A.	N.A.	N.A.	
Ce		1.37	1.12	N.A.	N.A.	N.A.	N.A.	N.A.	N.A.	N.A.	N.A.	N.A.	N.A.	N.A.	N.A.	N.A.	N.A.	N.A.	
Pb	500 ^{h, i, k}	53.5	50.8	18.7	25.6	110	47.1	59.3	137	0.117	71	0.069	18.8	0.2	2.05	0.09	9.8	20	
		150 ⁱ																	

^aLópez et al. (2005)^bLee et al. (2006) (*R1* Seoul, Incheon, Suwon, *R2* Deajon, Jeonju, *R3* Deagu, Ulsan, Pusan)^cWang et al. (2013)^dSilva et al. (2015)^eDongarrà et al. (2007) (*BD* Boccadifalco, *ID* Indipendenza, *GC* Giulio Cesare, *DB* Di Blasi)^fKemp (2002)^gJohansson et al. (2009)^hEuropean Commission Air Quality StandardsⁱWHO air quality guidelines for Europe^jNational Ambient Air Quality Standards of the US Environmental Protection Agency^kNational Air Quality Act of the South African Department of Environmental Affairs

some discrepancies with the PM₁₀ monitoring periods and frequencies, it appears reasonable to contextualise the selected metal concentrations as measured at PCD air quality observatory sites in Bangkok. As indicated in Table 1, the daily average concentrations of Al, V, Cr, Mn and Fe were comparable with those of Boccadifalco (Dongarrà et al. 2007), Zaragoza (López et al. 2005), Odense (Kemp 2002), Deajon, Jeonju and Kwangju (Lee et al. 2006), and Di Blasi (Dongarrà et al. 2007), respectively. In addition, the daily average concentrations of V, Cr, Mn, Ni and Pb were much lower than the existing ambient air quality guidelines and standard limit values for trace metal species (the WHO air quality guidelines for Europe, the European Commission Air Quality Standards, the National Ambient Air Quality Standards of the US EPA and the National Air Quality Act of the South African Department of Environmental Affairs) European Commission Air Quality Standards (2012).

Pearson correlation analysis

The average values of the selected trace elements analysed followed the order Al>Fe>Zn>Cu>Pb>Mn>Ba>V>Sb>Ni>As>Cr>Cd>Se>Ce>La>Co>Sc. The three maximum concentrations that were obtained from this study (i.e. Al, Fe and Zn) were similar to those of Zaragoza (López et al. 2005), Boccadifalco, Indipendenza, Giulio Cesare and Di Blasi (Dongarrà et al. 2007) but different from those of Baoshan (Wang et al. 2013). Several trace elements that were obtained from this study were primarily associated with the unique geographic location of Bangkok specifically and to the Chao Phraya Delta in general. While Al, Sc, V, Mn, Fe, As and Ba are plausibly from the impact of the closeness of the Asian continent and the crustal elements, Cr, Co, Ni, Cu, Zn and Cd are believed to be from anthropogenic inputs, mainly vehicular exhausts. This data interpretation is based on a detailed investigation of airborne trace metals and their potential major sources at Lhasa, the largest city in the Tibetan Plateau (Cong et al. 2011). Selected elements in the studied area followed a decreasing order of Fe>Zn>Cu>Cd, which was also consistent with a previous study of surface dust samples that were collected from the walls of residential buildings in Phitsanulok, Thailand (Srithawirat and Latif 2015), highlighting the fact that these four elements were predominantly associated with elemental crust.

In general, a high correlation coefficient between Fe and Zn indicates pollution emissions associated with human activities, incineration, imperfect combustion of hydrocarbon fuels or merely from natural sources (Gao et al. 2002). Because the correlation coefficient of these two elements was comparatively low ($R=0.20$), it appears reasonable to consider geographical input as a major source of Fe and Zn (Table 2). This interpretation agrees well with the relatively high positive correlation coefficients of Fe–Al ($R=0.95$), Fe–Sc ($R=0.95$), Fe–Cr ($R=0.81$), Fe–As ($R=0.91$), Fe–Ba ($R=0.71$) and Fe–Mn

($R=0.97$), indicating the predominance of crustal emissions on these elements over other sources (Table 2). In addition, the weak correlation coefficients of Ni–Pb ($R=-0.08$), Ni–Cr ($R=-0.03$) and Ni–Fe ($R=-0.23$) indicate that industrial activities are of minor importance because these metals are chemical markers of industrial emissions (Begum et al. 2004; Song et al. 2006; Yatkin and Bayram 2008a, b).

Spatial and temporal distribution of selected metals

To evaluate the spatial and temporal distribution of selected metals, the probability distribution function (PDF) was applied to all samples collected from the eight air quality observatory sites from January to June 2008, as previously mentioned in “Description of the air quality observatory sites and PM₁₀ sample collection”. The PDF is a function that describes the relative probability of this random variable taking on a provided value. The probability of a random variable falling within a particular region is given by the Gaussian distribution, which can be described as follows:

$$y = \frac{1}{\sigma\sqrt{2\pi}} \exp\left(\frac{-(x-\mu)^2}{2\sigma^2}\right) \quad (1)$$

where y , σ , σ^2 , μ and x represent the PDF, standard deviation, variance, average and atmospheric concentration of each selected metal, respectively. As a part of the analysis of random phenomena, skewness was used to measure the asymmetry of the probability distribution of selected metals in PM₁₀. In the case of unimodal distribution, negative skew suggests that the tail on the left side of the PDF is longer than the right side indicating that the mass of the distribution is concentrated on the right of the figure. If the mean of the selected metal concentrations is greater than the middle, the graph will be negative skew. This can be explained by several reasons such as unusually high level of selected metals from long-range transportation or accidental explosions (i.e. only few samples with unexpectedly high concentrations). On the contrary, positive skew underlines that the tail on the right side is longer than the left side. In other words, the mass of the distribution is concentrated on the left of the figure. This will happen when the mean of the selected metal concentrations is less than its own middle. A temporary low level of selected metals may responsible for this phenomena. If the mean is in the middle, it appears more likely to have a figure of symmetrical Gaussian distribution. This represents a conventional normal distribution without any interruptions from other extreme events (e.g. accidental explosions or long-range transportation).

As clearly illustrated in Fig. 3, some characteristic features can be extracted directly from the original images. First, a sharp symmetrical bell-shaped curve was detected for V and Cr. Because the observed values of the parameter are more

Table 2 Pearson correlation matrix of 18 selected metals with trace gaseous coupled with meteorological parameters

	Al	Sc	V	Cr	Mn	Fe	Co	Ni	Cu	Zn	As	Se	Cd	Sb	Ba	La	Ce	Pb	CO	O ₃	NO ₂	SO ₂	Rad	P	Rain	RH	T	WD	WS	
Al	<i>1.00</i>																													
Sc	<i>1.00</i>	<i>1.00</i>																												
V	0.17	0.22	<i>1.00</i>																											
Cr	0.69	0.68	0.29	<i>1.00</i>																										
Mn	0.96	0.96	0.24	0.76	<i>1.00</i>																									
Fe	0.95	0.95	0.33	0.81	0.97	<i>1.00</i>																								
Co	0.44	0.46	0.46	0.28	0.36	0.41	<i>1.00</i>																							
Ni	-0.28	-0.25	0.34	-0.03	-0.20	-0.23	0.12	<i>1.00</i>																						
Cu	-0.01	-0.02	0.27	0.01	0.05	0.05	0.25	-0.06	<i>1.00</i>																					
Zn	0.10	0.12	0.37	0.33	0.22	0.20	0.44	0.13	0.54	<i>1.00</i>																				
As	0.89	0.90	0.40	0.60	0.89	0.91	0.44	-0.26	0.19	0.23	<i>1.00</i>																			
Se	0.20	0.21	0.55	0.44	0.23	0.36	0.46	-0.12	0.16	0.36	0.25	<i>1.00</i>																		
Cd	0.51	0.51	0.02	0.31	0.59	0.46	0.07	-0.03	0.03	0.43	0.45	-0.03	<i>1.00</i>																	
Sb	0.84	0.85	0.39	0.67	0.87	0.87	0.54	-0.28	0.32	0.34	0.84	0.44	<i>1.00</i>																	
Ba	0.54	0.54	0.43	0.78	0.65	0.71	0.11	-0.11	-0.04	0.12	0.50	0.53	0.13	<i>0.64</i>																
La	0.98	0.98	0.16	0.64	0.95	0.94	0.41	-0.32	0.05	0.08	0.89	0.18	0.46	<i>0.87</i>	0.57	<i>1.00</i>														
Ce	0.99	0.99	0.16	0.65	0.96	0.95	0.41	-0.31	0.02	0.06	0.89	0.17	0.46	<i>0.86</i>	0.57	<i>1.00</i>														
Pb	0.45	0.47	0.51	0.46	0.42	0.50	0.81	-0.08	0.30	0.59	0.46	0.76	0.20	0.65	0.30	0.42	0.41	<i>1.00</i>												
CO	-0.25	-0.26	-0.27	0.07	-0.22	-0.20	-0.19	-0.20	-0.28	0.11	-0.37	0.06	-0.24	-0.15	0.24	-0.21	-0.23	-0.05	<i>1.00</i>											
O ₃	0.47	0.44	-0.33	0.03	0.27	0.27	0.34	-0.16	0.06	-0.16	0.38	-0.18	0.10	0.20	-0.25	0.43	0.45	0.11	-0.33	<i>1.00</i>										
NO ₂	0.09	0.09	0.31	0.10	0.13	0.01	0.05	-0.38	-0.02	-0.09	-0.02	0.00	-0.01	0.47	0.09	0.09	-0.06	<i>0.69</i>	-0.28	<i>1.00</i>										
SO ₂	-0.46	-0.45	0.01	-0.43	-0.46	-0.44	-0.24	-0.10	0.00	-0.20	-0.38	-0.09	-0.39	-0.35	-0.24	-0.42	-0.43	-0.17	0.04	-0.30	-0.16	<i>1.00</i>								
Rad	-0.06	-0.03	0.43	-0.18	-0.06	-0.10	0.23	0.77	-0.02	-0.12	-0.03	-0.18	-0.16	-0.02	-0.04	-0.05	-0.04	-0.08	-0.31	0.06	-0.03	0.06	<i>1.00</i>							
P	0.09	0.12	0.09	0.08	0.15	0.10	0.13	0.14	-0.11	0.06	0.22	-0.09	0.13	0.09	-0.15	0.05	0.08	0.10	-0.38	0.03	-0.37	0.41	0.15	<i>1.00</i>						
Rain	-0.15	-0.14	0.05	-0.05	-0.17	-0.10	-0.21	-0.19	-0.10	-0.15	-0.08	-0.16	-0.11	0.21	-0.15	-0.14	-0.14	-0.59	-0.34	0.68	0.02	-0.16	-0.38	<i>1.00</i>						
RH	-0.05	-0.03	-0.16	-0.22	-0.04	-0.12	-0.20	-0.24	-0.18	0.08	-0.02	-0.05	0.44	-0.13	-0.37	-0.14	-0.11	-0.04	-0.29	-0.02	-0.46	0.15	-0.29	0.40	-0.16	<i>1.00</i>				
T	-0.01	0.01	0.04	-0.07	-0.08	-0.09	0.33	0.35	-0.03	0.12	0.03	-0.07	-0.27	0.05	-0.25	0.01	0.00	0.22	0.01	0.34	-0.25	0.06	0.46	0.29	-0.42	-0.22	<i>1.00</i>			
WD	-0.25	-0.23	0.24	-0.24	-0.26	-0.26	0.15	0.06	0.10	-0.13	0.16	-0.40	0.02	-0.14	-0.23	0.10	0.01	-0.05	-0.34	0.42	0.33	0.25	-0.21	0.23	0.49	<i>1.00</i>				
WS	0.01	0.05	0.16	-0.18	0.05	-0.01	-0.14	-0.11	-0.26	0.11	0.18	-0.11	0.32	-0.02	-0.21	-0.03	-0.02	-0.08	-0.21	-0.18	-0.27	0.07	-0.06	0.30	-0.04	0.72	0.00	0.38	<i>1.00</i>	

Note that correlation coefficients with values greater than 0.6 are set in italics

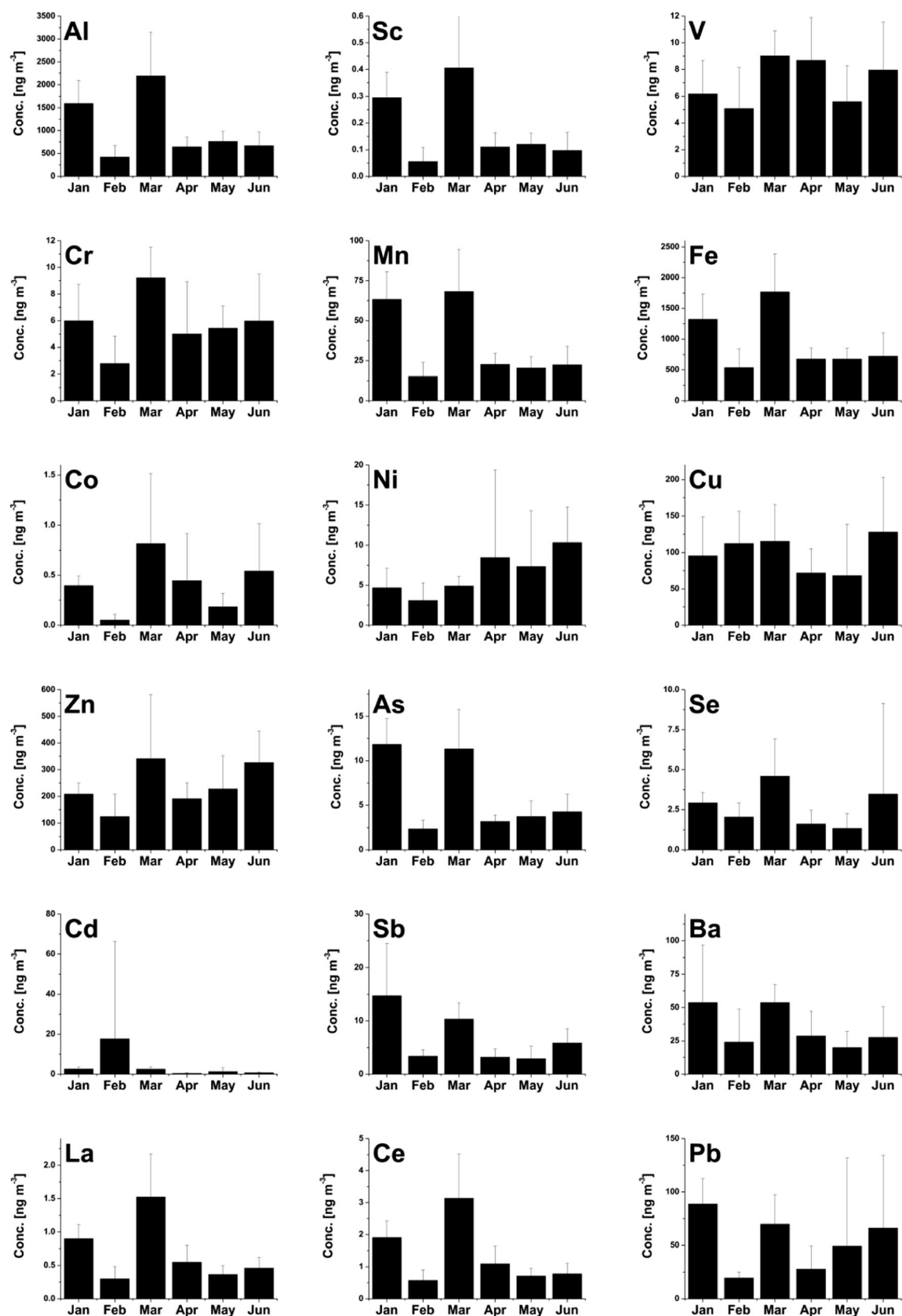


Fig. 2 Statistical descriptions of 18 selected metals collected from eight air quality observatory sites in Bangkok from January to June 2008

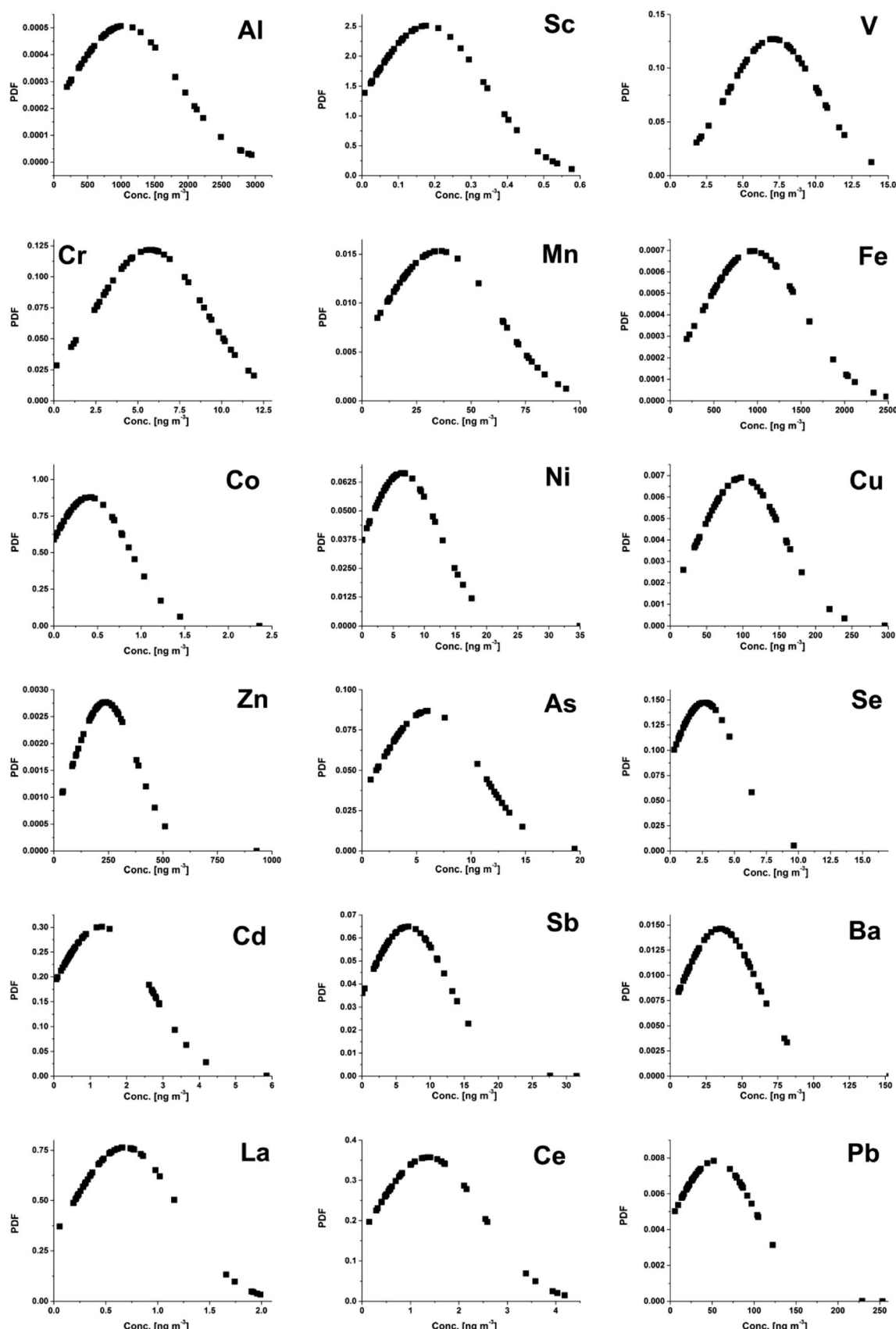


Fig. 3 Probability distribution function of 18 selected metals collected from eight air quality observatory sites in Bangkok from January to June 2008

Table 3 COD values between individual pairs of sampling sites computed individually for each element employing the entire data set for monthly concentrations

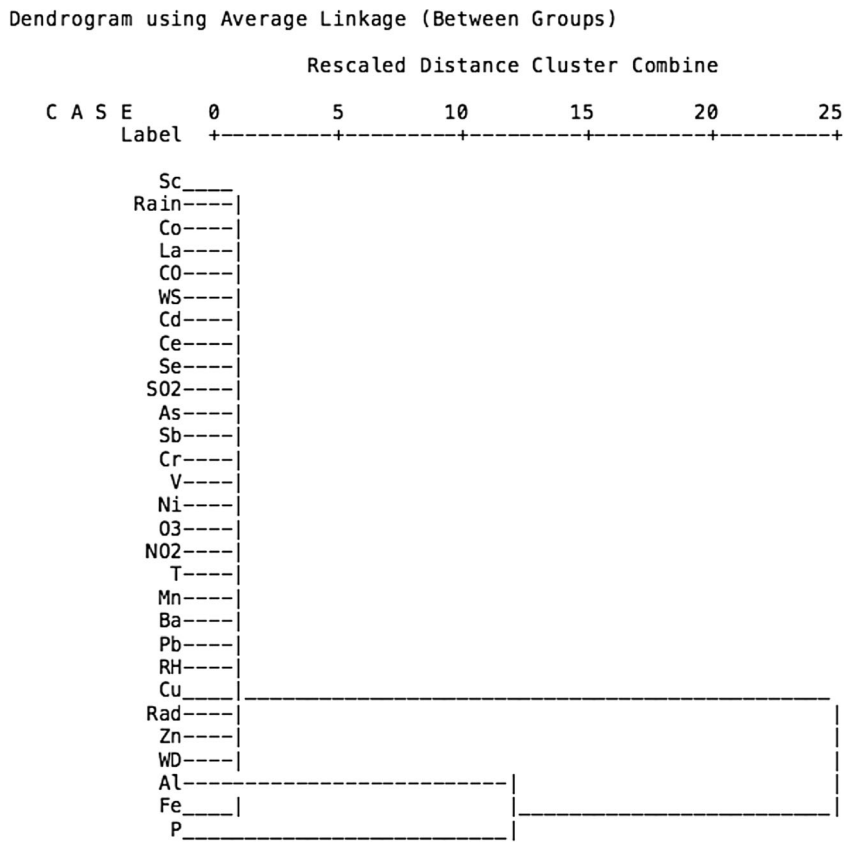
	Al	Sc	V	Cr	Mn	Fe	Co	Ni	Cu	Zn	As	Se	Cd	Sb	Ba	La	Ce	Pb
BHS-KHA	0.16	0.20	0.19	0.34	0.06	0.09	0.64	0.59	0.49	0.08	0.12	0.18	0.28	0.33	0.22	0.29	0.27	0.12
BHS-HHA	0.21	0.27	0.21	0.27	0.14	0.16	0.66	0.46	0.13	0.23	0.14	0.18	0.25	0.16	0.21	0.23	0.23	0.08
BHS-NWS	0.31	0.36	0.30	0.33	0.22	0.26	0.67	0.49	0.33	0.31	0.24	0.22	0.41	0.30	0.28	0.30	0.31	0.15
BHS-SPS	0.15	0.29	0.39	0.40	0.36	0.21	0.54	0.55	0.49	0.45	0.41	0.31	0.52	0.56	0.27	0.11	0.15	0.39
BHS-TPS	0.44	0.49	0.37	0.45	0.38	0.42	0.73	0.54	0.20	0.41	0.31	0.45	0.39	0.34	0.50	0.38	0.38	0.57
BHS-DHA	0.39	0.45	0.21	0.41	0.34	0.41	0.63	0.52	0.37	0.26	0.28	0.44	0.36	0.31	0.60	0.33	0.34	0.25
BHS-CPB	0.27	0.28	0.28	0.25	0.20	0.28	0.51	0.46	0.24	0.26	0.13	0.31	0.48	0.16	0.39	0.28	0.28	0.13
KHA-HHA	0.13	0.18	0.21	0.40	0.11	0.11	0.70	0.61	0.46	0.18	0.16	0.26	0.30	0.34	0.19	0.30	0.28	0.10
KHA-NWS	0.24	0.35	0.35	0.42	0.22	0.23	0.75	0.59	0.32	0.28	0.26	0.29	0.41	0.25	0.29	0.39	0.38	0.15
KHA-SPS	0.17	0.33	0.36	0.48	0.38	0.21	0.76	0.62	0.42	0.45	0.41	0.36	0.53	0.61	0.27	0.26	0.18	0.37
KHA-TPS	0.42	0.50	0.40	0.55	0.38	0.42	0.81	0.67	0.41	0.39	0.35	0.49	0.43	0.33	0.51	0.48	0.47	0.54
KHA-DHA	0.34	0.46	0.25	0.48	0.33	0.39	0.70	0.62	0.32	0.27	0.33	0.49	0.38	0.22	0.58	0.42	0.42	0.24
KHA-CPB	0.22	0.27	0.29	0.37	0.19	0.26	0.74	0.71	0.35	0.23	0.15	0.24	0.42	0.24	0.37	0.32	0.36	0.16
HHA-NWS	0.21	0.29	0.23	0.18	0.19	0.22	0.52	0.20	0.30	0.17	0.21	0.22	0.32	0.27	0.17	0.24	0.25	0.13
HHA-SPS	0.13	0.28	0.29	0.21	0.35	0.16	0.53	0.22	0.46	0.43	0.41	0.38	0.56	0.55	0.29	0.16	0.17	0.37
HHA-TPS	0.41	0.50	0.26	0.39	0.36	0.38	0.48	0.24	0.22	0.27	0.24	0.43	0.29	0.40	0.44	0.37	0.39	0.56
HHA-DHA	0.34	0.45	0.16	0.41	0.31	0.37	0.55	0.47	0.32	0.21	0.27	0.38	0.27	0.31	0.56	0.28	0.31	0.22
HHA-CPB	0.21	0.23	0.26	0.27	0.15	0.24	0.47	0.47	0.22	0.10	0.10	0.30	0.46	0.22	0.31	0.24	0.24	0.12
NWS-SPS	0.24	0.42	0.31	0.24	0.35	0.18	0.61	0.23	0.30	0.45	0.36	0.39	0.56	0.59	0.41	0.27	0.32	0.44
NWS-TPS	0.36	0.45	0.22	0.37	0.29	0.28	0.64	0.25	0.31	0.20	0.22	0.35	0.36	0.46	0.36	0.44	0.45	0.53
NWS-DHA	0.25	0.35	0.21	0.31	0.26	0.21	0.56	0.46	0.16	0.26	0.20	0.31	0.40	0.32	0.47	0.31	0.33	0.22
NWS-CPB	0.13	0.16	0.30	0.28	0.18	0.11	0.53	0.53	0.28	0.11	0.25	0.29	0.55	0.27	0.23	0.16	0.12	0.21
SPS-TPS	0.42	0.59	0.35	0.44	0.44	0.35	0.64	0.28	0.40	0.43	0.44	0.55	0.60	0.59	0.62	0.40	0.42	0.61
SPS-DHA	0.38	0.52	0.24	0.47	0.37	0.34	0.64	0.49	0.31	0.32	0.35	0.49	0.55	0.61	0.69	0.33	0.38	0.47
SPS-CPB	0.24	0.36	0.45	0.32	0.29	0.17	0.44	0.52	0.45	0.42	0.43	0.37	0.63	0.54	0.52	0.22	0.29	0.37
TPS-DHA	0.24	0.33	0.24	0.33	0.19	0.20	0.54	0.47	0.31	0.28	0.19	0.35	0.17	0.27	0.33	0.24	0.25	0.49
TPS-CPB	0.42	0.49	0.27	0.40	0.34	0.31	0.54	0.45	0.21	0.21	0.26	0.48	0.56	0.27	0.24	0.49	0.48	0.60
DHA-CPB	0.32	0.38	0.28	0.34	0.23	0.24	0.42	0.56	0.29	0.19	0.30	0.43	0.51	0.22	0.37	0.39	0.36	0.29

concentrated in the middle than in the tails, it seems rationale to assume a considerably strong homogeneous distribution of V and Cr in PM₁₀, which were much less affected by the human activities. This result can also be inferred as a consequence of the fairly convincing crustal emissions of these two metals.

Second, Al, Sc, Mn and Fe showed noticeably broad peaks with flat tops of right skewedness distributions, emphasising the higher degree of means than modes. These positive skewedness curves are consistent with the temporal distribution patterns of these four metals, as illustrated in Fig. 2, indicating the common sources of natural emissions, which are mainly associated with the geographic location of Bangkok. Third, Ba, Sb and Se demonstrated sharp positive skewedness curves, indicating that the bulk of metal concentrations were to the left of the mean. The similarities of the asymmetrical distribution curves of Ba, Sb and Se agree well with its own temporal distribution patterns and thus underline the

importance of anthropogenic activities on these three metals (see Figs. 2 and 3). It is also important to mention that the concentrations of these three metals are high in January and March. Several reasons are responsible for this trend. Since January and March are generally defined as cold period, a low-level atmospheric temperature inversion can be easily occurred and thus can lead to pollution such as smog and other metals being trapped close to the ground, with possible adverse effects on health. On the contrary, a comparatively high temperature in April is due to thermal expansion and subsequently dilutes the metal concentrations in Summer. Precipitations in May and June are also responsible for the reduction of selected metals during the rainy season. Previous studies also highlight the tyre and brake wear as a major source of Fe, Ba, Cu, Sn and Zn in PM₁₀, while plastic incineration and brake pad wears of automobiles were suspected as main contributors of Sb (Alves et al. 2015; Furuta et al. 2005). In addition, an unexpectedly high levels

Fig. 4 A dendrogram derived from hierarchical cluster analysis of selected metals and other meteorological parameters



of Ba, Sb and Se can be ascribed as a consequence of traffic congestion in the middle of new year celebration activities in the first week of January.

Intersite comparison-coefficient of divergence

One of the most difficult tasks in the data evaluation was merely the large number of selected metals coupled with its comparatively high deviations of PM₁₀-bounded chemical component concentrations. Furthermore, it appears problematic to evaluate the local and regional impacts on emission source strengths of selected metals. To assess the similarities or differences in the temporal distribution patterns of selected metals of the eight air quality observatory sites, the computation of coefficients of divergence (COD_{jk}) is suggested (Limbeck et al. 2009; Wilson et al. 2005), which can be described as follows:

$$\text{COD}_{jk} = \sqrt{\frac{1}{n} \sum_{i=1}^n \left(\frac{x_{ij} - x_{ik}}{x_{ij} + x_{ik}} \right)^2} \quad (2)$$

where x_{ij} denotes the atmospheric concentration of the selected metal on sampling event i at air quality observatory site j , x_{ik} is the atmospheric concentration of this element for the identical event i at air quality observatory site k , and n is the

number of total sampling events. It is important to mention that both short- and long-term measurements can be applied to the concept of using COD due to its self-normalising process (Wongphatarakul et al. 1998). When the COD value approaches zero, this trend can be interpreted as a strong similarity of emission sources between the two sites. In contrast, a COD value close to one indicates the dissimilarity of the two assessed air quality observatory sites.

As illustrated in Table 3, the majority of selected metals demonstrated comparatively low COD values (<0.30), indicating that the PM₁₀-bounded Al, Sc, V, Cr, Mn, Fe, Zn, As, Se, La and Ce levels of all eight sites were predominantly affected by comparable sources (e.g. regional crustal emissions or long-range transport) during the monitoring period and only to a minor magnitude by site-specific local emissions, which were expected to be accountable for the discrepancies between the individual air quality observatory sites. Relatively low COD average values ($n=28$) were observed for Fe (0.26 ± 0.10), Mn (0.27 ± 0.10), As (0.27 ± 0.10), Zn (0.28 ± 0.11), V (0.28 ± 0.07) and Al (0.28 ± 0.10), suggesting that emission sources are either spatially homogeneously dispersed or that there are no crucial specific emission sources and that the PM₁₀-bounded concentration of these metals might be occupied by regional crustal emissions and/or long-range transport. Because a previous study conducted in Vienna highlighted the re-suspension of road dust, the

weathering of facades and construction activities as three main sources of Al, Mn and Sb (Limbeck et al. 2009). It is logical to interpret the comparatively low COD values of these three elements as a consequence of a homogeneous mixture of air mass from road dust re-suspension coupled with construction activities in Bangkok. In addition, the comparatively low COD values that were observed for Ba (0.38 ± 0.15), Fe (0.26 ± 0.10) and Cu (0.33 ± 0.10) reflect the uniformity of emissions inside the city, such as brake abrasion of motor vehicles, which implies ubiquitous sources for these elements releasing uninterrupted independent from seasonal or meteorological fluctuations (Lough et al. 2005; Handler et al. 2008).

Potential source contributions of selected metals

HCA was performed to identify the homogeneous group of individual selected metals in PM₁₀ samples that were collected from eight PCD air quality observatory sites. The results in the dendrogram (Fig. 4) distinguish the 18 individual metals coupled with 11 meteorological parameters into two major clusters. The first major cluster ($n=26$) consists of Sc, Rain, Co, La, CO, WS, Cd, Ce, Se, SO₂, As, Sb, Cr, V, Ni, O₃, NO₂, T, Mn, Ba, Pb, RH, Cu, Rad, Zn and WD, as illustrated in Fig. 4. The first cluster shows fairly strong affinities of Co, La, Cd, Ce, Se, As, Sb, Cr, V and Ni with CO, SO₂, O₃ and NO₂, which are mainly produced by traffic emissions, underlining the importance of vehicular exhausts on these ten metals. Because Cu and Zn are highly associated with RH, Rad and WD in the first cluster, it appears reasonable to interpret this fact as a consequence of predominant geographical sources over these two metals. These findings are also consistent with those of the Pearson correlation analysis and PDF patterns as previously mentioned in “Pearson correlation analysis” and “Spatial and temporal distribution of selected metals”, respectively. The second sub-cluster contains Al, Fe and P. This result can be ascribed to the overwhelming influence of crustal emissions on these two metals, which agrees well with previous discussions comparing the PM₁₀-bounded selected metal concentrations in “Comparison of PM₁₀-bounded selected metal concentrations”.

Table 4 displays the principal component patterns for the Varimax-rotated components of the selected metal dataset coupled with meteorological parameters. To enable the further interpretation of potential selected metal sources, a PCA model with five significant PCs, each representing 37.74, 13.51, 11.32, 8.67 and 6.68 % of the variance, thus accounting for 77.92 % of the total variation in the data, was calculated. The first component (PC1) shows the high loading on crustal metals (i.e. Al, Fe and Mn), with no observed significant correlations in any trace gaseous species. Furthermore, the negative correlation of SO₂ (-0.51) in PC1 indicates that imperfect combustion of fossil fuels (e.g. coal) plays a minor role in this

Table 4 Principal component analysis of 18 selected metals with trace gaseous coupled with meteorological parameters

	Principal component (PC)				
	PC1	PC2	PC3	PC4	PC5
Al	0.98				
Sc	0.98				
V		0.61			
Cr	0.74				
Mn	0.97				
Fe	0.97				
Co		0.59			
Ni			0.79		
Cu		0.59			
Zn		0.74			
As	0.89				
Se		0.79			
Cd	0.53				
Sb	0.82				
Ba	0.62		0.60		
La	0.97				
Ce	0.98				
Pb		0.81			
CO			0.63		
O ₃			-0.71		
NO ₂			0.80		
SO ₂	-0.51				
Rad				0.92	
P					0.59
Rain			0.72		
RH					0.83
T				0.59	
WD					
WS					0.86
% of total variance	34.74	13.51	11.32	8.67	6.68

component. It is therefore logical to note that the crustal emissions contribute 34.7 %. The second component (PC2) has higher loadings for V, Co, Cu, Pb, Se and Zn. Previous studies have highlighted the importance of Se and Zn as elemental markers of coal combustion (Almeida et al. 2006; Hien et al. 2001; Lee et al. 2008). It is also important to note that Pb as well as V, Co and Zn are the most commonly used tracer element for identifying vehicular emissions. Despite the introduction of unleaded petrol in Thailand in 1992, lead is still used as an elementary marker because of its comparatively high persistence in road dust particles (Banerjee 2003). Therefore, PC2 can be considered representative of traffic emissions, explaining 13.5 % of the total PM₁₀.

PC3 indicates considerably strong positive correlations of Ba, CO and NO₂ coupled with a negative correlation of O₃.

Unlike those of trace gaseous CO and NO₂, the correlation coefficient of O₃ was negatively correlated with the others, highlighting the mechanism of O₃ formation from NO_x. Because Ba has been widely employed as an elementary marker for brake and tyre wear emissions (Lough et al. 2005; Gietl et al. 2010), it seems plausible to consider particle emissions from idling in traffic and frequent acceleration and braking as the main contributors of this PC, which is responsible for 11.3 % of the total variance. One of the main concerns when performing any source apportionment study employing multivariate methods is to confirm a high ratio between the number of samples collected and the number of variables being analysed, and if that ratio is extremely low, the data interpretations can be misleading (Pant and Harrison 2012). For instance, in this study, data from 48 samples were analysed for 29 variables. Additionally, the results from the HCA and PCA in many cases did not agree well with each other. For instance, while the HCA results indicated the strong affinity of Co, La, Cd, Ce, Se, As, Sb, Cr, V and Ni with trace gaseous species, reflecting vehicular emission as a major source of these elements, the results from the PCA showed only Ba to have good positive correlations with CO and NO₂ (Table 4).

Enrichment factors of the selected metals

The concept of the enrichment factor (EF) has been widely used to evaluate the contribution of vehicular exhaust (Zhang et al. 2015), industrial emissions (Li et al. 2012) and mining coupled with ore processing (Wang et al. 2014a, b) to atmospheric elemental contents. Although there is no specific rule for selecting the reference element, Si, Al and Fe are frequently used for the computations of EF (López et al. 2005). For individual selected metals, Fe was used as a reference assuming minor contributions of the pollutant Fe and the upper continental crustal composition given by Rudnick (2003). The EF of an element *E* in a PM₁₀ sample can be described as

$$\text{EF} = \frac{(E/R)_{\text{Air}}}{(E/R)_{\text{Crust}}} \quad (3)$$

where *R* is a reference element. If EF approaches one, the crustal can be considered the predominant emission source. The analytical results are displayed in Fig. 5, and the sequence of EF in Bangkok was Cd>Sb>Ba>Se>La>Ce>Cu>Zn>Pb>As>Ni>V>Cr>Mn>Co>Fe>Sc>Al. Additionally, the results can be categorised as follows (arbitrary scale) (Karageorgis et al. 2009). (i) Ni, V, Cr, Mn, Co, Fe, Sc and Al are not enriched (less than Log (EF)=1); (ii) Cu, Zn, Pb and As are slightly enriched (Log (EF) ranges from 1 to 3); (iii) Ba, Se, La and Ce are moderately enriched (Log (EF) ranges from 3 to 4); and (4) Cd and Sb are extremely strongly enriched

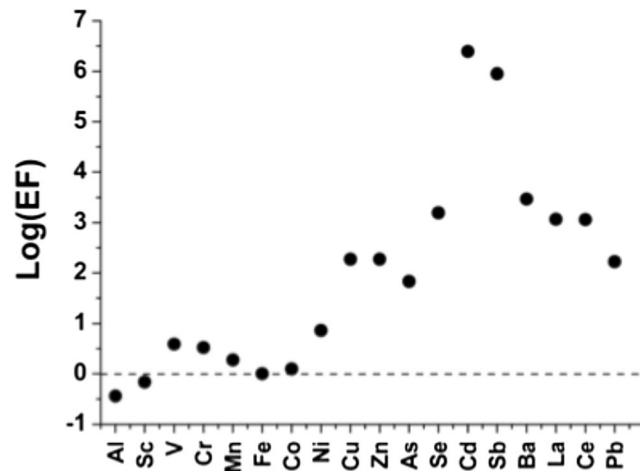


Fig. 5 Logarithms of EF of 18 selected metals collected at eight air quality observatory sites in Bangkok from January to June 2008

(Log (EF) is greater than 4). These results indicate that geographical sources, such as crustal emissions, the re-suspension of urban soils/road dusts, and maritime aerosols, are conceivably the prevailing sources for these selected metals. Comparable interpretations were also proposed by Wu et al. (1994), who reported that the majority of the atmospheric Al over Chesapeake Bay was derived from soil. The extremely low Log (EF) value of Al (-0.44) that was obtained in the current study is consistent with that of Wu et al. (1994). In contrast, the extremely high Log (EF) values (>4) that were obtained for Cd and Sb underline the strong influences of anthropogenic emissions on these two elements, plausibly vehicular emissions, which agrees well with previous studies (Lough et al. 2005; Almeida et al. 2006; Crawford et al. 2007; Begum et al. 2011). In addition, the comparatively high Log (EF) values of Ba and Se are consistent with those results of the PCA as previously discussed in “Potential source contributions of selected metals”, suggesting that traffic emissions are the main contributors of these two metals.

Conclusions

Apart from several limitations of the current study, including an inadequate number of samples (i.e. *n*<100), the use of unweighted models such as PCA, difficulties in most cases to distinguish vehicle exhaust from non-exhaust vehicle emissions, a comparatively low number of sampling sites and insufficient use of other organic markers, the Bangkok air quality can be categorised as relatively polluted with PM₁₀-bound metals under the current international air quality guidelines. The application of multivariate statistical tools was also useful for characterising the crustal emissions as well as the influence of vehicular exhaust and industrial release. The extremely high Log (EF) values of Cd and Sb coupled with the moderately high Log (EF) values of Ba, Se, La and Ce indicate that

these metals are not crustal derived and thus encourage policymakers to consider the full range of regulations including trace elements.

Acknowledgments This work was performed with the approval of the National Institute of Development Administration (NIDA), Thailand, and financial support from the Department of Regional Activation, Faculty of Regional Policy, Takasaki City University of Economics, Japan. The author acknowledges the research staff from the Pollution Control Department (PCD), Ministry of Natural Resources and Environment (MNRE), Thailand, for their contribution in the sampling and some laboratory work. The authors also acknowledge Ms. Mattanawadee Hattayanone and Ms. Thanpahatt Chaichombhoo for their contribution on graphic designs.

References

- Almeida SM, Pio CA, Freitas MC, Reis MA, Trancoso MA (2006) Source apportionment of atmospheric urban aerosol based on weekdays/weekend variability: evaluation of road re-suspended dust contribution. *Atmos Environ* 40:2058–2067
- Alves CA, Gomes J, Nunes T, Duarte M, Calvo A, Custódio D, Pio C, Karanasiou A, Querol X (2015) Size-segregated particulate matter and gaseous emissions from motor vehicles in a road tunnel. *Atmos Res* 153:134–144
- Banerjee ADK (2003) Heavy metal levels and solid phase speciation in street dusts of Delhi, India. *Environ Pollut* 123:95–105
- Begum BA, Kim E, Biswas SK, Hopke PK (2004) Investigation of sources of atmospheric aerosol at urban and semi-urban areas in Bangladesh. *Atmos Environ* 38:3025–3038
- Begum BA, Biswas SK, Hopke PK (2011) Key issues in controlling air pollutants in Dhaka, Bangladesh. *Atmos Environ* 45(40):7705–7713
- Berardi R, Pellei C, Valeri G, Pistelli M, Onofri A, Morgese F, Caramanti M, Mirza RM, Santoni M, De Lisa M, Savini A, Ballatore Z, Giuseppetti GM, Cascinu S (2015) Chromium exposure and germinal embryonal carcinoma: first two cases and review of the literature. *J Toxicol Environ Health A* 78(1):1–6
- Charlesworth S, Everett M, McCarthy R, Ordóñez A, de Miguel E (2003) A comparative study of heavy metal concentration and distribution in deposited street dusts in a large and a small urban area: Birmingham and Coventry, West Midlands, UK. *Environ Int* 29: 563–573
- Cong Z, Kang S, Luo C, Li Q, Huang J, Gao S, Li X (2011) Trace elements and lead isotopic composition of PM₁₀ in Lhasa, Tibet. *Atmos Environ* 45(34):6210–6215
- Crawford J, Chambers S, Cohen DD, Dyer L, Wang T, Zahorowski R (2007) Receptor modelling using positive matrix factorization, back trajectories and Radon-222. *Atmos Environ* 41:6823–6837
- Dongarà G, Mannoa E, Varricca D, Vultaggio M (2007) Mass levels, crustal component and trace elements in PM₁₀ in Palermo, Italy. *Atmos Environ* 41:7977–7986
- European Commission. Air quality standards [homepage on the Internet]. No date [updated 2012 Nov 30; cited 2013 Jan 24]. Available from: <http://ec.europa.eu/environment/air/quality/standards.htm>
- Furuta N, Iijima A, Kambe A, Sakai K, Sato K (2005) Concentrations, enrichment and predominant sources of Sb and other trace elements in size classified airborne particulate matter collected in Tokyo from 1995 to 2004. *J Environ Monit* 7(12):1155–1161
- Gao Y, Nelson ED, Field MP, Ding Q, Li H, Sherrell RM, Gigliotti CL, Van Ry DA, Glenn TR, Eisenreich SJ (2002) Characterization of atmospheric trace elements on PM_{2.5} particulate matter over the New York–New Jersey harbour estuary. *Atmos Environ* 36:1077–1086
- Gietl JK, Lawrence R, Thorpe AJ, Harrison RM (2010) Identification of brake wear particles and derivation of a quantitative tracer for brake dust at a major road. *Atmos Environ* 44:141–146
- Handler M, Puls C, Zbiral J, Marr I, Puxbaum H, Limbeck A (2008) Size and composition of particulate emissions from motor vehicles in the Kaiser-mühlen-Tunnel, Vienna. *Atmos Environ* 42:2173–2186
- Hien PD, Binh NT, Truong Y, Ngo NT, Sieu LN (2001) Comparative receptor modelling study of TSP, PM₂ and PM_{2–10} in Ho Chi Minh city. *Atmos Environ* 35:2669–2678
- Iijima A, Sato K, Fujitani Y, Fujimori E, Saitoh Y, Tanabe K, Ohara T, Kozawa K, Furuta N (2009) Clarification of the predominant emission sources of antimony in airborne particulate matter and estimation of their effects on the atmosphere in Japan. *Environ Chem* 6: 122–135
- Iijima A, Sato K, Ikeda T, Sato H, Kozawa K, Furuta N (2010) Concentration distributions of dissolved Sb(III) and Sb(V) species in size-classified inhalable airborne particulate matter. *J Anal At Spectrom* 25:356–363
- Johansson C, Norman M, Burman L (2009) Road traffic emission factors for heavy metals. *Atmos Environ* 43:4681–4688
- Karageorgis AP, Katsanevakis S, Kaberi H (2009) Use of enrichment factors for the assessment of heavy metal contamination in the sediments of Koumoundourou Lake, Greece. *Water Air Soil Pollut* 204: 243–258
- Kemp K (2002) Trends and sources for heavy metals in urban atmosphere. *Nucl Inst Methods Phys Res B* 189:227–232
- Lee BK, Lee HK, Jun NY (2006) Analysis of regional and temporal characteristics of PM₁₀ during an Asian dust episode in Korea. *Chemosphere* 63:1106–1115
- Lee S, Liu W, Wang Y, Russell AG, Edgerton ES (2008) Source apportionment of PM_{2.5}: comparing PMF and CMB results for four ambient monitoring sites in the southeastern United States. *Atmos Environ* 42:4126–4137
- Li YM, Pan YP, Wang YS, Wang YF, Li XR (2012) Chemical characteristics and sources of trace metals in precipitation collected from a typical industrial city in Northern China. *Huan Jing Ke Xue* 33(11): 3712–3717
- Limbeck A, Handler M, Puls C, Zbiral J, Bauer H, Puxbaum H (2009) Impact of mineral components and selected trace metals on ambient PM₁₀ concentrations. *Atmos Environ* 43:530–538
- López JM, Callén MS, Murillo R, García T, Navarro MV, de la Cruz MT, Mastral AM (2005) Levels of selected metals in ambient air PM₁₀ in an urban site of Zaragoza (Spain). *Environ Res* 99:58–67
- Lough GC, Schauer JJ, Park JS, Shafer MM, Deminter JT, Weinstein JP (2005) Emissions of metals associated with motor vehicle roadways. *Environ Sci Technol* 39:826–836
- Madrid F, Barrientos ED, Madrid L (2008) Availability and bioaccessibility of metals in the clay fraction of urban soils of Sevilla. *Environ Pollut* 605–610
- Milligan GW, Cooper MC (1987) A study of variable standardization. College of Administrative Science Working paper series, 87–63. The Ohio State University, Columbus, OH
- Pant P, Harrison R (2012) Critical review of receptor modelling for particulate matter: a case study of India. *Atmos Environ* 49:1–12
- Pongpiachan S (2013a) Diurnal variation, vertical distribution and source apportionment of carcinogenic polycyclic aromatic hydrocarbons (PAHs) in Chiang-Mai, Thailand. *Asian Pac J Cancer Prev* 14(3): 1851–1863
- Pongpiachan S (2013b) Vertical distribution and potential risk of particulate polycyclic aromatic hydrocarbons in high buildings of Bangkok, Thailand. *Asian Pac J Cancer Prev* 14(3):1865–77
- Pongpiachan S, Choochay C, Hattayanone M, Kositanont C (2013) Temporal and spatial distribution of particulate carcinogens and

- mutagens in Bangkok, Thailand. *Asian Pac J Cancer Prev* 14(3): 1879–1887
- Pongpiachan S, Tipmanee D, Khumsup C, Kittikoon I, Hirunyatrakul P (2015a) Assessing risks to adults and preschool children posed by PM_{2.5}-bound polycyclic aromatic hydrocarbons (PAHs) during a biomass burning episode in Northern Thailand. *Sci Total Environ* 508:435–444
- Pongpiachan S, Hattayanone M, Choochua C, Mekmok R, Wuttijak N, Ketratanakul A (2015b) Enhanced PM₁₀ bounded PAHs from shipping emissions. *Atmos Environ* 108:13–19
- Ratcliffe HE, Swanson GM, Fischer LJ (1996) Human exposure to mercury: a critical assessment of the evidence of adverse health effects. *J Toxicol Environ Health* 49(3):221–270
- Rosen JF (1995) Adverse health effects of lead at low exposure levels: trends in the management of childhood lead poisoning. *Toxicology* 97(1-3):11–17
- Rudnick RL (2003) “The Crust”, Volume 3 of the Treatise on Geochemistry, Elsevier
- Silva LID, Yokoyama L, Maia LB, Monteiro MIC, Pontes FVM, Carneiro MC, Neto AA (2015) Evaluation of bioaccessible heavy metal fractions in PM₁₀ from the metropolitan region of Rio de Janeiro city, Brazil, using a simulated lung fluid. *Microchem J* 118:266–271
- Song Y, Zhang Y, Xie S, Zeng L, Zheng M, Salmon LG, Shao M, Slanina S (2006) Source apportionment of PM_{2.5} in Beijing by positive matrix factorization. *Atmos Environ* 40:1526–1537
- Srithawirat T, Latif MT (2015) Concentration of selected heavy metals in the surface dust of residential buildings in Phitsanulok, Thailand. *Environ Earth Sci.* doi:[10.1007/s12665-015-4291-0](https://doi.org/10.1007/s12665-015-4291-0)
- Wang J, Hu Z, Chen Y, Chen Z, Xu S (2013) Contamination characteristics and possible sources of PM₁₀ and PM_{2.5} in different functional areas of Shanghai, China. *Atmos Environ* 68:221–229
- Wang W, Cheng S, Zhang D (2014a) Association of inorganic arsenic exposure with liver cancer mortality: a meta-analysis. *Environ Res* 135:120–125
- Wang L, Liang T, Zhang Q, Li K (2014b) Rare earth element components in atmospheric particulates in the Bayan Obo mine region. *Environ Res* 131:64–70
- Wilson JG, Kingham S, Pearce J, Sturman AP (2005) A review of intra-urban variations in particulate air pollution: implications for epidemiological research. *Atmos Environ* 39:6444–6462
- Wongphatarakul V, Friedlander SK, Pinto JP (1998) A comparative study of PM_{2.5} ambient aerosol chemical databases. *Environ Sci Technol* 32:3926–3934
- Wu ZY, Han M, Lin ZC, Ondov JM (1994) Chesapeake Bay atmospheric deposition study, year 1: sources and dry deposition of selected elements in aerosol particles. *Atmos Environ* 28(8):1471–1486
- Yang J, Kim EC, Shin DC, Jo SJ, Lim YW (2014) Human exposure and risk assessment of cadmium for residents of abandoned metal mine areas in Korea. *Environ Geochem Health.* doi:[10.1007/s10653-014-9650-3](https://doi.org/10.1007/s10653-014-9650-3)
- Yatkin S, Bayram A (2008a) Determination of major natural and anthropogenic source profiles for particulate matter and trace elements in Izmir, Turkey. *Chemosphere* 71:685–696
- Yatkin S, Bayram A (2008b) Source apportionment of PM₁₀ and PM_{2.5} using positive matrix factorization and chemical mass balance in Izmir, Turkey. *Sci Total Environ* 390:109–123
- Zhang H, Wang Z, Zhang Y, Ding M, Li L (2015) Identification of traffic-related metals and the effects of different environments on their enrichment in roadside soils along the Qinghai-Tibet highway. *Sci Total Environ* 521-522C:160–172
- Zwolak I (2014) Vanadium carcinogenic, immunotoxic and neurotoxic effects: a review of in vitro studies. *Toxicol Mech Methods* 24(1):1–12



Effects of day-of-week trends and vehicle types on PM_{2.5}-bounded carbonaceous compositions



Siwatt Pongpiachan ^{a,b,*}, Charnwit Kositanont ^c, Jittree Palakun ^d, Suixin Liu ^b, Kin Fai Ho ^b, Junji Cao ^b

^a NIDA Center for Research & Development of Disaster Prevention & Management, School of Social and Environmental Development, National Institute of Development Administration (NIDA), 118 Moo 3, Sereethai Road, Klong-Chan, Bangkapi, Bangkok 10240, Thailand

^b SKLQG, Institute of Earth Environment, Chinese Academy of Sciences (IEECAS), Xi'an 710075, China

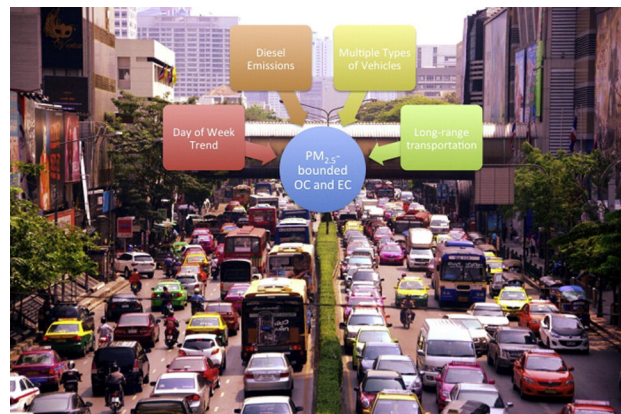
^c Department of Microbiology, Faculty of Sciences, Chulalongkorn University, Bangkok 10330, Thailand

^d Faculty of Education, Valaya Alongkorn Rajabhat University under the Royal Patronage (VRU), No.1 Moo 20, Phaholyothin Road, Klong luang, Pathumthani 13180, Thailand

HIGHLIGHTS

- Traffic emissions play an important role in governing OC and EC during weekdays.
- Time series analysis shows the existence of day-of-week trends of OC and EC.
- Diesel vehicles are the main contributors of carbonaceous compositions.

GRAPHICAL ABSTRACT



ARTICLE INFO

Article history:

Received 20 April 2015

Received in revised form 11 June 2015

Accepted 13 June 2015

Available online xxxx

Editor: D. Barcelo

Keywords:

Carbonaceous compositions

Vehicle types

Bangkok

Day-of-week trends

ABSTRACT

Carbonaceous compositions of PM_{2.5} were measured in the heart of Bangkok from 17th November 2010 to 19th January 2012, and a data set of 94 samples was constructed. Effects of day-of-week trends and vehicle types on PM_{2.5}-bound TC, OC, and EC were carefully investigated. In this study, OC was the most important contributor to the total PM_{2.5} mass concentration. The average PM_{2.5}-bound OC content measured at CHAOS ($18.8 \pm 9.18 \mu\text{g m}^{-3}$) was approximately 11 times higher than at Chaumont, Switzerland ($1.7 \mu\text{g m}^{-3}$), but approximately five times lower than at Xi'an, China ($93.0 \mu\text{g m}^{-3}$). The application of diagnostic binary ratios of OC/EC and estimations of secondary organic carbon (SOC) coupled with autocorrelation plots (Box and Jenkins) highlight the enhanced impacts of traffic emissions, especially from diesel vehicles, on PM_{2.5}-bound carbonaceous compositions on weekdays relative to weekends. Hierarchical cluster analysis (HCA) coupled with principal component analysis (PCA) underline the importance of diesel emissions as the primary contributors of carbonaceous aerosols, particularly during weekdays.

© 2015 Elsevier B.V. All rights reserved.

* Corresponding author at: NIDA Center for Research & Development of Disaster Prevention & Management, School of Social and Environmental Development, National Institute of Development Administration (NIDA), 118 Moo 3, Sereethai Road, Klong-Chan, Bangkapi, Bangkok 10240, Thailand.

E-mail address: pongpijun@gmail.com (S. Pongpiachan).

1. Introduction

Chemical characteristics of aerosols, particularly the compositions of organic carbon (OC) and elemental carbon (EC), have been constantly evaluated predominantly in Asian countries during the past few years (Pongpiachan et al., 2013a, 2013b, 2014a, 2014b; Srivastava et al., 2014; Zhang et al., 2009). Rapid industrialization and urbanization, especially in China, are apparently responsible for the enhancement of carbonaceous aerosols in this region (Huang et al., 2013; Zhang et al., 2011). Recently, numerous studies have highlighted the impacts of burning agricultural waste and forest fires in Southeast Asian countries and southern China as the main contributors of OC and EC in fine particles (Pongpiachan et al., 2014a; Zhang et al., 2010). Previous studies have shown associations between carbonaceous aerosols and the number of patients with respiratory diseases as well as some major contributions on the climate system (Künzi et al., 2013; Repine et al., 2008; US-EPA, 2012).

As a consequence, many scientific studies have focused on annual average, monthly and seasonal trends in the concentrations of carbonaceous compositions (Fu et al., 2014; Tao et al., 2012), which are extremely advantageous to a comprehensive view on the average contributions of sources of particulate OC and EC. However, it is extremely difficult to investigate the influences of day-of-week trends only given knowledge of annual or monthly average carbonaceous concentrations. In most incidents, the impacts of numerous source emissions coupled with photochemical transformations can greatly affect the day-of-week trends of atmospheric pollutants (Chow, 2003). Furthermore, traffic emissions seem to govern the diurnal variations and weekly trends of OC and EC (Bae et al., 2004). While others have examined the effects of anthropogenic activities on both diurnal and weekly fluctuations, only a few studies have demonstrated in-depth, quantitative evidence associated with the behaviour of carbonaceous aerosols in tropical countries (Li et al., 2012; Pongpiachan et al., 2009; Safai et al., 2014).

Despite copious studies involving the clarification of emission factors of OC/EC compositions from different fuel and vehicle types (Shen et al., 2014; Wei et al., 2014), little is known about their correlations in the tropical atmosphere. Although vehicle conditions can play a major role in the emission source strength of carbonaceous aerosols, there have been no studies to date that examine the relationship between vehicle types and OC/EC compositions. To our knowledge, there is no information available on intensive monitoring of fine particle

bounded carbonaceous compositions in Thailand. Overall, the principle objectives of this study were to (i) assess the day-of-week trends of OC/EC compositions through an intensive monitoring campaign of PM_{2.5} and (ii) elucidate the correlations between vehicle types and carbonaceous aerosols in the heart of metropolitan Bangkok, Thailand.

2. Experiment

2.1. Description of sampling sites

In this study, the roof of the Mahamakut Building, Chulalongkorn University (CHAOS: 13°44'9.07"N 100°31'50.26"E), was selected as the air quality observatory site because the site is positioned in the most densely populated area of Bangkok and is surrounded by shopping malls, restaurants, multiplex movie theatres, and business buildings (see Fig. 1). There were no barriers in the neighbourhood of the sampling equipment, which was deliberately situated to be accessible to winds from all directions. The sampling method was based on the "Quality Assurance Guidance Document 2.12; Monitoring PM_{2.5} in Ambient Air Using Designated Reference or Class I Equivalent Methods" (US-EPA, 1998).

2.2. Filter sample collection & meteorological data

To ensure that the quantity of carbonaceous compositions present in the samples was much greater than the instrumental detection limit, MiniVol™ portable air samplers (Airmetrics) were employed to collect PM_{2.5} for 72 h at CHAOS. The MiniVol's pump draws air at 5 L min⁻¹ through a particle size separator (impactor) and then through a 47 mm filter. The 2.5-micron particle (PM_{2.5}) separation is achieved by impaction. In this study, PM_{2.5} samples were collected on 47 mm Whatman quartz microfiber filters (QM/A) for the chemical detection of OC/EC compositions. All samples (*n* = 94) were collected in three consecutive day intervals from 17th November 2010 to 19th January 2012 at CHAOS. Prior to the PM_{2.5} sample collection, the QM/A were baked at 800 °C for at least three hours to remove any organic contaminants and were wrapped individually in DCM pre-cleaned aluminium foil until loaded into the filter holder cassette. The QM/A were equilibrated for 24 h at a constant temperature between 20 °C and 23 °C and RH between 35% and 45% in a laboratory at the Institute of Earth Environment, Chinese Academy of Sciences (IEECA), Xi'an, China, prior to PM_{2.5} mass measurement.

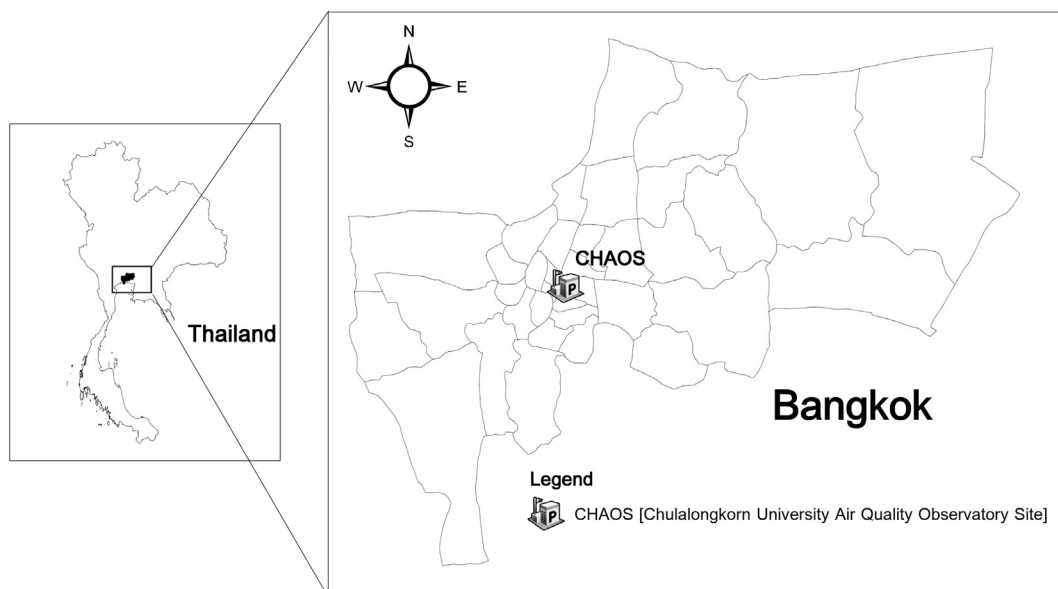


Fig. 1. Map of Chulalongkorn University Air Quality Observatory Site (CHAOS).

Table 1Average OC and EC concentrations and the OC/EC ratios in PM_{2.5} collected at CHAOS.

Sampling date	PM _{2.5} [$\mu\text{g m}^{-3}$]	TC [$\mu\text{g m}^{-3}$]	OC [$\mu\text{g m}^{-3}$]	EC [$\mu\text{g m}^{-3}$]	OC/EC ratio	TC [%]	OC [%]	EC [%]
11/17/10	39.24	17.84	11.17	6.67	1.68	45.5	28.5	17.0
11/20/10	54.72	35.59	24.40	11.19	2.18	65.0	44.6	20.4
11/23/10	35.21	18.29	11.91	6.37	1.87	51.9	33.8	18.1
11/26/10	27.08	17.34	12.89	4.45	2.90	64.0	47.6	16.4
12/02/10	35.62	12.39	8.18	4.21	1.94	34.8	23.0	11.8
12/05/10	55.69	23.95	16.83	7.11	2.37	43.0	30.2	12.8
12/08/10	60.97	25.22	16.71	8.51	1.97	41.4	27.4	13.9
12/11/10	30.89	10.25	6.64	3.62	1.84	33.2	21.5	11.7
12/14/10	25.56	15.29	9.78	5.51	1.77	59.8	38.3	21.6
12/17/10	39.03	22.75	17.63	5.11	3.45	58.3	45.2	13.1
12/20/10	75.35	45.13	33.04	12.09	2.73	59.9	43.9	16.0
12/23/10	62.57	37.67	23.86	13.81	1.73	60.2	38.1	22.1
12/26/10	32.78	16.03	11.47	4.56	2.51	48.9	35.0	13.9
12/29/10	68.68	43.65	31.30	12.36	2.53	63.6	45.6	18.0
01/01/11	58.12	29.69	22.05	7.65	2.88	51.1	37.9	13.2
01/04/11	49.86	30.67	21.19	9.48	2.23	61.5	42.5	19.0
01/07/11	37.29	20.95	15.03	5.93	2.54	56.2	40.3	15.9
01/10/11	54.37	32.95	23.59	9.36	2.52	60.6	43.4	17.2
01/13/11	47.08	27.09	18.94	8.15	2.32	57.5	40.2	17.3
01/16/11	53.26	23.50	17.66	5.84	3.03	44.1	33.2	11.0
01/19/11	74.17	47.79	33.49	14.30	2.34	64.4	45.2	19.3
01/22/11	52.99	44.04	32.78	11.26	2.91	83.1	61.9	21.3
01/25/11	49.86	32.21	23.32	8.89	2.62	64.6	46.8	17.8
01/28/11	40.07	32.27	23.71	8.56	2.77	80.5	59.2	21.4
01/31/11	57.22	44.01	32.07	11.94	2.68	76.9	56.0	20.9
02/03/11	58.54	44.96	33.28	11.68	2.85	76.8	56.8	19.9
02/06/11	52.71	28.39	21.43	6.96	3.08	53.9	40.7	13.2
02/09/11	33.68	15.74	10.40	5.33	1.95	46.7	30.9	15.8
02/12/11	32.50	9.90	6.37	3.53	1.81	30.5	19.6	10.9
02/15/11	35.35	14.14	7.68	6.46	1.19	40.0	21.7	18.3
02/18/11	29.72	13.22	9.10	4.12	2.21	44.5	30.6	13.9
02/21/11	41.88	20.86	13.07	7.79	1.68	49.8	31.2	18.6
02/24/11	24.72	6.70	3.73	2.96	1.26	27.1	15.1	12.0
02/27/11	33.61	27.50	21.46	6.05	3.55	81.8	63.8	18.0
03/02/11	57.36	25.99	17.16	8.83	1.94	45.3	29.9	15.4
03/05/11	74.31	38.20	27.62	10.58	2.61	51.4	37.2	14.2
03/08/11	27.36	7.65	4.71	2.93	1.61	27.9	17.2	10.7
03/11/11	62.92	39.62	30.55	9.07	3.37	63.0	48.6	14.4
04/27/11	20.63	3.97	1.93	2.04	0.94	19.3	9.3	9.9
04/30/11	18.82	6.55	3.88	2.67	1.46	34.8	20.6	14.2
05/03/11	15.35	5.04	2.85	2.19	1.30	32.8	18.5	14.3
05/05/11	15.97	6.88	5.33	1.54	3.46	43.0	33.4	9.6
08/13/11	67.43	37.55	29.58	7.97	3.71	55.7	43.9	11.8
08/16/11	48.68	18.26	14.31	3.94	3.63	37.5	29.4	8.1
08/19/11	54.58	19.09	15.32	3.76	4.07	35.0	28.1	6.9
08/22/11	49.79	16.54	12.36	4.18	2.96	33.2	24.8	8.4
08/25/11	43.82	20.80	14.85	5.96	2.49	47.5	33.9	13.6
08/28/11	20.21	11.20	7.71	3.50	2.20	55.4	38.1	17.3
08/31/11	74.31	46.88	36.66	10.22	3.59	63.1	49.3	13.8
09/03/11	58.54	38.91	30.02	8.89	3.38	66.5	51.3	15.2
09/06/11	66.74	40.39	31.80	8.59	3.70	60.5	47.6	12.9
09/09/11	60.90	35.98	29.25	6.73	4.35	59.1	48.0	11.0
09/12/11	50.07	21.10	15.83	5.28	3.00	42.1	31.6	10.5
09/15/11	45.49	21.40	15.69	5.70	2.75	47.0	34.5	12.5
09/30/11	13.82	8.65	8.30	3.60	2.30	62.6	60.0	2.6
09/24/11	41.94	25.37	16.95	8.42	2.01	60.5	40.4	20.1
09/27/11	33.82	21.66	17.43	4.24	4.11	64.1	51.5	12.5
09/18/11	53.26	28.78	21.34	7.44	2.87	54.0	40.1	14.0
10/03/11	69.65	40.16	29.90	10.25	2.92	57.7	42.9	14.7
10/06/11	74.24	45.67	33.99	11.68	2.91	61.5	45.8	15.7
10/09/11	87.78	57.46	43.00	14.46	2.97	65.5	49.0	16.5
10/12/11	79.24	51.24	39.86	11.38	3.50	64.7	50.3	14.4
10/15/11	53.47	25.90	19.74	6.16	3.20	48.4	36.9	11.5
10/18/11	46.18	22.21	17.46	4.76	3.67	48.1	37.8	10.3
10/21/11	34.10	13.54	9.90	3.65	2.72	39.7	29.0	10.7
10/24/11	28.54	26.26	19.77	6.49	3.05	92.0	69.3	22.7
10/27/11	48.33	18.29	13.10	5.19	2.53	37.8	27.1	10.7
10/30/11	68.26	38.94	31.03	7.91	3.92	57.0	45.5	11.6
11/02/11	62.43	33.16	25.49	7.68	3.32	53.1	40.8	12.3
11/05/11	35.90	28.27	22.23	6.05	3.68	78.7	61.9	16.8
11/08/11	53.96	24.18	18.20	5.99	3.04	44.8	33.7	11.1
11/11/11	52.15	27.26	20.74	6.52	3.18	52.3	39.8	12.5
11/14/11	54.24	23.35	17.28	6.08	2.84	43.1	31.9	11.2
11/17/11	45.14	21.01	15.83	5.19	3.05	46.5	35.1	11.5
11/20/11	55.42	24.42	18.08	6.34	2.85	44.1	32.6	11.4
11/23/11	64.44	35.56	26.20	9.36	2.80	55.2	40.7	14.5

Table 1 (continued)

Sampling date	PM _{2.5} [µg m ⁻³]	TC [µg m ⁻³]	OC [µg m ⁻³]	EC [µg m ⁻³]	OC/EC ratio	TC [%]	OC [%]	EC [%]
11/26/11	38.33	17.60	12.54	5.07	2.47	45.9	32.7	13.2
11/29/11	58.96	35.41	28.92	6.49	4.46	60.1	49.1	11.0
12/02/11	36.67	18.17	14.20	3.97	3.57	49.5	38.7	10.8
12/05/11	46.18	14.64	11.20	3.44	3.26	31.7	24.3	7.4
12/08/11	41.67	12.39	9.10	3.29	2.77	29.7	21.8	7.9
12/11/11	42.36	14.46	10.16	4.30	2.37	34.1	24.0	10.1
12/14/11	42.01	27.77	22.43	5.33	4.21	66.1	53.4	12.7
12/17/11	27.92	14.28	11.17	3.11	3.59	51.2	40.0	11.1
12/20/11	54.03	27.81	21.63	6.18	3.50	51.5	40.0	11.4
12/23/11	61.04	29.69	23.41	6.28	3.73	48.6	38.4	10.3
12/26/11	59.79	30.51	24.40	6.10	4.00	51.0	40.8	10.2
12/29/11	41.60	16.92	13.31	3.62	3.68	40.7	32.0	8.7
01/04/12	59.44	25.46	18.64	6.82	2.73	42.8	31.4	11.5
01/07/12	9.24	6.12	5.91	2.10	2.82	66.3	64.0	2.2
01/10/12	39.58	16.71	11.71	5.01	2.34	42.2	29.6	12.7
01/13/12	39.65	17.84	13.31	4.53	2.93	45.0	33.6	11.4
01/16/12	59.44	30.44	23.92	6.52	3.67	51.2	40.2	11.0
01/19/12	70.42	37.40	29.43	7.97	3.69	53.1	41.8	11.3
Average	47.6 ± 16.4	25.4 ± 11.9	18.8 ± 9.18	6.65 ± 2.94	2.80 ± 0.77	52.1 ± 13.6	38.4 ± 11.8	13.6 ± 4.00

2.3. Organic carbon (OC) & elemental carbon (EC)

A 0.5-cm² punch from each QM/A was examined for carbonaceous compositions with a Desert Research Institute (DRI) Model 2001 Thermal/Optical Carbon Analyzer (Atmoslytic Inc., Calabasas, CA, USA) for four organic carbon (OC) fractions (OC1, OC2, OC3, and OC4) in a helium atmosphere, three elemental carbon (EC) fractions (EC1, EC2, and EC3) in a 2% oxygen–98% helium atmosphere, and OP, a pyrolysed carbon fraction following the IMPROVE (Interagency Monitoring of Protected Visual Environments) thermal/optical reflectance (TOR) protocol (Chow et al., 2001; Fung et al., 2002). For this study, OC and EC were described as the sum of OC fractions (OC1 + OC2 + OC3 + OC4) and EC fractions (EC1 + EC2 + EC3 + OP), respectively, based on the IMPROVE TOC (Interagency Monitoring to Protect Visual Environments Total Organic Carbon) protocol (Chow et al., 2001; Fung et al., 2002). Total organic carbon (TOC) was defined as the sum of OC and EC. The quality control and quality assurance (QA/QC) protocols have been previously discussed in detail in Cao et al. (2003).

2.4. Traffic count database and statistical analysis

The Traffic and Transportation Department (TTD), Bangkok Metropolitan Administration (BMA), provided all traffic data used in this study. To formulate effective policy for traffic volume control and develop the traffic and transportation information system for planning and public dissemination, TTD strategically determined 153 traffic flow observatory sites for counting the number of vehicles based on their corresponding category, namely pickups/vans, trucks, cars, buses and Tuktuks (i.e., a three wheel motorcycle). The data synchronization between the two databases (i.e., vehicle counts and OC/EC compositions) was conducted manually for further advanced statistical analysis. In addition, the Statistical Program for Social Sciences (SPSS) version 13 was used for Simple Linear Regression Analysis (SLRA), Analysis of Variance (ANOVA), Hierarchical Cluster Analysis (HCA), and Principal Component Analysis (PCA).

2.5. Estimation of secondary organic carbon (SOC)

Because several factors can cause relatively high OC/EC ratios in ambient aerosols, it is crucial to conduct further estimation of secondary organic carbon (SOC), which is frequently associated with long-range transport (Wang et al., 2012; Zhou et al., 2012). In this study, the calculation of SOC was performed using the method reported by Na et al. (2004). The principle of this technique is based on the assumption

that PM_{2.5} samples that possess the smallest OC/EC ratios comprise almost entirely primary carbonaceous compositions (Castro et al., 1999). For the PM_{2.5} samples detected at CHAOS, the average of the three lowest OC/EC ratios was 1.13 ± 0.17 and thus can be used to estimate SOC. It is also essential to note that the three lowest OC/EC ratios are assumed to have solely primary OC, and the influence of a small proportion of SOC is of minor importance. The concentration of SOC is calculated by

$$OC_{sec} = OC_{tot} - EC \times (OC/EC)_{primary}, \quad (1)$$

where OC_{sec}, OC_{tot}, and (OC/EC)_{primary} are SOC, TOC, and the average value of the three lowest OC/EC ratios, respectively.

2.6. Probability distribution function of carbonaceous compositions

The probability distribution function (PDF) was applied to PM_{2.5}-bound TC, OC, and EC collected at CHAOS. Generally, a PDF is a function that describes the relative probability for a random parameter to take a provided value. The Gaussian distribution describes the probability that a random parameter will fall within a specific interval

$$y = \frac{1}{\sigma\sqrt{2\pi}} \exp\left(\frac{-(x-\mu)^2}{2\sigma^2}\right), \quad (2)$$

where y, σ, σ², μ and x are the probability distribution function, standard deviation, variance, average and concentrations of carbonaceous compositions, respectively.

2.7. Time series approach

During the past few years, autocorrelation plots have been widely employed in several atmospheric environmental studies, including an investigation of the impact of meteorological parameters and trace gas concentrations on daily hospital walk-ins and admissions in Chiang-Mai, Thailand (Pongpiachan and Paowa, 2014), long-term observations and modelling of aerosol loading over the Indo-Gangetic plains (IGP), India (Soni et al., 2014), and pedestrian exposure to PM_{2.5} in Sydney, Australia (Greaves et al., 2008). Because autocorrelation represents the similarity between observations as a function of the time lag between them, it appears reasonable to evaluate the randomness of carbonaceous compositions with time using this mathematical tool. This randomness can be investigated by computing autocorrelations for each parameter at different time lags. In the case of random signals, such autocorrelations should hypothetically approach zero for all

time-lag intervals. In the case of non-random, one or more of the autocorrelations will be significantly non-zero. The calculation of autocorrelation plots is described below. Primarily, the vertical axis symbolizes the autocorrelation coefficient, which is computed from Eq. (3):

$$R_h = \frac{C_h}{C_0} \quad (3)$$

where R_h is the autocorrelation coefficient of the atmospheric parameters (i.e., $\text{PM}_{2.5}$, TC, OC, and EC) and ranges between -1 and $+1$. Note that C_h is the autocovariance function, which can be explained in Eq. (4):

$$C_h = \frac{1}{N} \sum_{t=1}^{N-h} (Y_t - \bar{Y})(Y_{t+h} - \bar{Y}) \quad (4)$$

where N , t , h , Y_t , \bar{Y} , Y_{t+h} are the total number of individual atmospheric parameters, time, time lag, concentration of the atmospheric parameter at time t , average of the atmospheric parameter concentrations, and concentration of the atmospheric parameter at time $t + h$, respectively. It is also important to note that C_0 is the variance function, which can be described as follows:

$$C_0 = \frac{\sum_{t=1}^N (Y_t - \bar{Y})^2}{N}. \quad (5)$$

Furthermore, the horizontal axis denotes the time lag h ($h = 1, 2, 3, \dots$). Finally, the confidence bands have fixed width that depend on the sample size and can be computed using Eq. (6):

$$\pm \frac{Z_{1-\alpha/2}}{\sqrt{N}} \quad (6)$$

where N is the sample size, Z is the cumulative distribution function of the standard normal distribution, and α is the significance level.

3. Results & discussion

The statistical descriptions and their percentage contributions of $\text{PM}_{2.5}$, TC, OC and EC measured during the sampling period at CHAOS are listed in Table 1. The percentage contribution of TC ranged from 19.3 to 92%, with an average of $52.1 \pm 13.6\%$, and OC varied from 9.3 to 69.3%, with an average of $38.4 \pm 11.8\%$. EC ranged from 2.2 to 22.7%, with an average of $13.6 \pm 4.0\%$. These findings show that OC was the most important contributor to the total $\text{PM}_{2.5}$ mass concentration.

3.1. OC/EC ratios and estimation of secondary organic carbon (SOC)

During the past decades, OC/EC ratios have been extensively applied for elucidating the photolysis process of carbonaceous compositions and the formation of secondary organic aerosol (SOA) and for categorizing their emission sources (Turpin and Huntzicker, 1995). In this study, the OC/EC ratios varied from 0.94 to 4.46, with an average of 2.80 ± 0.77 , as listed in Table 1. Generally, the average OC/EC ratio at CHAOS was very similar to that of Chaumont, Switzerland (2.8), Guangzhou, China (2.8 ± 2.8), and Xi'an, China (2.9 ± 2.7) (Cao et al., 2003, 2005; Hueglin et al., 2005). Several reasons can be used to explain the comparatively high OC/EC ratios observed in this study. Firstly, previous studies have highlighted the importance of the formation of secondary OC via long-range transport (Wang et al., 2012; Zhou et al., 2012). For instance, the moderately high $\text{PM}_{2.5}$ -bound OC/EC ratios (range: 1.6–10.4; average: 5.2 ± 1.8) observed at Mount Heng, China were considered to be a consequence of in-cloud secondary organic aerosol (SOA) formation coupled with long-range transport (Zhou et al., 2012). The increase in the photochemical age of the air mass during the spring and summer

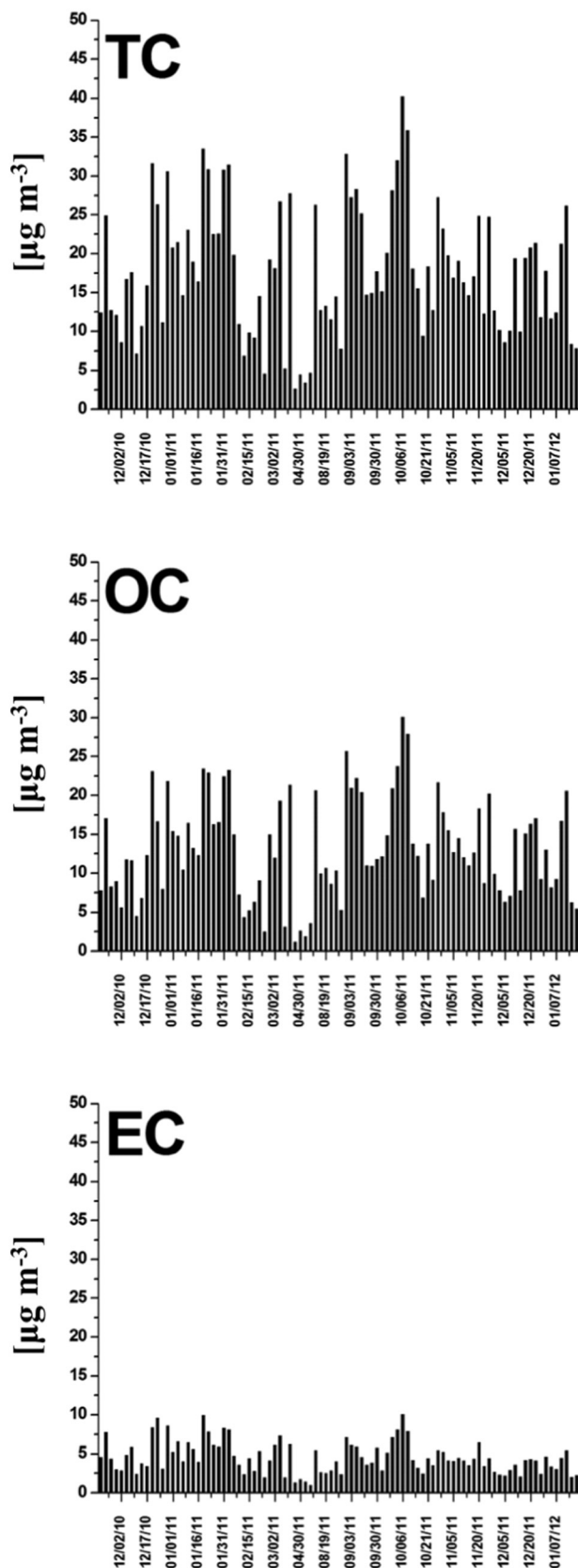


Fig. 2. Temporal variability in fine carbonaceous aerosol from November 2010 to January 2012 in CHAOS.

also played an important role in relatively high OC/EC ratios in the North China Plain (Wang et al., 2012). Alternatively, the fairly high OC/EC ratios simply can be attributed to the extraordinarily low EC

levels in rural areas, and thus the OC/EC ratio tended to be high. It is also important to note the probable relationship between biomass burning and the formation of SOA (Zeng and Wang, 2011). As a consequence, the burning of agricultural waste coupled with forest fires could have been responsible for the high OC/EC ratios.

Using Eq. (1), the PM_{2.5}-bound OC_{sec} concentrations and percentage contributions at CHAOS were $12.6 \pm 6.20 \mu\text{g m}^{-3}$ and $68.9 \pm 7.22\%$, respectively. The average percentage contribution was almost equivalent to that of Claremont, US PM_{2.5} (65%, Na et al., 2004) but almost four times and 1.7 times higher than those of Birmingham, UK (17%, Castro et al., 1999) and Kaohsiung (40.0%, Lin and Tai, 2001), respectively. This emphasizes the importance of long-range transport as the primary mechanism responsible for the relatively high observed OC/EC ratios at CHAOS, and thus other mechanisms, such as local agricultural waste and biomass burning, can be considered negligible.

3.2. Day-of-week trends of OC/EC ratios and OC_{soc}

Over the past few years, the application of OC/EC ratios has been widely used for elucidating the relationship between day-of-week trends and vehicular emission sources (Chinkin et al., 2003; Harley et al., 2005). As illustrated in the first and second sets of plots in Fig. 2, most of the tendencies in carbonaceous compositions were due to fluctuations in OC contents. Slight deviations were detected in day-of-week average concentrations of OC and EC (Fig. 2). Three-day average OC varied from $11.29 \pm 5.84 \mu\text{g m}^{-3}$ (Tuesday-to-Thursday) to $15.39 \pm 6.51 \mu\text{g m}^{-3}$ (Sunday-to-Tuesday), and the EC contributions differed from $4.16 \pm 1.55 \mu\text{g m}^{-3}$ (Tuesday-to-Thursday) to $5.06 \pm 1.78 \mu\text{g m}^{-3}$ (Sunday-to-Tuesday). Similarly, three-day average OC/EC ratios were between 2.48 ± 0.83 (Wednesday-to-Friday) to 3.18 ± 0.70 (Friday-to-Sunday), and the OC_{soc} values were between $65.56 \pm 9.28\%$ (Wednesday-to-Friday) to $72.22 \pm 4.82\%$ (Friday-to-Sunday). Although there were subtle changes in carbonaceous compositions, no statistically significant differences ($p < 0.05$) were found in the three-day average samples. This can be simply explained by the comparatively long sampling period of three days (i.e., 72 h). To investigate the impacts of the day-of-week trends on carbonaceous contents, all of the data were separated into two sets: a weekday group (i.e., the average of Monday to Wednesday, Tuesday to Thursday, and Wednesday to Friday) and a weekend group (i.e., Friday to

Sunday). After rearranging the variables into the two data sets, the OC/EC ratios and OC_{soc} of the weekend group were statistically larger ($p < 0.05$) than those of the weekday group. Thus it seems reasonable to assume that driving patterns were the most important factor governing PM_{2.5}-bound carbonaceous contents in Bangkok and surpassed other factors, such as meteorology and emission source strength.

Further attempts to analyse the day-of-week trends were conducted by separating the OC/EC ratios and OC_{soc} into four different quartiles based on their values (see Table 2). The relatively low OC/EC ratios were observed during the Tuesday-to-Thursday (25% in Q1) and Wednesday-to-Friday sampling periods (25% in Q1). Likewise, comparatively low OC_{soc} values were detected in the Tuesday-to-Thursday (20.8% in Q1), Wednesday-to-Friday (20.8% in Q1), and Thursday-to-Saturday (20.8% in Q1) monitoring intervals. These findings underline the prominence of vehicular emissions as a key factor controlling black carbon content and SOC formation in the urban atmosphere during the week. The fact that 26.1% of OC_{soc} in Q4 were observed in the Saturday-to-Monday samples indicates that the low traffic densities might have allowed long-range transport of fine particles (i.e., higher contents of OC_{soc}) that approached the city during the weekend.

As noticeably seen in Fig. 3, some distinguishing features can be obtained directly from the original Gaussian distribution curve. Firstly, a sharp symmetrical bell-shape curve was found for the EC samples in comparison to those of OC and TC. Because the detected values of EC are more concentrated in the middle than in the tails, it is reasonable to assume that this is the result of less spatial variance of EC in the background air mass, which was much less affected by atmospheric photo-oxidation, thermal degradation, homogeneous and/or heterogeneous chemical reactions. This can also be inferred as a consequence of a prevalent contribution of vehicular exhaust on the EC levels, particularly in the urban atmosphere. On the contrary, TC and OC show exceedingly broad peaks with flat tops between $18 \mu\text{g m}^{-3}$ and $13 \mu\text{g m}^{-3}$, respectively, which underlines the higher degree of variance than for EC. These flat symmetrical distribution curves also reveal that OC was more sensitive to meteorology and thus displays a broader peak than EC. This was in good agreement with the comparatively high percentage contribution of OC_{soc} observed at CHAOS ($68.9 \pm 7.22\%$), which supports the idea that OC appears to be more susceptible to meteorology than EC.

Table 2

The OC/EC ratios and OC_{soc} in PM_{2.5} coupled with its percentage contributions at CHAOS in four different quartiles based on their values.

	OC/EC – 1 ^a	OC/EC – 2 ^b	OC/EC – 3 ^c	OC/EC – 4 ^d	OC _{soc} – 1 ^a	OC _{soc} – 2 ^b	OC _{soc} – 3 ^c	OC _{soc} – 4 ^d
Monday–Wednesday	1	5	5	1	2	6	1	3
Tuesday–Thursday	6	2	2	5	5	3	5	2
Wednesday–Friday	6	3	1	3	5	3	2	3
Thursday–Saturday	4	6	2	2	5	2	4	2
Friday–Sunday	2	3	4	5	2	5	3	4
Saturday–Monday	4	2	5	4	3	3	4	6
Sunday–Tuesday	1	2	4	3	2	1	4	3
Total count	24	23	23	23	24	23	23	23
<i>Percentage contribution</i>								
Monday–Wednesday	4.2	21.7	21.7	4.3	8.3	26.1	4.3	13.0
Tuesday–Thursday	25.0	8.7	8.7	21.7	20.8	13.0	21.7	8.7
Wednesday–Friday	25.0	13.0	4.3	13.0	20.8	13.0	8.7	13.0
Thursday–Saturday	16.7	26.1	8.7	8.7	20.8	8.7	17.4	8.7
Friday–Sunday	8.3	13.0	17.4	21.7	8.3	21.7	13.0	17.4
Saturday–Monday	16.7	8.7	21.7	17.4	12.5	13.0	17.4	26.1
Sunday–Tuesday	4.2	8.7	17.4	13.0	8.3	4.3	17.4	13.0
Total %	100	100	100	100	100	100	100	100

^a First quartile (Q1).

^b Second quartile (Q2).

^c Third quartile (Q3).

^d Fourth quartile (Q4).

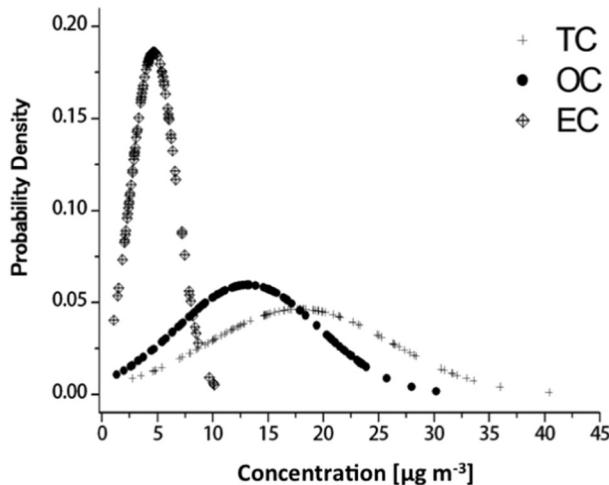


Fig. 3. Probability distribution of TC, OC and EC in $\text{PM}_{2.5}$ collected at CHAOS.

3.3. Autocorrelation of $\text{PM}_{2.5}$ and carbonaceous compositions

Generally, a correlogram is a mathematical tool for investigating randomness in a data set, which can be determined by calculating autocorrelations for data values at fluctuating time lags as described in Eqs. (3)–(5). In the case of random time series, such correlograms should be near zero for any and all time-lag intervals. In other words, the autocorrelation function should drop suddenly from 1 at zero lag to nearly zero at lags equal to one or larger. If non-random, then one or more of the correlograms will be significantly non-zero. Despite some differences in variance found in some atmospheric parameters, the time series approach employing autocorrelation plots showed a

fairly strong sinusoidal wave in $\text{PM}_{2.5}$, TC, OC, and EC, as displayed in the correlograms (see Fig. 4). Because all of the autocorrelation plots showed sinusoidal wave patterns, it is reasonable to state that the stochastic oscillations of the atmospheric parameters were not random. It is also crucial to stress that the majority of the R_h values of all atmospheric parameters were lower than the confidence bands (see Fig. 4). This reveals a higher degree of impacts that may be governed by the periodic component (i.e., the day-of-week trend) rather than other confounding factors (i.e., photo degradation, thermo degradation, heterogeneous and homogeneous chemical reactions, and meteorology). In addition, the similarities of the autocorrelation plots between TC and OC were in good agreement with the comparatively high percentage contribution of OC_{soc} previously mentioned in Section 3.1, which indicates that $\text{PM}_{2.5}$ -bound carbonaceous compositions in Bangkok were dominated by secondary organic carbon.

3.4. Simple linear regression analysis (SLRA)

As previously mentioned in Section 3.1, the comparatively high OC to EC ratios at CHAOS were possibly associated with high OC rather than low EC values. There are three probable reasons: anthropogenic emissions, biogenic emissions, and long-range transport of carbonaceous compositions from outside of Bangkok. Because previous studies have highlighted the importance of traffic emissions on air quality in Bangkok (Pongpiachan, 2013; Pongpiachan et al., 2013a, 2013b, 2014b), biogenic emissions of carbonaceous aerosols were not likely a major source of the measured high OC contents at CHAOS. The comparative contributions of long-range transport and local biogenic emissions were investigated using a simple linear regression analysis between OC and EC contents. If the majority of the particulate OC around CHAOS was influenced by biogenic emissions, the R -value of OC and EC should be low because EC are mainly released from transportation. On the contrary, if the R -values of OC and EC are high, it can be reasonably

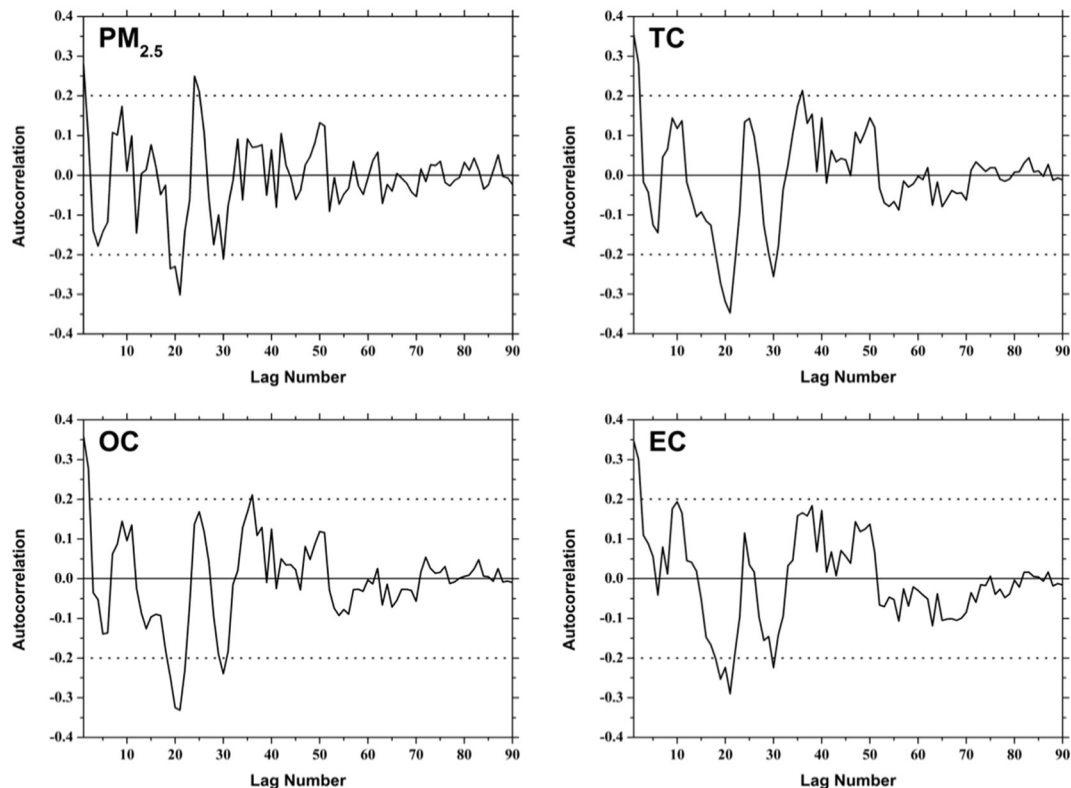


Fig. 4. Plots of autocorrelation using contents of TC, OC and EC in $\text{PM}_{2.5}$ collected at CHAOS.

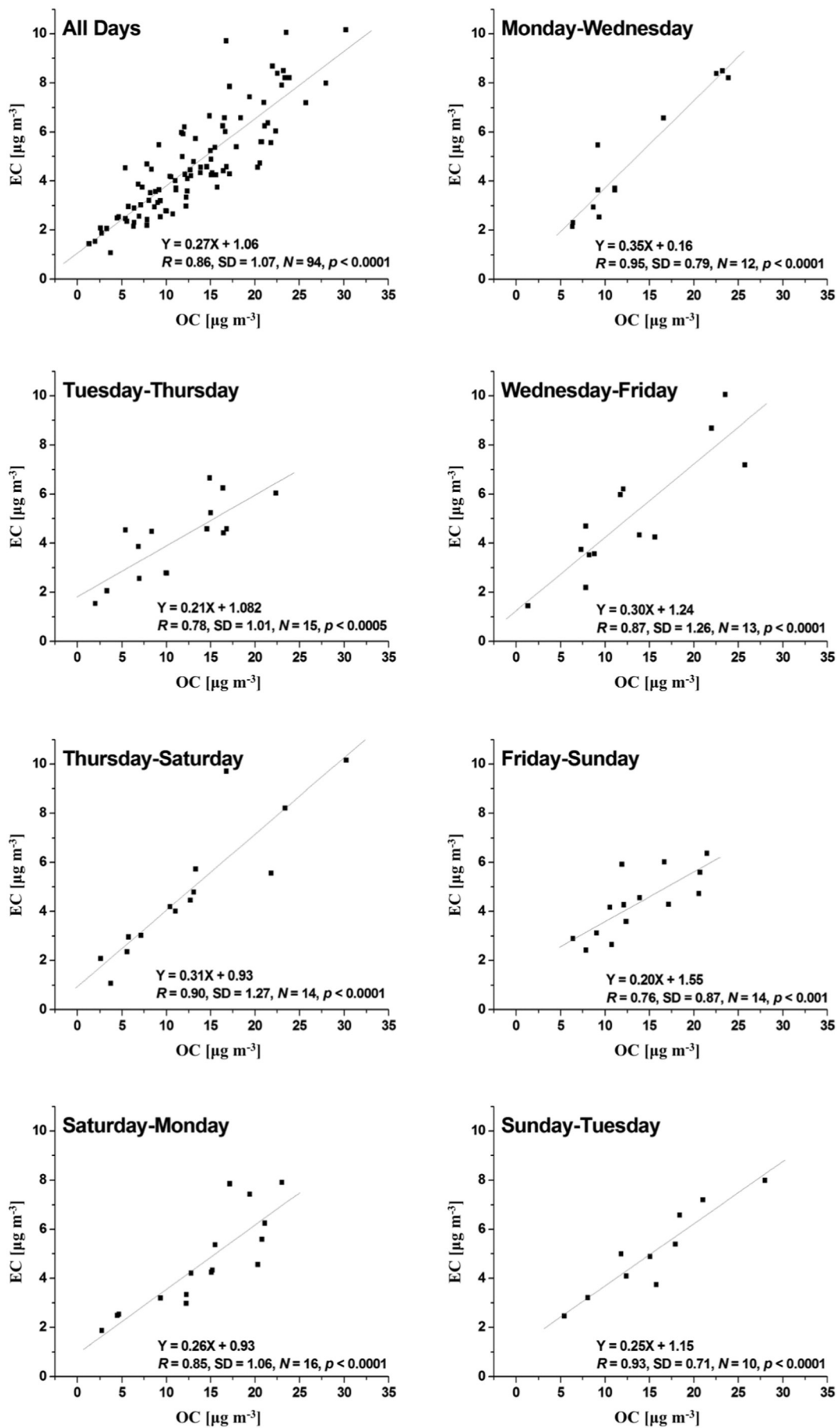


Fig. 5. Linear regression analysis of OC and EC observed in CHAOS.

concluded that both are emitted simultaneously from a single source, namely transportation (Chen et al., 2012).

To test this hypothesis and to assess the impact of the day-of-week trend to carbonaceous composition levels at CHAOS, a linear regression between the OC and EC contents in each sampling interval was applied (See Fig. 5). In general, a high R -value ($R = 0.86$) coupled with a lower p -value ($p < 0.0001$) was found in all of the sampling periods, which suggests a single dominant emission source (mostly traffic-related) in Bangkok. This finding is in good agreement with a previous study conducted in the southern China coastal area at Xiamen, which found a strong positive correlation ($R = 0.91$) between OC and EC during the winter monsoon season as a consequence of prevailing vehicular exhausts (Chen et al., 2012). On the contrary, the lowest R -value ($R = 0.76$, $p < 0.0001$) was detected in the Friday-to-Sunday samples. These results reflect a comparatively smaller contribution of mobile emissions on carbonaceous content during the weekend, which was consistent with the relatively high OC_{soc} ($72.22 \pm 4.82\%$) observed from Friday-to-Sunday (see Section 3.2). The highest R -value ($R = 0.95$, $p < 0.0001$) observed in the Monday-to-Wednesday samples indicates that both OC and EC were released simultaneously and thus underlines the importance of transportation on carbonaceous compositions during working days.

3.5. Hierarchical cluster analysis (HCA)

To obtain more information on the origins of the carbonaceous compositions collected at CHAOS, HCA was conducted on the eight variables ($n = 94$), which were TC, OC, EC, buses, Tuktuks, trucks, pick-ups/vans, and cars. The cluster analysis revealed the presence of three different groups, as displayed in the dendrogram in Fig. 6. The first cluster consisted of TC, OC, EC, buses, Tuktuks, and trucks. Because the majority of buses and trucks are powered by diesel engines, this cluster clearly indicates that heavy-duty vehicles (HDVs) appear to have been responsible for the increase of ambient carbonaceous compositions. These findings are consistent with previous studies of measurements of particulate matter from on-road vehicles and inside a tunnel, which highlighted that diesel engines had higher emission rates than did gasoline and LPG engines for most carbonaceous fractions (Cheng et al., 2010; He et al., 2006). The second sub-cluster was composed of pick-ups/vans, which is indicative of a mixing of the three types of fuel, namely "diesel", "gasohol", and "benzene". Gasohol is a mixture of gasoline and ethanol, which is an alternative fuel to 100% gasoline and helps lessen the consumption of gasoline, and has been on the market since 2001 in Thailand. (See Fig. 6.)

The third cluster contained only personal cars, for which gasohol is the main fuel. On January 1, 2013, the Thailand government abandoned

the sale of regular octane 91 gasoline to promote gasohol usage. As a consequence, ethanol consumption rapidly rose from 1.3 million L day $^{-1}$ in 2012 to 2.0 million L day $^{-1}$ in 2014. The Department of Alternative Energy Development and Efficiency, Ministry of Energy, launched the new energy policy with a target to enhance ethanol usage, primarily of E20 and E85, to 3.0 million L day $^{-1}$ in 2015 and to 9.9 million L day $^{-1}$ in 2021. This will inevitably affect the emission factors of OC and EC from vehicular exhausts and thus the atmospheric contents of carbonaceous aerosols in the near future. As a consequence, it is reasonable to conclude that the proximity in the dendrogram of vehicle type vs. carbonaceous compositions is directly related to the fuel and engine types. In addition, driving patterns coupled with road conditions can dramatically change the emission factors of OC and EC and thus need to be considered in future work.

3.6. Principal component analysis (PCA)

Generally, PCA can be applied as a multivariate statistical tool to reduce a set of original variables (i.e., PM_{2.5}-bound carbonaceous compositions and vehicle types) and to extract a small number of latent factors (i.e., principal components, PCs), to investigate associations among the measured parameters. The data that were accepted for investigation were organized into a matrix, where each column was a parameter component and the samples were in the rows. The data matrices were analysed using PCA, which permitted the reviewed data to be further assessed and plotted in three dimensions. In this study, the principal component patterns for Varimax rotated components were composed of three components, namely PC1 (36.9%), PC2 (27.2%) and PC3 (17.2%), which accounted for 81.3% of the total variance.

The clearest 3D plot features displayed in Fig. 7 are (i) the TC, OC, EC, and pick-ups/vans are grouped together, (ii) Tuktuks and buses are highly separated from the carbonaceous compositions and pick-ups/vans, and (iii) the cars and trucks are closer to the TC, OC, and EC group than Tuktuks and buses. While the dendrogram shows the close proximities of carbonaceous composition groups with buses, Tuktuks, and trucks (see Section 3.5), the PCA 3D plots show the strong associations between carbonaceous aerosols and pick-ups/vans. This discrepancy may merely reflect a difference in the statistical analogy between PCA and HCA. While PCA is a multivariate statistical technique used for reducing a set of elements by selecting the attributes with the most variation, HCA is an unsupervised learning method to find groups of similarities based on attribute values. Despite the differences in these two statistical tools, the strong influence of diesel vehicles (e.g., buses, pick-ups/vans, trucks) on PM_{2.5}-bounded carbonaceous particles is undoubtedly obvious. Because the majority of pick-ups/vans consume

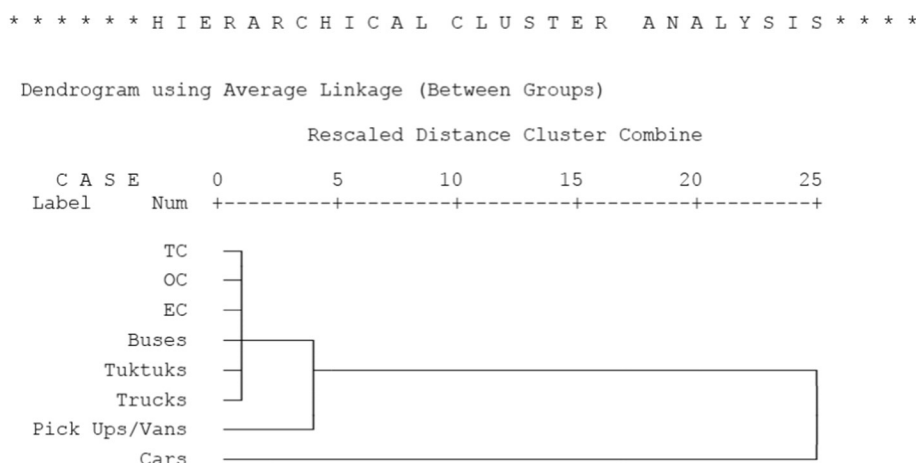


Fig. 6. Dendrogram of hierarchical cluster analysis using average linkage (between groups).

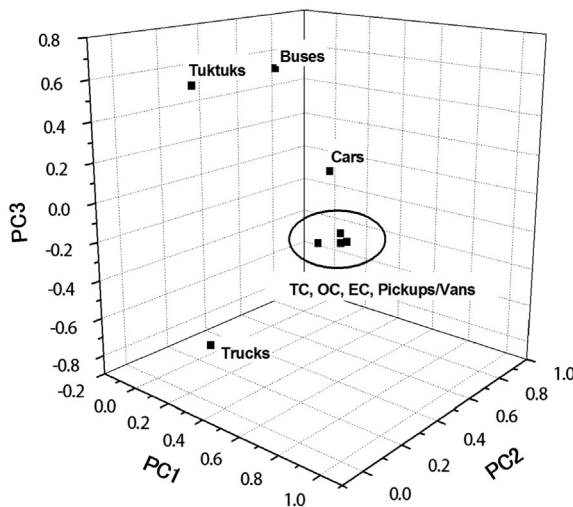


Fig. 7. Three-dimensional plots of principal components of TC, OC, EC, pickups/vans, trucks, cars, buses and Tuktuks.

diesel fuels, it appears reasonable to ascribe the strong affinity between carbonaceous compositions and pick-up/vans as a consequence of the diesel engine combustion process. This interpretation is also supported by the 3D proximity of cars and trucks with the carbonaceous aerosols. In addition, it is also noteworthy that the air sample collections in the tunnel prove that diesel engine emissions contribute most of the carbonaceous compositions in the urban atmosphere (Cheng et al., 2010; He et al., 2006).

4. Conclusions

This study attempts to conduct the time series analysis based on the long term monitoring of PM_{2.5}-bounded OC/EC collected at ONE monitoring site. According to our best knowledge, this is the only long term monitoring data of PM_{2.5}-bounded carbonaceous fractions in Thailand. Since this study use the 48 h sampling period data, it appears reasonable to interpret that the impacts of local thermal circulation are minor of importance. The analysis of day-of-week trends of OC/EC ratios, the time series results and OC_{soot} reveal that vehicle fleets are the most influential factors governing the atmospheric content of PM_{2.5}-bound carbonaceous compositions. Although traffic emissions played an important role in controlling carbonaceous aerosols during the week, multiple types of emission sources, including the long-range transport, appear to have been the main contributors on weekends. Irrespective of some discrepancies that occurred from the application of HCA and PCA to investigate the relationship between carbonaceous compositions and vehicle types, the overwhelming contribution from diesel emissions on the PM_{2.5}-bound TC, OC, and EC is unquestionably evident. This leads to greater public health concerns of urban air quality. Overall, a variety of emission control strategies for different categories of in-use HDVs, coupled with multiple effective solutions for most fleets in both weekday and weekend periods, will be required to improve air quality in Bangkok.

Acknowledgements

This work was performed with the approval of the Institute of Earth Environment, Chinese Academy of Sciences (IEE CAS) and the National Institute of Development Administration (NIDA). The authors acknowledge the academic staffs from the Faculty of Sciences, Chulalongkorn University, for their assistances with the PM_{2.5} field sampling.

References

- Bae, M.S., Schauer, J.J., DeMinter, J.T., Turner, J.R., 2004. Hourly and daily patterns of particle-phase organic and elemental carbon concentrations in the urban atmosphere. *J. Air Waste Manage. Assoc.* 54 (7), 823–833.
- Cao, J.J., Lee, S.C., Ho, K.F., Zhang, X.Y., Zou, S.C., Fung, K.K., Chow, J.C., Watson, J.G., 2003. Characteristics of carbonaceous aerosol in Pearl River Delta region, China during 2001 winter period. *Atmos. Environ.* 37 (11), 1451–1460.
- Cao, J.J., Wu, F., Chow, J.C., et al., 2005. Characterization and source apportionment of atmospheric organic and elemental carbon during fall and winter of 2003 in Xi'an, China. *Atmos. Chem. Phys.* 5, 3127–3137.
- Castro, M.L., Pio, A.C., Harrison, M.R., Smith, T.J.D., 1999. Carbonaceous aerosols in urban and rural European atmospheres: estimation of secondary organic carbon concentrations. *Atmos. Environ.* 33 (17), 2771–2781.
- Chen, B., Du, K., Wang, Y., Chen, J., Zhao, J., Wang, K., Zhang, F., Xu, L., 2012. Emission and transport of carbonaceous aerosols in urbanized coastal areas in China. *Aerosol Air Qual. Res.* 12, 371–378.
- Cheng, Y., Lee, S.C., Ho, K.F., Chow, J.C., Watson, J.G., Louie, P.K.K., Cao, J.J., Hai, X., 2010. Chemically-specified on-road PM_{2.5} motor vehicle emission factors in Hong Kong. *Sci. Total Environ.* 408 (7), 1621–1627 (1 March 2010).
- Chinkin, L.R., Coe, D.L., Funk, T.H., Hafner, H.R., Roberts, P.T., Ryan, P.A., Lawson, D.R., 2003. Weekday versus weekend activity patterns for ozone precursor emissions in California's South Coast Air Basin. *J. Air Waste Manage. Assoc.* 53 (7), 829–843.
- Chow, J.C., 2003. Introduction to special topic: weekend and weekday differences in ozone levels. *J. Air Waste Manage. Assoc.* 53 (7), 771.
- Chow, J.C., Watson, J.G., Crow, D., Lowenthal, D.H., Merrifield, T.M., 2001. Comparison of IMPROVE and NIOSH carbon measurements. *Aerosol Sci. Technol.* 34 (1), 23–34.
- Fu, X., Wang, X., Guo, H., Cheung, K., Ding, X., Zhao, X., He, Q., Gao, B., Zhang, Z., Liu, T., Zhang, Y., 2014. Trends of ambient fine particles and major chemical components in the Pearl River Delta region: observation at a regional background site in fall and Winter. *Sci. Total Environ.* 497–498, 274–281.
- Fung, K.K., Chow, J.C., Watson, J.G., 2002. Evaluation of OC/EC speciation by thermal manganese dioxide oxidation and the IMPROVE method. *J. Air Waste Manage. Assoc.* 52 (11), 1333–1341.
- Greaves, S., Issarayangyun, T., Liu, Q., 2008. Exploring variability in pedestrian exposure to fine particulates (PM_{2.5}) along a busy road. *Atmos. Environ.* 42 (8), 1665–1676.
- Harley, R.A., Marr, L.C., Lehner, J.K., Giddings, S.N., 2005. Changes in motor vehicle emissions on diurnal to decadal time scales and effects on atmospheric composition. *Environ. Monit. Sci. Technol.* 39 (14), 5356–5362.
- He, L.Y., Hu, M., Huang, X.F., Zhang, Y.H., Yu, B.D., Liu, D.Q., 2006. Chemical characterization of fine particles from on-road vehicles in the Wutong tunnel in Shenzhen, China. *Chemosphere* 62, 1565–1573.
- Huang, X.F., Xue, L., Tian, X.D., Shao, W.W., Sun, T.L., Gong, Z.H., Ju, W.W., Jiang, B., Hu, M., He, L.Y., 2013. Highly time-resolved carbonaceous aerosol characterization in Yangtze River Delta of China: composition, mixing state and secondary formation. *Atmos. Environ.* 64, 200–207.
- Hueglin, C., Gehrig, R., Baltensperger, U., et al., 2005. Chemical characterisation of PM_{2.5}, PM₁₀ and coarse particles at urban, near-city and rural sites in Switzerland. *Atmos. Environ.* 39, 637–651.
- Künzi, L., Mertes, P., Schneider, S., Jeannet, N., Menzi, C., Dommen, J., Baltensperger, U., Prévôt, A.S.H., Salathe, M., Kalberer, M., Geiser, M., 2013. Responses of lung cells to realistic exposure of primary and aged carbonaceous aerosols. *Atmos. Environ.* 8, 143–150.
- Li, C., Tsay, C.S., Hsu, C.N., Kim, Y.J., Howell, G.S., Huebert, J.B., Ji, Q., Jeong, J.M., Wang, H.S., Hansell, A.R., Bell, W.S., 2012. Characteristics and composition of atmospheric aerosols in Phimai, central Thailand during BASE-ASIA. *Atmos. Environ.* 78, 60–71.
- Lin, J.J., Tai, S.H., 2001. Concentrations and distributions of carbonaceous species in ambient particles in Kaohsiung City, Taiwan. *Atmos. Environ.* 35 (15), 2627–2636.
- Na, K., Sawant, A.A., Song, C., Cocker III, D.R., 2004. Primary and Secondary Carbonaceous Species in the Atmosphere of Western Riverside County, California. *Atmos. Environ.* 38, 1345–1355.
- Pongpiachan, S., 2013. Vertical distribution and potential risk of particulate polycyclic aromatic hydrocarbons in high buildings of Bangkok, Thailand. *Asian Pac. J. Cancer Prev.* 14 (3), 1865–1877.
- Pongpiachan, S., Paowa, T., 2014. Hospital out-and-in-patients as functions of trace gaseous species and other meteorological parameters in Chiang-Mai, Thailand. *Aerosol Air Qual. Res.* X, 1–15 (doi: 10.4209/aaqr.2013.09.0293).
- Pongpiachan, S., Thammanu, K., Ho, K.F., Lee, S.C., Sompongchaiyakul, P., 2009. Predictions of gas-particle partitioning coefficients (K_p) of polycyclic aromatic hydrocarbons at various occupational environments of Songkhla Province, Thailand. *Southeast Asian J. Trop. Med. Public Health* 40 (6), 1377–1394.
- Pongpiachan, S., Ho, K.F., Cao, J., 2013a. Estimation of gas-particle partitioning coefficients (K_p) of carcinogenic polycyclic aromatic hydrocarbons by carbonaceous aerosols collected at Chiang-Mai, Bangkok and Hat-Yai, Thailand. *Asian Pac. J. Cancer Prev.* 14 (4), 3369–3384.
- Pongpiachan, S., Choochay, C., Hattayanone, M., Kositanont, C., 2013b. Temporal and spatial distribution of particulate carcinogens and mutagens in Bangkok, Thailand. *Asian Pac. J. Cancer Prev.* 14 (3), 1879–1887.
- Pongpiachan, S., Ho, K.F., Cao, J., 2014a. Effects of biomass and agricultural waste burnings on diurnal variation and vertical distribution of OC/EC in Hat-Yai City, Thailand. *Asian J. Appl. Sci.* <http://dx.doi.org/10.3923/ajaps.2014>.
- Pongpiachan, S., Kudo, S., Sekiguchi, K., 2014b. Chemical characterization of carbonaceous PM₁₀ in Bangkok, Thailand. *Asian J. Appl. Sci.* <http://dx.doi.org/10.3923/ajaps.2014>.
- Repine, E.J., Reiss, K.O., Elkins, N., Chughtai, R.A., Smith, M.D., 2008. Effects of fine carbonaceous particles containing high and low unpaired electron spin densities on lungs of female mice. *Transl. Res.* 152 (4), 185–193.

- Safai, P.D., Raju, M.P., Rao, P.S.P., Pandithurai, G., 2014. Characterization of carbonaceous aerosols over the urban tropical location and a new approach to evaluate their climatic importance. *Atmos. Environ.* 92, 493–500.
- Shen, G., Xue, M., Chen, Y., Yang, C., Li, W., Shen, H., Huang, Y., Zhang, Y., Chen, H., Zhu, Y., Wu, H., Ding, A., Tao, S., 2014. Comparison of carbonaceous particulate matter emission factors among different solid fuels burned in residential stoves. *Atmos. Environ.* 89, 337–345.
- Soni, K., Kapoor, S., Parmar, K.S., Kaskaoutis, D.G., 2014. Statistical analysis of aerosols over the Gangetic–Himalayan region using ARIMA model based on long-term MODIS observations. *Atmos. Res.* 149, 174–192.
- Srivastava, A.K., Bisht, D.S., Ram, K., Tiwari, S., Srivastava, M.K., 2014. Characterization of carbonaceous aerosols over Delhi in Ganga basin: seasonal variability and possible sources. *Environ. Sci. Pollut. Res. Int.* 21 (14), 8610–8619. <http://dx.doi.org/10.1007/s11356-014-2660-y>.
- Tao, J., Shen, Z., Zhu, C., Yue, J., Cao, J., Liu, S., Zhu, L., Zhang, R., 2012. Seasonal variations and chemical characteristics of sub-micrometer particles (PM1) in Guangzhou, China. *Atmos. Res.* 118, 222–231.
- Turpin, B.J., Huntzicker, J.J., 1995. Identification of secondary organic aerosol episodes and quantitation of primary and secondary organic aerosol concentrations during SCAQS. *Atmos. Environ.* 29, 3527–3544.
- US-EPA, 1998. Quality Assurance Guidance Document 2.12; Monitoring PM2.5 in Ambient Air Using Designated Reference or Class I Equivalent Methods. <http://www.epa.gov/ttnamti1/files/ambient/pm25/qa/m212covid.pdf>.
- US-EPA, 2012. Report to Congress on Black Carbon. Department of the interior, environment, and related agencies appropriations act, 2010 (EPA-450/R-12-001).
- Wang, Z., Wang, T., Guo, J., Gao, R., Xue, L., Zhang, J., Zhou, Y., Zhou, X., Zhang, Q., Wang, W., 2012. Formation of secondary organic carbon and cloud impact on carbonaceous aerosols at Mount Tai, North China. *Atmos. Environ.* 46, 516–527.
- Wei, S., Shen, G., Zhang, Y., Xue, M., Xie, H., Lin, P., Chen, Y., Wang, X., Tao, S., 2014. Field measurement on the emissions of PM, OC, EC and PAHs from indoor crop straw burning in rural China. *Environ. Pollut.* 184, 18–24.
- Zeng, T., Wang, Y., 2011. Nationwide summer peaks of OC/EC ratios in the contiguous United States. *Atmos. Environ.* 45, 578–586.
- Zhang, R., Ho, K.F., Cao, J., Han, Z., Zhang, M., Cheng, Y., Lee, S.C., 2009. Organic carbon and elemental carbon associated with PM10 in Beijing during spring time. *J. Hazard. Mater.* 172 (2–3), 970–977.
- Zhang, G., Li, J., Li, X.D., Xu, Y., Guo, L.L., Tang, J.H., Lee, C.S.L., Liu, X., Chen, Y.J., 2010. Impact of anthropogenic emissions and open biomass burning on regional carbonaceous aerosols in South China. *Environ. Pollut.* 158 (11), 3392–3400.
- Zhang, F., Zhao, J., Chen, J., Xu, Y., Xu, L., 2011. Pollution characteristics of organic and elemental carbon in PM2.5 in Xiamen, China. *J. Environ. Sci.* 23 (8), 1342–1349.
- Zhou, S., Wang, Z., Gao, R., Xue, L., Yuan, C., Wang, T., Gao, X., Wang, X., Nie, W., Xu, Z., Zhang, Q., Wang, W., 2012. Formation of secondary organic carbon and long-range transport of carbonaceous aerosols at Mount Heng in South China. *Atmos. Environ.* 63, 203–212.

RESEARCH ARTICLE

Assessment of Reliability when Using Diagnostic Binary Ratios of Polycyclic Aromatic Hydrocarbons in Ambient Air PM₁₀

Siwatt Pongpiachan

Abstract

The reliability of using diagnostic binary ratios of particulate carcinogenic polycyclic aromatic hydrocarbons (PAHs) as chemical tracers for source characterisation was assessed by collecting PM10 samples from various air quality observatory sites in Thailand. The major objectives of this research were to evaluate the effects of day and night on the alterations of six different PAH diagnostic binary ratios: An/(An + Phe), Fluo/(Fluo + Pyr), B[a]A/(B[a]A + Chry), B[a]P/(B[a]P + B[e]P), Ind/(Ind + B[g,h,i]P), and B[k]F/Ind, and to investigate the impacts of site-specific conditions on the alterations of PAH diagnostic binary ratios by applying the concept of the coefficient of divergence (COD). No significant differences between day and night were found for any of the diagnostic binary ratios of PAHs, which indicates that the photodecomposition process is of minor importance in terms of PAH reduction. Interestingly, comparatively high values of COD for An/(An + Phe) in PM10 collected from sites with heavy traffic and in residential zones underline the influence of heterogeneous reactions triggered by oxidising gaseous species from vehicular exhausts. Therefore, special attention must be paid when interpreting the data of these diagnostic binary ratios, particularly for cases of low-molecular-weight PAHs.

Keywords: Diagnostic binary ratios - PAHs - photolysis - spatial distribution

Asian Pac J Cancer Prev, **16** (18), 8605-8611

Introduction

Over recent decades, major advances have been made in elucidating the environmental fate and behaviour of polycyclic aromatic hydrocarbons (PAHs) in various environmental situations (Pongpiachan, 2013a,b, 2014, 2015; Pongpiachan et al., 2013a,b,c, 2015a,b). The principal reasons for investigating environmental concentrations of PAHs relate to their adverse effects on health, such as their potential to disrupt the endocrine system (Annamalai and Namasivayam, 2015), increase anxiety-related behaviour and decrease regional brain metabolism in adult male rats (Crépeaux et al., 2012), and cause adverse reproductive outcomes (Šrám et al., 1999), DNA damage to lungs (Müller et al., 2004), the development of solid tumours in mice (Wang and Xue, 2015), and increased risks of coupled lung and breast cancers (Venkatachalam et al., 2014; Moorthy et al., 2015). As a consequence of the numerous adverse health effects, several studies have used receptor models, including principal component analysis (Pongpiachan, 2013b), positive matrix factorisation (Jang et al., 2013), and a chemical mass balance model (Hanedar et al., 2011), to quantitatively identify potential sources of atmospheric PAHs.

Selecting one among the many source-apportionment

models is undoubtedly an important and difficult task because of the requirements for specific skill, knowledge, and experience. Conversely, the application of diagnostic binary ratios of PAH congeners to categorise their potential sources is a comparatively simple process, which provides a broad comprehensive perspective of source classification. For these particular reasons, diagnostic binary ratios of PAHs have been used widely as promising chemical tracers in marine deposits, terrestrial soils, atmospheric particles, and agricultural products (Tipmanee et al., 2012; Alam et al., 2013; Pongpiachan, 2014, 2015; Pongpiachan et al., 2015a,b).

Despite their capability in classifying emission source types, some ambiguities remain regarding the reliability of diagnostic binary ratios of PAHs. Generally, the vast majority of studies associated with the application of PAH binary ratios have paid little attention to adsorption, volatilisation, photolysis, and chemical and microbial degradation, which can selectively decrease the atmospheric contents of low-molecular-weight (LMW) PAHs in comparison with those of high-molecular-weight (HMW) congeners. Previous studies have highlighted the importance of meteorological parameters (e.g., ambient temperature and relative humidity), sub-cooled liquid vapour pressures (p^oL), the octanol-air partitioning coefficient (KOA), and the soot-air partitioning coefficient

(KSA) on the gas-particle partitioning coefficient of PAHs (Dachs and Eisenreich, 2000; Odabasi et al., 2006; Pongpiachan, 2010; Pongpiachan et al., 2010, 2013b; Wang et al., 2013). According to Gao et al. (2015), gas-particle partitioning can play a significant role in estimations of the source apportionment of atmospheric PAHs and their toxicity using positive matrix factorisation. Furthermore, PAHs can be degraded by sulphate anion radicals in atmospheric aqueous droplets (Wang et al., 2008) as well as by photo-decomposition by UV light (Wang et al., 2005) coupled with both homogeneous and heterogeneous chemical reactions with atmospheric oxidants (Ringuet et al., 2012a; Zhang et al., 2013).

Although several factors can dramatically affect the reduction of each PAH congener with different magnitudes, little is known about the reliability of using their binary ratios as chemical tracers of emission sources, particularly in the tropical atmosphere. One of the many crucial aspects of the current study concerned the effects of day and night on the variations of diagnostic binary ratios of PM_{10} -bounded PAHs collected from three different cities in Thailand. During the past few years, numerous studies have investigated the impact of diurnal variations on the fluctuation of atmospheric contents of PAHs (Ringuet et al., 2012b; Liu et al., 2013; Ohura et al., 2013) but none has examined the impacts of day and night on the alteration of their binary ratios. Furthermore, the influence of sampling site on the fluctuation of each PAH diagnostic binary ratio remains unclear and its elucidation is critical. Overall, the principal objectives of this study were (*i*) to investigate the impacts of day and night on the variation of PAH diagnostic binary ratios, including anthracene and phenanthrene ($\text{An}/(\text{An} + \text{Phe})$), fluoranthene and pyrene ($\text{Fluo}/(\text{Fluo} + \text{Pyr})$), benzo[a]anthracene and chrysene ($\text{B}[a]\text{A}/(\text{B}[a]\text{A} + \text{Chry})$), benzo[a]pyrene and benzo[e] pyrene ($\text{B}[a]\text{P}/(\text{B}[a]\text{P} + \text{B}[e]\text{P})$), indeno[1,2,3,-c,d] pyrene and benzo[g,h,i]perylene ($\text{Ind}/(\text{Ind} + \text{B}[g,h,i]\text{P})$), and benzo[k]fluoranthene and indeno[1,2,3,-c,d]pyrene ($\text{B}[k]\text{F}/\text{Ind}$), and (*ii*) to assess the influence of air quality observatory sites on the fluctuation of PAH diagnostic binary ratios; specifically, $\text{An}/(\text{An} + \text{Phe})$ and $\text{Fluo}/(\text{Fluo} + \text{Pyr})$. In addition, in the current paper, the concept of the coefficient of divergence (COD) is introduced and discussed further.

Materials and Methods

Description of air quality observatory sites and PM_{10} sample collection

The monitoring campaign adopted in this study can be broadly categorised into three sections. Firstly, the Spatial Distributions of PM_{10} -bounded PAHs based on a Monitoring Campaign (SDPMC) were carefully assessed using seven air quality monitoring sites operated by the Pollution Control Department of the Ministry of Natural Resources and Environment, Thailand: Klongchan National Housing Authority (KHA; $13^{\circ}49'11.761''\text{N}$, $100^{\circ}34'33.190''\text{E}$), Nonsreewitayakom High School (NWS; $13^{\circ}42'28.937''\text{N}$, $100^{\circ}32'50.443''\text{E}$), Singharaj Pitayakhom High School (SPS), Thonburi Power Substation (TPS; $13^{\circ}43'39.205''\text{N}$, $100^{\circ}29'11.776''\text{E}$),

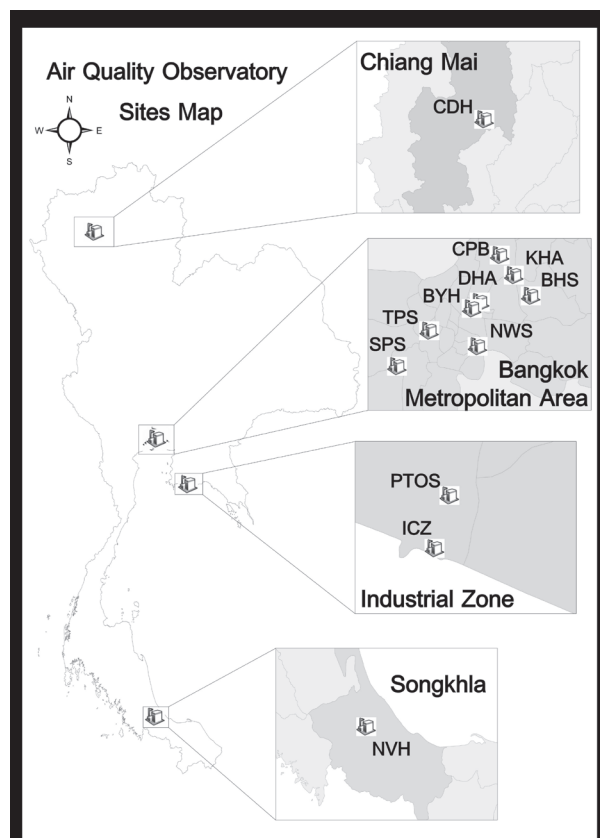


Figure 1. Map of Air Quality Observatory Sites in this Study

Chokchai 4 Police Box (CPB; $13^{\circ}47'33.474''\text{N}$, $100^{\circ}35'45.879''\text{E}$), Dindang National Housing Authority (DHA; $13^{\circ}46'59.544''\text{N}$, $100^{\circ}32'25.618''\text{E}$), and Badindecha High School (BHS; $13^{\circ}46'10.745''\text{N}$, $100^{\circ}36'52.433''\text{E}$) (see Figure 1). It should be noted that sites CPB, KHA, and DHA were situated adjacent to traffic routes, reflecting PAH emissions from vehicular exhausts, whilst sites NWS, SPS, TPS, and BHS, located in residential areas, reflected residential background PAH emissions. Air quality observation campaigns were conducted concurrently at all monitoring sites on a normal weekday every month from January 2006 to December 2006, which provided a database of 84 individual PM_{10} samples (i.e., $12 \times 7 = 84$).

Secondly, the Diurnal variations of PM_{10} -bounded PAHs based on an Intensive Monitoring Campaign (DPIMC) were prudently chosen using three different air quality monitoring sites: the Baiyoke Suite Hotel (BYH; $13^{\circ}45'10.65''\text{N}$, $100^{\circ}32'24.92''\text{E}$), Centara Duangtawan Hotel (CDH; $18^{\circ}47'03.46''\text{N}$, $98^{\circ}59'56.72''\text{E}$), and Novotel Centara Hat-Yai Hotel (NVH; $7^{\circ}00'20.65''\text{N}$, $100^{\circ}28'15.65''\text{E}$), as clearly illustrated in Figure 1. It is worth mentioning that BYH, CDH, and NVH are located in the city centre of Bangkok, Chiang-Mai, and Hat-Yai, respectively. In the case of BYH, PM_{10} samples were collected every three hours consecutively from 21:00 local time (LT) 18 February to 21:00 LT 21 February 2008, whilst those of CDH were sampled every three hours sequentially from 21:00 LT 25 February to 21:00 LT 28 February 2008. In addition, the variations of PM_{10} -bounded PAHs were measured at NVH every three hours consecutively from 21:00 LT 17 December to 21:00 LT 20

Assessment of Reliability when Using Diagnostic Binary Ratios of Polycyclic Aromatic Hydrocarbons in Ambient Air PM₁₀

December 2007. These measurements provided a database of 72 individual PM₁₀ samples (i.e., 8 × 3 × 3 = 72).

Thirdly, Concurrent Monitoring of PM₁₀-bounded PAHs in Industrial Areas (CMPIA) was performed at the Pluakgate Temple Observatory Station (PTOS) (12°39'41.70"N, 101°18'53.62"E) and IRPC Complex Zone Observatory Station (ICZOS) (12°39'10.46"N, 101°18'7.66"E). The PTOS is situated within a petrochemical industrial area of Tumbol Cherngnern, Muang District in Rayong Province, which is located approximately 1.2 km northeast of the IRPC refineries (Figure 1). The ICZOS (12°39'10.46"N, 101°18'7.66"E) was chosen because of its proximity to the IRPC seaport (i.e., a distance of approximately 1.4 km), meaning that it could be considered representative of a mixture of shipping and industrial emissions. Graseby-Anderson (TE-6001) high volume air samplers were used to achieve unmanned 24-h and 3-h samplings of PM₁₀ for SDPMC coupled with CMPIA and DPIMC, respectively. Samples of PM₁₀ were collected on 20 × 25 cm Whatman glass fibre filters under an airflow rate of about 1.133 m³ min⁻¹ (i.e., 40 cfm). A comprehensive explanation of the air sampling method is given in "Compendium Method IO-2.2. Sampling of Ambient Air for PM₁₀ using an Andersen Dichotomous Sampler" (US-EPA, 1999). Samples of total ambient PM₁₀ from both PTOS and ICZOS were collected on 75 days in discontinuous sequences from 1-10 February 2010 (n = 10), 19-28 April 2011 (n = 10), 5-14 March 2012 (n = 10), 27-31 October 2012 (n = 5), 22-31 March 2013 (n = 10), and 7 June to 6 July 2013 (n = 30). Samples of PM₁₀ were collected simultaneously at both sites for 24 h every day from 09:00 LT to 09:00 LT on the following day. These observations provided a database of 150 individual PM₁₀ samples (i.e., 75 × 2 = 150).

Analysis of PAHs

All organic solvents (i.e., dichloromethane and hexane) were HPLC grade, purchased from Fisher Scientific. A cocktail of 11 PAHs to Norwegian Standard NS 9815: S-4008-100-T (phenanthrene (Phe), anthracene (An), fluoranthene (Fluo), pyrene (Pyr), benz[a]anthracene (B[a]A), chrysene (Chry), benzo[k]fluoranthene (B[k]F), benzo[a]pyrene (B[a]P), benzo[e]pyrene (B[e]P), indeno[1,2,3-c,d]pyrene (Ind), and benzo[g,h,i]perylene (B[g,h,i]P); each 100 µg mL⁻¹ in toluene: unit: 1 × 1 mL) and a mixture of recovery Internal Standard PAHs (d₁₂-perylene (d₁₂-Per), d₁₀-fluorene (d₁₀-Fl)); each 100 µg mL⁻¹ in xylene: unit: 1 × 1 mL) were supplied by Chiron AS (Stiklestadveine 1, N-7041 Trondheim, Norway). Standard stock solutions of 4 µg mL⁻¹ of deuterated PAHs (used as internal standards) and 100 µg mL⁻¹ of native PAHs were prepared in nonane. The dilution of the working standards was conducted using n-cyclohexane. A half-cut sample of the glass fibre filter was transferred to a 250 mL Soxhlet extractor and then 50 µL of d₁₂-Per and d₁₀-Fl was spiked to the glass fibre filter sample as an internal standard. These samples were treated in 200 mL of dichloromethane for 8 h in a Soxhlet extractor, following which solvent removal was conducted using a nitrogen blow-down evaporator.

The glass container was washed repeatedly with

hexane and the fractionation/clean-up and blow-down processes adhered strictly to the method suggested by Gogou et al. (1996). The congeners and concentrations of PAHs were both qualitatively and quantitatively analysed using GC/MS (Varian Saturn 2000 GC/MS) installed with a fused silica capillary column (60-m length × 0.25-mm i.d. of DB5 capillary column coated with a 0.25-µm-thickness film) and a Saturn workstation program. High-purity He gas (99.99%) was used as the carrier gas. The GC temperature programming and the quantification and identification of the congeners are clearly explained in Pongpiachan et al. (2009). Quality assurance and quality control were evaluated using the standard SRM 1941b. Mean recovery (based on the extraction of matrix-matched certified reference materials, (n = 8) was within the range 77-119%. The precision of the analytical method, computed as the relative standard deviation on the duplicate samples, was <15%. All PAH concentrations were quantified using standardised relative response factors run with each batch (Pongpiachan et al., 2009).

Statistical analysis

As a part of the effort to assess the reliability of using diagnostic binary ratios of PAHs as chemical tracers, the arithmetic mean, standard deviation, t-Test, and analysis of variance were calculated using statistical software (SPSS v.13.0; SPSS Inc., Chicago, IL, USA).

Results and Discussion*Effects of photolysis on variations of diagnostic binary ratios of PAHs*

Photolysis is the main process that influences the residence time and behaviour of atmospheric particulate PAHs, both in the atmosphere and after wet/dry deposition. A study by Kim et al. (2013) highlighted the importance of both fast photodegradation and fast diffusion kinetics on the reduction of LMW PAHs (with 2-3 rings) in comparison with HMW PAHs (with 4 or more rings). Although the photodegradation rates of 16 U.S. EPA-priority PAHs follow first-order kinetics, UV-B (315-280 nm) exposure can dramatically accelerate the photolysis rate of PAHs adsorbed onto fly ash particles (Niu et al., 2007). However, this is not the case for the photodecomposition of PAHs at ground level, because the majority of UV-B radiation is absorbed by the ozone layer in the stratosphere (Caldwell and Flint, 1994). As illustrated in Table 1, no significant differences between day and night were found for any of the diagnostic binary ratios of PAHs, irrespective of differences in their source emission characteristics, and the geographical and meteorological conditions of the three air quality monitoring sites (i.e., BYH, CDH, and NVH). This indicates that photolysis plays a minor role in altering the diagnostic binary ratios of PAHs in PM₁₀. These findings are consistent with a previous report by Wortham et al. (1993), which suggested that in the absence of oxidising gaseous species, photodegradation is negligible for comparatively short irradiation times, e.g., <2 h for An, Fluo, Pyr, B[a]P, B[g,h,i]P, and B[b]F. As the sampling time of DPIMC was three hours, it is reasonable to interpret the "non-significant differences" for all the

diagnostic binary ratios of PAHs as a consequence of comparatively low irradiation in the absence of oxidising gases.

Inter-site comparison of coefficient of divergence (COD)

One of the most challenging problems is to assess the degree to which site-specific conditions affect the PAH diagnostic binary ratios. If these ratios are influenced to some extent by source emission characteristics (e.g., vehicle types and driving cycle patterns), and environmental (e.g., geographic and building morphologies) and meteorological conditions (e.g., wind speed and direction), which are dependent variables of the sampling sites, careful consideration should be given to the interpretation of the data. Furthermore, it is difficult to assess the local and regional effects on the emission source strengths of the selected PAH diagnostic binary ratios. To evaluate the deviations in the temporal distributions of the selected PAH binary ratios at the seven air quality monitoring sites, the computation of the COD is recommended (Wilson et al., 2005; Limbeck et al., 2009), as explained below:

$$COD = \sqrt{\frac{1}{n} \sum_{i=1}^n \left(\frac{x_{ij} - x_{ik}}{x_{ij} + x_{ik}} \right)^2} \quad (1)$$

where x_{ij} indicates the PAH ratio for sampling event i at

Table 1. Comparison of Diagnostic Binary Ratios of Polycyclic Aromatic Hydrocarbons Collected During the Day and Night

Sampling Site	Bangkok				
	Sampling Period		Feb-08		t-Test
	Day	Night	Avg.	Std. dev.	
	Avg.	Std. dev.	Avg.	Std. dev.	(p<0.05)
An/(An + Phe)	0.604	0.523	0.576	0.306	NS
Fluo/(Fluo + Pyr)	0.507	0.062	0.483	0.196	NS
B[a]A/(B[a]A+Chry)	0.38	0.184	0.465	0.208	NS
B[a]P/(B[a]P+B[e]P)	0.4	0.129	0.518	0.208	NS
Ind/(Ind+B[g,h,i]P)	0.411	0.235	0.358	0.246	NS
B[k]F/Ind	0.502	0.324	0.34	0.303	NS
Sampling Site					
Sampling Period	Chiang-Mai				
	Sampling Time		Feb-08		t-Test
	Day	Night	Avg.	Std. dev.	
	Avg.	Std. dev.	Avg.	Std. dev.	(p<0.05)
An/(An + Phe)	0.127	0.0608	0.0933	0.00334	NS
Fluo/(Fluo + Pyr)	0.39	0.0658	0.413	0.0272	NS
B[a]A/(B[a]A+Chry)	0.421	0.0868	0.433	0.0614	NS
B[a]P/(B[a]P+B[e]P)	0.408	0.0648	0.466	0.0886	NS
Ind/(Ind+B[g,h,i]P)	0.639	0.181	0.615	0.165	NS
B[k]F/Ind	0.143	0.0463	0.149	0.0309	NS
Sampling Site					
Sampling Period	Hat-Yai				
	Sampling Time		Dec-07		t-Test
	Day	Night	Avg.	Std. dev.	
	Avg.	Std. dev.	Avg.	Std. dev.	(p<0.05)
An/(An + Phe)	0.35	0.201	0.41	0.202	NS
Fluo/(Fluo + Pyr)	0.121	0.0884	0.217	0.118	NS
B[a]A/(B[a]A+Chry)	0.37	0.0404	0.358	0.0409	NS
B[a]P/(B[a]P+B[e]P)	0.544	0.0527	0.481	0.0737	NS
Ind/(Ind+B[g,h,i]P)	0.487	0.0967	0.452	0.131	NS
B[k]F/Ind	0.199	0.0621	0.329	0.198	NS

sampling site j, x_{ik} is the PAH ratio for the identical event i at sampling site k, and n is the number of total sampling events. It is crucial to stress that both short- and long-term observations can be adapted to the principle of employing the COD because of the self-normalising characteristics of the process (Wongphatarakul et al., 1998). If the COD value approaches zero, it can be inferred that strong affinity exists between the emission sources of the two sampling sites. Conversely, if the COD value approaches one, it suggests divergence between the emission sources of the two investigated air sampling stations.

As displayed in Table 2, the average value of An/(An + Phe) is three times more significant ($p < 0.001$) than Fluo/(Fluo + Pyr). This reflects greater divergence in the spatial distribution of An/(An + Phe), which can be attributed to several causes. According to a previous study, the overall rate of photodegradation of irradiated 2-3-ring PAHs on soot particles is affected by fast photolysis and fast diffusion kinetics, while that of PAHs with 4 or more rings is evidently governed by either the combination of slow photolysis and slow diffusion kinetics, or by extremely slow diffusion kinetics alone (Kim et al., 2013). Therefore, the comparatively high COD value of An/(An + Phe) reflects the greater fragility of these LMW congeners in comparison with those of Fluo and Pyr. It is also interesting to note that the three highest COD values of An/(An + Phe) were observed for the combinations of KHA-BHS (0.495), CPB-BHS (0.465), and SPS-BHS (0.455), as illustrated in Table 2.

As the KHA and CPB sampling sites are representative of traffic routes and the BHS site is situated in a residential area, the comparatively high COD values observed for these two combinations might simply reflect differences in the characteristics of the emission sources between the two sites. Furthermore, a study by Valavanidis et al. (2009) found that ozone from vehicular emissions was responsible for the generation of hydroxyl radicals, which are frequently referred to as the “detergent” of the troposphere because they react with various types of air pollutants including PAHs (Jariyasopit et al., 2014). Heterogeneous reactions of PM_{10} -bound PAHs with NO_3/N_2O_5 , OH radicals, and O_3 released from traffic exhausts can also dramatically reduce the atmospheric concentrations of PAHs (Jariyasopit et al., 2014) and thus, they might alter the diagnostic binary ratios of An/(An + Phe) at KHA and CPB. Conversely, the three lowest COD values for An/(An + Phe) were observed for the combinations of TPS-NWS (0.117), DHA-TPS (0.139), and DHA-NWS (0.187). Because these three air quality monitoring sites are all categorised as representative of an urban residential background, it is reasonable to ascribe the relatively low COD values to the strong similarities in the temporal variation of An/(An + Phe) between the two sampling sites.

Influence of traffic emissions on PAH diagnostic binary ratios

The impact of traffic emissions on PAH diagnostic binary ratios has been investigated as part of the CMPIA project at two monitoring sites: PTOS and ICZOS. As the PTOS is located only a few hundreds of metres from

Assessment of Reliability when Using Diagnostic Binary Ratios of Polycyclic Aromatic Hydrocarbons in Ambient Air PM10
a highway, it is reasonable to ignore contributions to the PAH aerosol concentrations caused by non-traffic sources and other atmospheric chemical and/or physical processes. However, it is crucial to stress that the ICZOS is situated within the IRPC Complex Zone. Thus, differences in the PM₁₀-bounded PAH concentrations between the PTOS and ICZOS can only be attributed to vehicular exhausts. If the effects of traffic emissions are larger than those of industrial combustion and other potential industrial sources, some significant differences of PAH diagnostic binary ratios between the two observatory sites should be observed. Conversely, if the influence of traffic emissions is minor, then no significant differences in the binary ratios should be detected.

The t-test statistic can be used to determine whether

Table 2. Coefficient of Divergence for An/(An + Phe) and Fluo/(Fluo + Pyr) Measured at seven Air quality monitoring sites in Bangkok

	An/(An + Phe)	Fluo/(Fluo + Pyr)
CPB-DHA	0.35	0.084
CPB-TPS	0.338	0.141
CPB-SPS	0.267	0.119
CPB-KHA	0.315	0.176
CPB-NWS	0.269	0.168
CPB-BHS	0.465	0.174
DHA-TPS	0.139	0.143
DHA-SPS	0.339	0.139
DHA-KHA	0.382	0.199
DHA-NWS	0.187	0.171
DHA-BHS	0.305	0.193
TPS-SPS	0.322	0.104
TPS-KHA	0.345	0.157
TPS-NWS	0.117	0.086
TPS-BHS	0.295	0.107
SPS-KHA	0.328	0.15
SPS-NWS	0.293	0.135
SPS-BHS	0.455	0.177
KHA-NWS	0.305	0.161
KHA-BHS	0.495	0.158
NWS-BHS	0.323	0.132
Avg.	0.316	0.146
Std. dev.	0.093	0.032

Note: KHA – Klongchan National Housing Authority, NWS – Nonsreewitayakom High School, SPS – Singharaaj Pitayakhom High School, TPS – Thonburi Power Substation, CPB – Chokchai 4 Police Box, DHA – Dindang National Housing Authority, and BHS – Badindecha High School

Table 3. Statistical Descriptions and t-Test Results for Diagnostic Binary ratios of PM10-bounded Polycyclic Aromatic Hydrocarbons Collected at the Pluakgate Temple Observatory Station (PTOS) and IRPC Complex Zone Observatory Station (ICZOS)

	PTOS		ICZOS		
	Avg.	Std. dev.	Avg.	Std. dev.	t-Test
An/(An + Phe)	0.223	0.207	0.234	0.214	NS
Fluo/(Fluo + Pyr)	0.405	0.156	0.383	0.124	NS
B[a]A/(B[a]A+Chry)	0.434	0.187	0.42	0.191	NS
B[a]P/(B[a]P+B[e]P)	0.394	0.245	0.371	0.248	NS
Ind/(Ind+B[g,h,i]P)	0.432	0.189	0.389	0.198	NS
B[k]F/Ind	1.763	1.959	1.863	1.59	NS

*NS means not significant

two independent populations have different mean values on some measure. Thus, the average values of the PAH diagnostic binary ratios collected at the two monitoring sites were calculated and compared. As can be clearly seen from Table 3, there is no significant difference ($p < 0.001$) in any of the six PAH diagnostic binary ratios between the two monitoring sites. As the CMPIA project covered the measurement of particulate PAHs from 2010 to 2013, the comparatively long four-year observation period underlines the reliability of using PAH ratios as alternative chemical tracers for source categorisation. It is also crucial to note that these two monitoring sites are located within the coastal region of Rayong Province, i.e., an area predominantly governed by both sea and land breezes. These prevailing winds could have been responsible for the comparatively homogeneous air mass over the monitoring area, which led to the lack of significant differences in PAH binary ratios between the two stations. Another explanation for these findings is the extremely low concentrations of PAHs observed in this coastal area in comparison with other cities around the world (Pongpiachan et al., 2015b). As discussed in the previous section, oxidising gaseous species from vehicular exhausts can play an important role in reducing some LMW PAHs, which could be responsible for the alteration of the diagnostic binary ratios in areas with heavy traffic congestion. In addition, the application of PAH ratios only functions properly if the air quality observations are conducted in a clean air environment with relatively low concentrations of oxidising gaseous species.

In conclusion, the conclusions of this study are drawn based on the evidence that the photolysis process and vehicular exhausts play minor roles in altering PAH ratios. For application of the diagnostic binary ratios in areas of heavy traffic congestion, particularly careful attention should be given the data interpretation because NO₃/N₂O₅, OH radicals, and O₃ from vehicles can cause dramatic fluctuations of the PAH ratios. While the Fluo/(Fluo + Pyr) ratios did show some small inter-site differences with comparatively low COD values, careful examination of the binary ratios of An/(An + Phe) is crucial for a more precise elucidation of source categorisation for PM₁₀-bounded PAHs.

Acknowledgements

This work was performed with the approval of the National Institute of Development Administration (NIDA), Thailand. The author acknowledges the research staff of the Pollution Control Department (PCD), Ministry of Natural Resources and Environment (MNRE), Thailand for its contributions to the field sampling and some laboratory work.

References

- Alam MS, Delgado-Saborit JM, Stark C, et al (2013). Using atmospheric measurements of PAH and quinone compounds at roadside and Urban background sites to assess sources and reactivity. *Atmos Environ*, **77**, 24-35.
- Annamalai J, Namasivayam V (2015). Endocrine disrupting

- chemicals in the atmosphere: their effects on humans and wildlife. *Environ Int*, **76**, 78-97.
- Caldwell MM, Flint SD (1994). Stratospheric ozone reduction, Solar UV-B radiation and terrestrial ecosystems. *Climatic Change*, **28**, 375-94.
- Crépeaux G, Kremarik PB, Sikhayeva N, et al (2012). Late Effects of a Perinatal Exposure to a 16 PAH Mixture: increase of anxiety-related behaviours and decrease of regional brain metabolism in adult male rats. *Toxicol Lett*, **211**, 105-13.
- Dachs J, Eisenreich SJ (2000). Adsorption onto aerosol soot carbon dominates gas-particle partitioning of polycyclic aromatic hydrocarbons. *Environ Sci Technol*, **34**, 3690-7.
- Gao B, Wang XM, Zhao XY, et al (2015). Source apportionment of atmospheric PAHs and their toxicity using PMF: impact of Gas/Particle partitioning. *Atmos Environ*, **103**, 114-20.
- Gogou A, Stratigakis N, Kanakidou M, et al (1996). Organic aerosol in eastern mediterranean: component source reconciliation by using molecular markers and atmospheric back trajectories. *Org Geochem*, **25**, 79-96.
- Hanedar A, Alp K, Kaynak B, et al (2011). Concentrations and Sources of PAHs at Three Stations in Istanbul, Turkey. *Atmos Res*, **99**, 391-9.
- Jang E, Alam MS, Harrison RM (2013). Source apportionment of polycyclic aromatic hydrocarbons in urban air using positive matrix factorization and spatial distribution analysis. *Atmos Environ*, **79**, 271-85.
- Jariyasopit N, Zimmermann K, Schrlau J, et al (2014). Heterogeneous Reactions of Particulate Matter-Bound PAHs and NPAHs with NO₃/N₂O₅, OH Radicals, and O₃ under simulated long-range atmospheric transport conditions: reactivity and mutagenicity. *Environ Sci Technol*, **48**, **10**, 155-64.
- Kim D, Young TM, Anastasio C (2013). Phototransformation rate constants of PAHs associated with soot particles. *Sci Total Environ*, **443**, 896-903.
- Limbeck A, Handler M, Puls C, et al (2009). Impact of mineral components and selected trace metals on ambient PM₁₀ concentrations. *Atmos Environ*, **43**, 530-8.
- Liu J, Li J, Lin T, et al (2013). Diurnal and nocturnal variations of PAHs in the Lhasa atmosphere, tibetan plateau: implication for local sources and the impact of atmospheric degradation processing. *Atmos Res*, **124**, 34-43.
- Moorthy B, Chu C, Carlin DJ (2015). Polycyclic aromatic hydrocarbons: from metabolism to lung cancer. *Toxicol Sci*, **145**, 5-15.
- Müller AK, Farombi EO, Möller P, et al (2004). DNA damage in lung after oral exposure to diesel exhaust particles in big blue® rats. *Mutat Res-Fund Mol M*, **550**, 123-32.
- Niu J, Sun P, Schramm KW (2007). Photolysis of Polycyclic Aromatic Hydrocarbons Associated with Fly Ash Particles under Simulated Sunlight Irradiation. *J Photoc Photobio A*, **186**, 93-8.
- Odabasi M, Cetin E, Sofuoğlu A (2006). Determination of octanol-air partition coefficients and super-cooled liquid Vapor Pressures of PAHs as a function of temperature: application to gas-particle partitioning in an urban atmosphere. *Atmos Environ*, **40**, 6615-25.
- Ohura T, Horii Y, Kojima M, et al (2013). Diurnal variability of chlorinated polycyclic aromatic hydrocarbons in Urban Air, Japan. *Atmos Environ*, **81**, 84-91.
- Pongpiachan S, Bualert S, Sompongchaiyakul P, et al (2009). Factors affecting sensitivity and stability of polycyclic aromatic hydrocarbons. *Anal Lett*, **42**, 2106-30.
- Pongpiachan S (2010). Atmospheric lifetimes and traveling distances of airborne carcinogenic polycyclic aromatic hydrocarbons. *Chinese J Clinic (Electronic Edition)*, **16**.
- (<http://journal.shouxi.net/qikan/articledes.php?id=537551>).
- Pongpiachan S, Ho KF, Lee SC (2010). A Study of Gas-Particle Partitioning of PAH According to Adsorptive Models and Season. In Air Pollution XVIII, WIT press, pp. 37-48. ISBN: 978-1-84564-450-5, ISSN (Online): 1743-3541, ISSN (Print): 1746-448X, June 2010. (Conference Book)
- Pongpiachan S (2013a). Vertical distribution and potential risk of particulate polycyclic aromatic hydrocarbons in high buildings of Bangkok, Thailand. *Asian Pac J Cancer Prev*, **14**, 1865-77.
- Pongpiachan S (2013b). Diurnal variation, vertical distribution and source apportionment of carcinogenic polycyclic aromatic hydrocarbons (PAHs) in Chiang-Mai, Thailand. *Asian Pac J Cancer Prev*, **14**, 1851-63.
- Pongpiachan S, Choochua C, Hattayanone M, et al (2013a). Temporal and spatial distribution of particulate carcinogens and mutagens in bangkok, Thailand. *Asian Pac J Cancer Prev*, **14**, 1879-87.
- Pongpiachan S, Ho KF, Cao J (2013b). Estimation of gas-particle partitioning coefficients (kp) of carcinogenic polycyclic aromatic hydrocarbons by carbonaceous aerosols collected at chiang-mai, Bangkok and Hat-Yai, Thailand. *Asian Pac J Cancer Prev*, **14**, 3369-84.
- Pongpiachan S, Tipmanee D, Deelaman W, et al (2013c). Risk assessment of the presence of polycyclic aromatic hydrocarbons (PAHs) in coastal areas of Thailand affected by the 2004 Tsunami. *Mar Pollut Bull*, **76**, 370-8.
- Pongpiachan S (2014). Application of binary diagnostic ratios of polycyclic aromatic hydrocarbons for identification of tsunami 2004 backwash sediments in khao lak, Thailand. *Scientific World J*, **485068**, 14.
- Pongpiachan S (2015). A preliminary study of using polycyclic aromatic hydrocarbons as chemical tracers for traceability in soybean products. *Food Control*, **47**, 392-400.
- Pongpiachan S, Tipmanee D, Khumsup C, et al (2015a). Assessing Risks to Adults and Preschool Children Posed by PM_{2.5}-bound polycyclic aromatic hydrocarbons (pahs) during a biomass burning episode in northern Thailand. *Sci Total Environ*, **508**, 435-44.
- Pongpiachan S, Hattayanone M, Choochua C, et al (2015b). Enhanced PM₁₀ Bounded PAHs from shipping emissions. *Atmos Environ*, **108**, 13-9.
- Ringuet J, Albinet A, Garziandia EL, et al (2012a). Reactivity of polycyclic aromatic compounds (PAHs, NPAHs and OPAHs) adsorbed on natural aerosol particles exposed to atmospheric oxidants. *Atmos Environ*, **61**, 15-22.
- Ringuet J, Albinet A, Garziandia EL, et al (2012b). Diurnal/nocturnal concentrations and sources of particulate-bound PAHs, OPAHs, and NPAHs at traffic and suburban sites in the region of Paris (France). *Sci Total Environ*, **437**, 297-305.
- SrAm RJ, BinkovA B, Rossner P, et al (1999). Adverse Reproductive Outcomes from Exposure to Environmental Mutagens. *Mutat Res-Fund Mol M*, **428**, 203-15.
- Tipmanee D, Deelaman W, Pongpiachan S, et al (2012). Using polycyclic aromatic hydrocarbons (PAHs) as a chemical proxy to indicate tsunami 2004 backwash in khao lak coastal area, Thailand. *Nat Hazards Earth Syst Sci*, **12**, 1441-51.
- US-EPA (1999). Compendium of Methods for the Determination of Inorganic Compounds in Ambient Air. Compendium method IO-2.2. Sampling of Ambient Air for PM₁₀ Using an Andersen Dichotomous Sampler. EPA/625/R-96/010a. Available from: <http://www.epa.gov/ttnamti1/files/ambient/inorganic/mthd-2-2.pdf>.
- Valavanidis A, Loridas S, Vlahogianni T, et al (2009). Influence of ozone on traffic-related particulate matter on the generation of hydroxyl radicals through a heterogeneous synergistic effect. *J Hazard Mater*, **162**, 886-92.

- Assessment of Reliability when Using Diagnostic Binary Ratios of Polycyclic Aromatic Hydrocarbons in Ambient Air PM10*
- Venkatachalam S, Kuppusamy P, Kuppusamy B, et al (2014). The potency of essential nutrient taurine on boosting the antioxidant status and chemopreventive effect against benzo(a)pyrene-induced experimental lung cancer. *Biomed Prev Nutr*, **4**, 251-5.
- Wang D, Chen J, Xu Z, et al (2005). Disappearance of polycyclic aromatic hydrocarbons sorbed on surfaces of pine [pinus thunbergii] needles under irradiation of sunlight: volatilization and photolysis. *Atmos Environ*, **39**, 4583-91.
- Wang D, Li Y, Yang M, et al (2008). Decomposition of polycyclic aromatic hydrocarbons in atmospheric aqueous droplets through sulfate anion radicals: an experimental and theoretical study. *Sci Total Environ*, **393**, 64-71.
- Wang Z, Na G, Ma X, et al (2013). Occurrence and gas/particle partitioning of PAHs in the atmosphere from the north pacific to the arctic ocean. *Atmos Environ*, **77**, 640-6.
- Wang Q, Xue Y (2015). Characterization of solid tumors induced by polycyclic aromatic hydrocarbons in mice. *Med Sci Monit Basic Res*, **21**, 81-5.
- Wilson JG, Kingham S, Pearce J, et al (2005). A review of intra-urban variations in particulate air pollution: implications for epidemiological research. *Atmos Environ*, **39**, 6444-62.
- Wongphatarakul V, Friedlander SK, Pinto JP (1998). A comparative study of PM_{2.5} ambient aerosol chemical databases. *Environ Sci Technol*, **32**, 3926-34.
- Wortham H, Nguyen EB, Masclet P (1993). Study of heterogeneous reactions of polycyclic aromatic hydrocarbons I: Weakening of PAH-support bonds under photonic irradiation. *Sci Total Environ*, **128**, 1-11.
- Zhang Y, Shu J, Liu C, et al (2013). Heterogeneous Reaction of Particle-Associated Triphenylene with NO₃ Radicals. *Atmos Environ*, **68**, 114-9.



ELSEVIER

Contents lists available at ScienceDirect

Materials Letters

journal homepage: www.elsevier.com/locate/matlet

Visualizing reactive oxygen species inside cancer cells after stimulation with polycyclic aromatic hydrocarbon *via* spontaneous formation of Au nanoclusters

Chalermchai Pilapong ^{a,*1}, Siwatt Pongpiajun ^b, Samlee Mankhetkorn ^a^a Center of Excellence for Molecular Imaging (CEMI), Department of Radiologic Technology, Faculty of Associated Medical Science, Chiang Mai University, Chiang Mai 50200, Thailand^b NIDA Center for Research & Development of Disaster Prevention & Management, School of Social and Environmental Development, National Institute of Development Administration (NIDA), Bangkok 10240, Thailand

ARTICLE INFO

Article history:

Received 14 July 2014

Accepted 30 October 2014

Available online 7 November 2014

Keywords:

Gold nanocluster

Reactive oxygen species

Chloroauric acid

ABSTRACT

This research was designed to visualize cellular response – in particular the generation of intracellular ROS – to stimulation by polycyclic aromatic hydrocarbon (PAH). We used chloroauric acid (HAuCl_4) as a molecular probe for visualizing intracellular ROS generated by the stimulation of benzo[a]pyrene (BaP). The chloroauric acid undergoes a spontaneous reduction reaction, assisted by the intracellular ROS, into gold nanoclusters (AuNCs). As a result, we can visualize the ROS *via* optical imaging technique. According to MTT assay, the chloroauric acid exhibited good biocompatibility. The AuNCs produced in the cells were approximately 2–3 nm in diameter with a green fluorescent property. Cellular imaging showed that BaP induced the formation of AuNCs within the cells, leading to a high relative cellular fluorescent intensity with a considerable extent of scatter light. Thus, this probe is an efficient molecular imaging probe for visualizing intracellular ROS.

© 2014 Elsevier B.V. All rights reserved.

1. Introduction

Polycyclic aromatic hydrocarbons (PAHs) can cause cancer, heritable genetic damage and sensitization by skin contact, among other health issues. Exposure to PAHs may lead cells, as an early-stage response, to overproduce intracellular reactive oxygen species (ROS), causing oxidative stress [1–3]. Generally, abnormal overproduction of intracellular ROS is closely associated with various pathological processes, including cancer, cardiovascular disease and neurological disorders [4]. Various fluorescent probes for detecting ROS have been developed, including small molecule-based and nanoparticle-based probes. However, use of these probes is limited by their toxicity and they cannot be used for spontaneous imaging. Moreover, some probes cannot be used to

spontaneously monitor intracellular ROS induced by a highly toxic reagent [5–11].

To overcome these limitations, we build on the concept that metal nanoclusters and nanoparticles can be simultaneously synthesized by using various kinds of reducing agents – such as a highly toxic agent (NaBH_4) [12], biomolecules (RNase A, ovalbumin) [13,14] and ROS compounds [15,16] – to form fluorescent metal nanoclusters in order to visualize intracellular ROS in hepatocellular carcinoma cells after being stimulated with PAH compounds (benzo[a]pyrene, BaP). We postulated that BaP molecules enter cells and stimulate them to produce intracellular ROS. In the presence of chloroauric salt (HAuCl_4) within the cell, HAuCl_4 can undergo a rapid and efficient spontaneous reduction by intracellular ROS into fluorescent gold nanoclusters. Thus, we could spontaneously visualize intracellular ROS, induced by polycyclic aromatic hydrocarbon, *via* optical imaging technique.

2. Experimental details

Physical characterization: Size of AuNCs, obtained from the cells by a repetitive freeze–thaw method, was measured with a field-emission transmission electron microscope (TEM, JEOL JEM-2100).

* Corresponding author at: Center of Excellence for Molecular Imaging (CEMI), Department of Radiologic Technology, Faculty of Associated Medical Science, Chiang Mai University, Chiang Mai 50200, Thailand. Tel.: +66 53 94 9306; fax: +66 53 21 3218.

E-mail address: chalermchai.pilapong@cmu.ac.th (C. Pilapong).

¹ Post-Doctoral Research Fellow, National Institute Development Administration (NIDA), Bangkok 10240, Thailand.

Fluorescence and excitation spectra of AuNCs were determined with an LS55 luminescence spectrometer. UV-vis absorbance was measured on an Agilent 8453 UV-visible spectrometer.

Cell viability: HepG2 cells (hepatocellular carcinoma cells) or HepG2.2.15 cells (hepatitis B virus infected hepatocellular carcinoma cells) were trypsinized and resuspended in DMEM. The cells were seeded in a 24-well plate at a density of 5×10^4 cells/mL and incubated overnight at 37 °C in 5% CO₂ atmosphere. After washing, DMEM containing HAuCl₄ was loaded in each well with final concentrations of 0, 0.1, 1, 10, 100 and 1000 μM. After 48 h incubation, the culture medium was discarded and the cells were washed twice with PBS buffer and further incubated with 200 μL of solution containing 5 mg MTT/mL phosphate-buffered saline at 37 °C for 4 h. The MTT solution was removed and the intracellular formazan crystals were dissolved with 500 μL DMSO for 15 min at 37 °C. The absorbance of formazan solution was measured through spectroscopy at 570 nm with DMSO as blank.

Cellular imaging study: The trypsinized cells were seeded at a density of 5×10^4 cells/well and incubated in DMEM at 37 °C in 5% CO₂. After 24 h incubation, the cells were washed twice with PBS buffer and further incubated with the culture medium containing BaP alone, HAuCl₄ alone or co-incubation of BaP and HAuCl₄. After 24 h incubation, the cells were washed with PBS and observed under a Leica DMI 4000B microscope.

3. Results and discussion

TEM and fluorescence analysis were used to confirm the formation of AuNCs within the cells. Figs. 1a and S1 show, respectively, the TEM image and EDS spectrum of AuNCs produced inside HepG2 cells after incubation with the appropriate amount of HAuCl₄ and BaP for 24 h. The AuNCs were measured as approximately 2–3 nm without any impurity elements. The HRTEM image (Fig. 1a(inset)) reveals a lattice fringe with a spacing of ~2.4 Å, which is in good agreement with the lattice spacing in the (111) planes of face centered cubic gold. The AuNCs exhibited an optimum excitation wavelength of 450 nm and a maximum emission wavelength of 525 nm (Fig. 1b); the origin of PL band centered at ~530 nm is ascribed to the presence of Au₁₃ species, which act as main emitters inside the cells [17]. These results confirmed that cells stimulated with BaP spontaneously produced intracellular fluorescent AuNCs. The formation of fluorescent AuNCs inside the cells might be due to a reduction of Au (III) by competing with reduction of dioxygen and/or the intracellular ROS e.g., superoxide anion (O₂•), and subsequent surface capping by

specific ligands inside the cells [18,19]. However, the formation mechanism is still unclear, and beyond the scope of this study.

To demonstrate a potential use of HAuCl₄ as a biocompatible ROS imaging probe, we initially tested the cytotoxicity of HAuCl₄ toward HepG2 and HepG2.2.15 cells by using MTT assay. As shown in Fig. 2, no toxicity was observed in the cells incubated with 0–100 μM of HAuCl₄, indicating this probe's good biocompatibility. At an even higher concentration of HAuCl₄ (1000 μM), the cellular viability remained approximately 80%. These MTT assays indicated that HAuCl₄ has low cytotoxicity.

To show the feasibility of HAuCl₄ as a spontaneous fluorescent imaging probe for visualizing intracellular ROS produced inside cancer cells after BaP stimulation, the HepG2 cells were incubated with the culture medium containing BaP alone, HAuCl₄ alone or co-incubation of BaP and HAuCl₄. After 24 h incubation, the cells were washed with PBS several times and observed under a Leica DMI 4000B fluorescence microscope. As shown in Fig. 3, a higher relative cellular green fluorescent intensity was observed in the HepG2 cells incubated with both HAuCl₄ and BaP (Fig. 3e), and even higher as the concentration of BaP was increased (Figs. 3f and S2). The higher fluorescent intensity demonstrated that BaP induced the formation of AuNCs via a spontaneous reduction reaction assisted by the intracellular ROS. This confirms that HAuCl₄ is an efficient molecular imaging probe for inflammation induced by a highly toxic compound (e.g., PAHs). Furthermore, we observed a strong green fluorescence near cell membranes, indicating an active location for AuNCs formation inside the cells. This result accords well with previous reports, which indicated

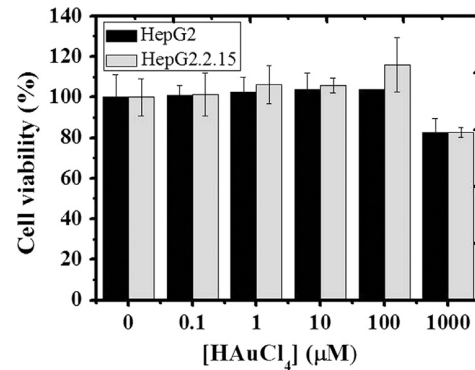


Fig. 2. Cell viability determined by MTT assay in HepG2 and HepG2.2.15 cells.

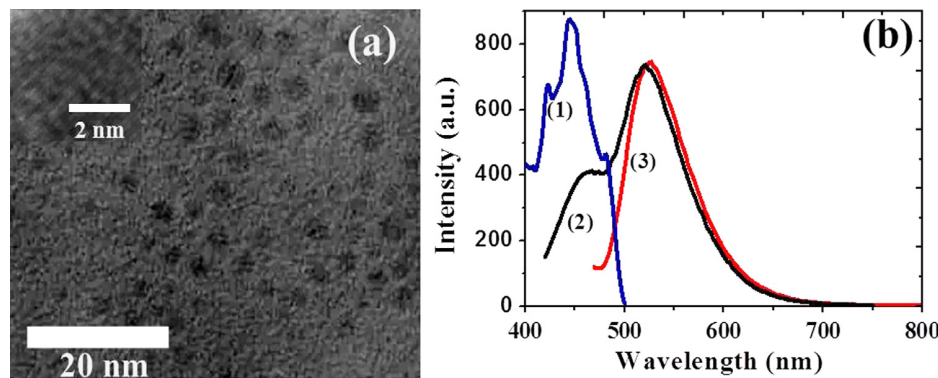


Fig. 1. (a) TEM image of AuNCs obtained from the cells by a repetitive freeze-thaw method (scale bar = 20 nm), (b) fluorescent spectra of the AuNCs obtained using 400 nm excitation wavelength (2) and 450 excitation wavelength (3) with their excitation spectra (1).

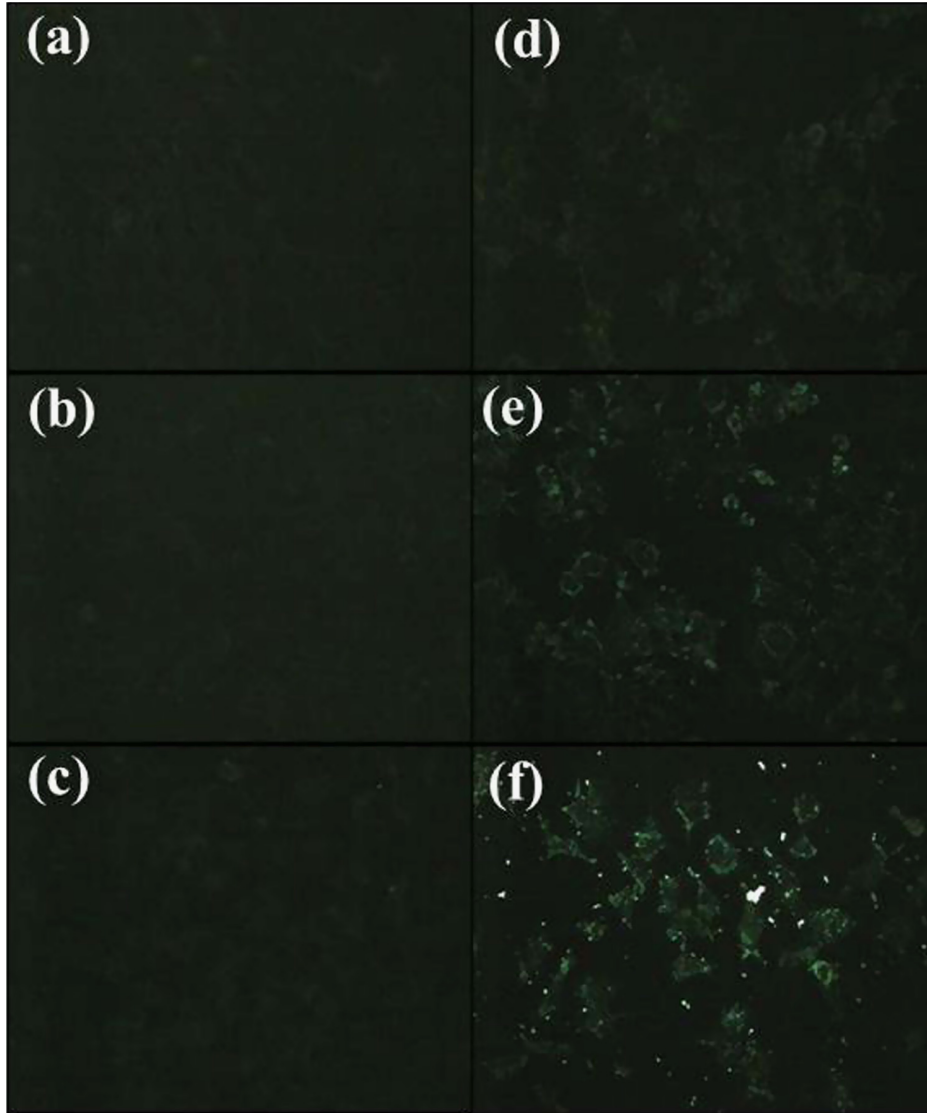


Fig. 3. Fluorescence images of untreated HepG2 cells (a), 0.1 μM BaP treated cells (b), 1 μM BaP treated cells (c), 0.5 mM HAuCl₄ treated cells (d), 0.5 mM HAuCl₄+0.1 μM BaP treated cells (e), and 0.5 mM HAuCl₄+1 μM BaP treated cells (f).

important enzymatic pools near cell membranes [20,21]. While the probe was suitable for visualizing the ROS pool in cancer cells, it was not specific to individual ROS. In addition to fluorescence imaging, dark field imaging is normally used for analyzing biological samples containing scattered nanomaterials e.g., gold nanoparticles. Dark field images of HepG2 cells (Fig. 4) showed that a higher accumulation of AuNCs were observed in the cells treated with both HAuCl₄ and BaP. These results are in good accordance with those observed in fluorescence imaging. Therefore, we can simultaneously visualize intracellular ROS *via* both fluorescence and dark field imaging techniques by using a biocompatible HAuCl₄ as molecular probe.

The same strategy was also applied for HepG2.2.15 cells. As shown in Fig. S2, a much higher fluorescent intensity was observed in both HepG2 and HepG2.2.15 cells co-incubated with HAuCl₄ and BaP, compared to HAuCl₄ alone. This is also due to an over-generated intracellular ROS after BaP stimulation, leading to a high relative cellular fluorescent intensity. This confirms that our

molecular probe can visualize ROS inside both HepG2 and HepG2.2.15 cells after being stimulated by BaP.

4. Conclusion

We utilized HAuCl₄ as a molecular probe for visualizing ROS inside cancer cells after stimulation with a highly toxic agent (benzo[a]pyrene, BaP). The intracellular ROS reduces HAuCl₄ into fluorescent AuNCs. The presence of AuNCs inside the cells can be confirmed by TEM and fluorescent spectrum. According to cellular fluorescent and dark field imaging, BaP induced the formation of AuNCs inside the cancer cells, observed as a high relative cellular fluorescent intensity and scattered light, respectively. Thus, this molecular probe can be used to study cellular response (ROS generation) to stimulation by a highly toxic polycyclic aromatic hydrocarbon, *via* optical imaging technique.

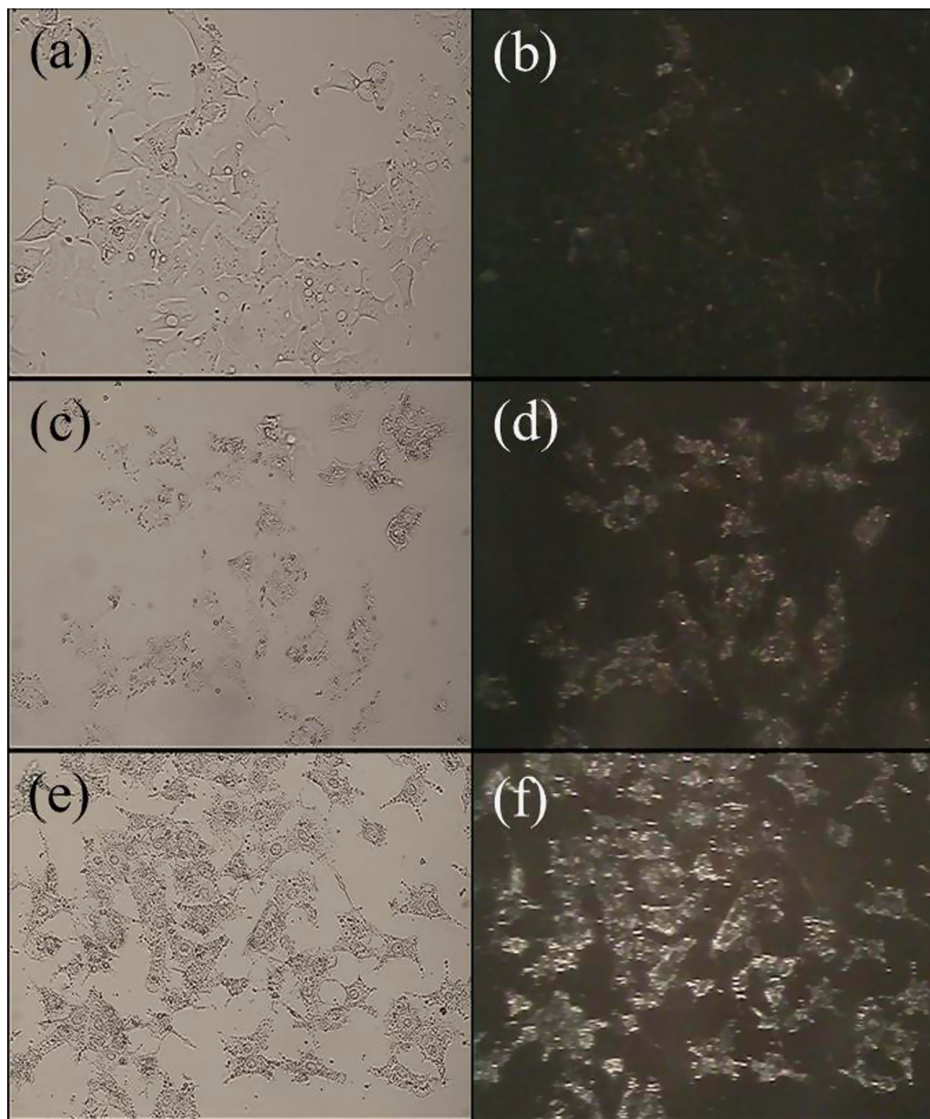


Fig.4. Bright field and dark field images of untreated HepG2 cells (a), 0.5 mM HAuCl₄ treated cells (b) and 0.5 mM HAuCl₄+1 μM BaP treated cells (c).

Acknowledgments

We would like to thank National Institute Development Administration (NIDA), Thailand, for providing financial support through Post-Doctoral Research Fellowship.

Appendix A. Supporting information

Supplementary data associated with this article can be found in the online version at <http://dx.doi.org/10.1016/j.matlet.2014.10.157>.

References

- [1] Wilk A, Waligórska P, Lassak A, Vashistha H, Lurette D, Tate D, et al. *J Cell Physiol* 2013;228:2127–38.
- [2] Chung SW, Chung HY, Toriba A, Kameda T, Tang N, Kizu R, et al. *Toxicol Sci* 2007;95:348–55.
- [3] Song MK, Kim YJ, Song M, Choi HS, Park YK, Ryu JC. *Cancer Sci* 2011;102:1636–44.
- [4] Medzhitov R. *Nature* 2008;454:428–35.
- [5] Beltran-Huarac J, Tomar MS, Singh SP, Perales O, Rivera L, Peña S. *NSTI-Nanotech* 2010;3:405–8.
- [6] Soh N. *Anal Bioanal Chem* 2006;386:532–43.
- [7] Hempel SL, Buettner GR, O’Malley YQ, Wessels DA, Flaherty DM. *Free Radic Biol Med* 1999;27:146–59.
- [8] Miller EW, Tulyathan O, Isacoff EY, Chang CJ. *Nat Chem Biol* 2007;3:263–7.
- [9] Lee D, Khaja S, Velasquez-Castano JC, Dasari M, Sun C, Petros J, et al. *Nat Mater* 2007;6:765–9.
- [10] Pu K, Shuhendler AJ, Rao J. *Angew Chem Int Ed* 2013;52:10325–9.
- [11] Chen T, Hu Y, Cen Y, Chu X, Lu Y. *J Am Chem Soc* 2013;135:11595–602.
- [12] Yin J, He X, Wang K, Qing Z, Wu X, Shi H, et al. *Nanoscale* 2012;4:110–2.
- [13] Qiao J, Mu X, Qi L, Deng J, Mao L. *Chem Commun (Camb)* 2013;49:8030–2.
- [14] Kong Y, Chen J, Gao F, Brydson R, Johnson B, Heath G, et al. *Nanoscale* 2013;5:1009–17.
- [15] Li Q, Lu B, Zhang L, Lu C. *J Mater Chem* 2012;22:13564–70.
- [16] Liu X, Xu H, Xia H, Wang D. *Langmuir* 2012;28:13720–6.
- [17] Chattoraj S, Bhattacharyya K. *J Phys Chem C* 2014;118:22339–46.
- [18] Turrens JF. *J Physiol* 2003;552:335–44.
- [19] Wang J, Zhang G, Li Q, Jiang H, Liu C, Amatore C, et al. *Sci Rep* 2013;3:1157.
- [20] Amatore C, Arbaud S, Guile M, Guile M. *Chem Rev* 2008;108:2585–621.
- [21] Wiseman H, Halliwell B. *Biochem J* 1996;313:17–29.



เลขที่อนุสิทธิบัตร 10250

อสป/200 - ข

อนุสิทธิบัตร

อาศัยอำนาจตามความในพระราชบัญญัติสิทธิบัตร พ.ศ. 2522

เกี่ยวกับเพิ่มเติมโดยพระราชบัญญัติสิทธิบัตร (ฉบับที่ 3) พ.ศ. 2542

ดังนี้
ได้กรรมทรัพย์สินทางปัญญาอุปกรณ์สิทธิบัตรฉบับนี้ให้แก่

รศ.ดร.ศิริวัช พงษ์เพียจันทร์

สำหรับการประดิษฐ์ตามรายละเอียดการประดิษฐ์ ข้อถือสิทธิ และรูปเขียน (ถ้ามี)
ดังนี้
ลักษณะภายนอกในอนุสิทธิบัตรนี้

หมายเลขที่คำขอ 1403001502

ข้อรับอนุสิทธิบัตร 17 พฤษภาคม 2557

ประดิษฐ์ รศ.ดร.ศิริวัช พงษ์เพียจันทร์

ผลงานการประดิษฐ์ วิธีการบ่งชี้แหล่งเพาะปลูกของพืชผลทางการเกษตรด้วยสารเคมีชีวภาพและโรมาริดิกไซโตรัวร์บอน

ให้ผู้ทรงอนุสิทธิบัตรทราบและหน้าที่ตามกฎหมายว่าด้วยสิทธิบัตรทุกประการ

ออกให้	ณ	วันที่	18	เดือน	สิงหาคม	พ.ศ.	2558
หมดอายุ	ณ	วันที่	16	เดือน	พฤษภาคม	พ.ศ.	2563



พนักงานเจ้าหน้าที่

- หมายเหตุ
- ผู้ทรงอนุสิทธิบัตรต้องชำระค่าธรรมเนียมรายปีเริ่มแต่ปีที่ 5 ของอนุสิทธิบัตร มีฉะนั้น อนุสิทธิบัตรจะถือว่าอายุ 2 ปี โดยยกเว้นค่าธรรมเนียมรายปีล่วงหน้าโดยชำระทั้งหมดในคราวเดียวได้
 - ภายใน 90 วันก่อนวันสิ้นอายุอนุสิทธิบัตร ผู้ทรงอนุสิทธิบัตรมีสิทธิขอต่ออายุอนุสิทธิบัตรได้ 2 คราว มีกำหนดคราวละ 2 ปี โดยยกเว้นค่าตอบแทน 2 คราว
 - การอนุญาตให้ใช้สิทธิตามอนุสิทธิบัตรและการโอนอนุสิทธิบัตรต้องทำเป็นหนังสือและจดทะเบียนต่อพนักงานเจ้าหน้าที่ 021961



คำขอรับสิทธิบัตร/อนุสิทธิบัตร

- การประดิษฐ์
 การออกแบบผลิตภัณฑ์
 อนุสิทธิบัตร

ข้าพเจ้าผู้ถุงลายมือชื่อในคำขอรับสิทธิบัตร/อนุสิทธิบัตรนี้
 ขอรับสิทธิบัตร/อนุสิทธิบัตร ตามพระราชบัญญัติสิทธิบัตร พ.ศ.2522
 แก้ไขเพิ่มเติมโดยพระราชบัญญัติสิทธิบัตร (ฉบับที่ 2) พ.ศ.2535
 และพระราชบัญญัติสิทธิบัตร (ฉบับที่ 3) พ.ศ.2542

สำหรับเจ้าหน้าที่

วันรับคำขอ 17 มิ.ย. 2561

เลขที่คำขอ

วันยื่นคำขอ

1403001502

สัญลักษณ์สำเนาการประดิษฐ์ระหว่างประเทศ

ใช้กับแบบผลิตภัณฑ์

ประเภทผลิตภัณฑ์

วันประกาศโழฆณา

เลขที่ประกาศโழฆณา

วันออกสิทธิบัตร/อนุสิทธิบัตร

เลขที่สิทธิบัตร/อนุสิทธิบัตร

ลายมือชื่อเจ้าหน้าที่

1. ชื่อที่แสดงถึงการประดิษฐ์/การออกแบบผลิตภัณฑ์

วิธีการบ่งชี้แหล่งเพาเวอร์กูลของพืชผลทางการเกษตรด้วย PAHs

2. คำขอรับสิทธิบัตรการออกแบบผลิตภัณฑ์นี้เป็นคำขอสำหรับแบบผลิตภัณฑ์อย่างเดียวกันและเป็นคำขอลำดับที่

ในจำนวน คำขอ ที่ยื่นในคราวเดียวกัน

3. ผู้ขอรับสิทธิบัตร/อนุสิทธิบัตร และที่อยู่ (เลขที่ ถนน ประเทศไทย)

รศ. ดร. ศิริวัช พงษ์เพียจันทร์

อยู่ที่ 37/69 เวลาสิงตัน รามคำแหง 40 หัวหมาก บางกะปิ กรุงเทพฯ 10240

ประเทศไทย

3.1 สัญชาติ ไทย

3.2 โทรศัพท์

3.3 โทรสาร

3.4 อีเมล์

4. สิทธิในการขอรับสิทธิบัตร/อนุสิทธิบัตร

 ผู้ประดิษฐ์/ผู้ออกแบบ ผู้รับโอน ผู้ขอรับสิทธิโดยเหตุอื่น

5. ตัวแทน (ถ้ามี)/ที่อยู่ (เลขที่ ถนน จังหวัด รหัสไปรษณีย์)

นางสาวตติชนุ ก้าวหน้าชัยมงคล และ/หรือ นางสาวจุฬาจิต ศรีประสานน์
และ/หรือ นายรัชพงษ์ ทองดีแท้

บริษัท ที่ปรึกษาภูมายางากล จำกัด

เลขที่ 175 อาคารสาขาวิชชาทั่ววาร์ ชั้น 18 ถนนสาทรใต้
แขวงทุ่งมหาเมฆ เขตสาทร กรุงเทพมหานคร

5.1 ตัวแทนเลขที่ 1775 และ/หรือ 1956 และ/หรือ 1971

5.2 โทรศัพท์ 02 6796005

5.3 โทรสาร 02 6796041-2

5.4 อีเมล์ ipgroup@ilct.co.th

6. ผู้ประดิษฐ์/ผู้ออกแบบผลิตภัณฑ์ และที่อยู่ (เลขที่ ถนน ประเทศไทย)

รศ. ดร. ศิริวัช พงษ์เพียจันทร์

อยู่ที่ 37/69 เวลาสิงตัน รามคำแหง 40 หัวหมาก บางกะปิ กรุงเทพฯ 10240 ประเทศไทย

7. คำขอรับสิทธิบัตร/อนุสิทธิบัตรนี้แยกจากหรือเกี่ยวข้องกับคำขอเดิม

ผู้ขอรับสิทธิบัตร/อนุสิทธิบัตร ขอให้ถือว่าได้ยื่นคำขอรับสิทธิบัตร/อนุสิทธิบัตรนี้ ในวันเดียวกับคำขอรับสิทธิบัตร

เลขที่ _____ วันยื่น _____ เพราะคำขอรับสิทธิบัตรนี้แยกจากหรือเกี่ยวข้องกับคำขอเดิม เพราะ

 คำขอเดิมมีการประดิษฐ์หลายอย่าง ถูกคัดค้านเนื่องจากผู้ขอไม่มีสิทธิ ขอเปลี่ยนแปลงประเภทของสิทธิ

8. การยื่นคำขอกราชอาญาจกร

วันยี่นคำขอ	เลขที่คำขอ	ประเภท	สัญลักษณ์จำแนกการประดิษฐ์ระหว่างประเทศ	สถานะคำขอ
8.1				
8.2				
8.3				
8.4 <input type="checkbox"/> ผู้ขอรับสิทธิบัตร/อนุสิทธิบัตรขอสิทธิให้ถือว่าได้ยื่นคำขอนี้ในวันที่ได้ยื่นคำขอรับสิทธิบัตร/อนุสิทธิบัตรในต่างประเทศเป็นครั้งแรกโดย <input checked="" type="checkbox"/> ได้ยื่นเอกสารหลักฐานพร้อมคำขอนี้ <input type="checkbox"/> ขอยื่นเอกสารหลักฐานหลังจากวันยื่นคำขอนี้				
9. การแสดงการประดิษฐ์ หรือการออกแบบพลิตภัณฑ์ ผู้ขอรับสิทธิบัตร/อนุสิทธิบัตร ได้แสดงการประดิษฐ์ที่หน่วยงานของรัฐเป็นผู้จัด วันแสดง		วันเปิดงานแสดง	ผู้จัด	
10. การประดิษฐ์เกี่ยวกับจุลชีพ				
10.1 เลขทะเบียนฝาแก้บ	10.2 วันที่ฝาแก้บ		10.3 สถาบันฝาแก้บ/ประเทศ	
11. ผู้ขอรับสิทธิบัตร/อนุสิทธิบัตร ขอยื่นเอกสารภาษาต่างประเทศก่อน ในวันยื่นคำขอนี้ และจะจัดยื่นคำขอรับสิทธิบัตร/อนุสิทธิบัตรนี้ที่จัดทำเป็นภาษาไทยภายใน 90 วัน นับจากวันยื่นคำขอนี้ โดยขอยื่นเป็นภาษา <input type="checkbox"/> อังกฤษ <input type="checkbox"/> ฝรั่งเศส <input type="checkbox"/> เมอร์มัน <input type="checkbox"/> ญี่ปุ่น <input type="checkbox"/> อื่น ๆ				
12. ผู้ขอรับสิทธิบัตร/อนุสิทธิบัตร ขอให้อธิบดีประกาศโฆษณาคำขอรับสิทธิบัตร หรือรับจดทะเบียน และประกาศโฆษณาอนุสิทธิบัตรนี้ หลังจากวันที่ เดือน พ.ศ.		<input type="checkbox"/> ผู้ขอรับสิทธิบัตร/อนุสิทธิบัตรขอให้ใช้รูปเปลี่ยนหมายเลข ในการประกาศโฆษณา		
13. คำขอรับสิทธิบัตร/อนุสิทธิบัตรนี้ประกอบด้วย ก. แบบพิมพ์คำขอ 2 หน้า ข. รายละเอียดการประดิษฐ์ 11 หน้า หรือคำบรรยายแบบพลิตภัณฑ์ หน้า ค. ข้อถือสิทธิ 2 หน้า ง. รูปเปลี่ยน 4 รูป 4 หน้า จ. ภาพแสดงแบบพลิตภัณฑ์ <input type="checkbox"/> รูปเปลี่ยน รูป หน้า <input type="checkbox"/> ภาพถ่าย รูป หน้า ฉ. บทสรุปการประดิษฐ์ 1 หน้า		14. เอกสารประกอบคำขอ <input checked="" type="checkbox"/> เอกสารแสดงสิทธิในการขอรับสิทธิบัตร/อนุสิทธิบัตร <input type="checkbox"/> หนังสือรับรองการแสดงการประดิษฐ์/การออกแบบพลิตภัณฑ์ <input checked="" type="checkbox"/> หนังสือมอบอำนาจ <input type="checkbox"/> เอกสารรายละเอียดเกี่ยวกับจุลชีพ <input type="checkbox"/> เอกสารการขอันบันยันคำขอในต่างประเทศเป็นวันยื่นคำขอในประเทศไทย <input type="checkbox"/> เอกสารขอเปลี่ยนแปลงประเภทของสิทธิ <input type="checkbox"/> เอกสารอื่น ๆ		
15. ข้อเข้าขอรับรองว่า <input checked="" type="checkbox"/> การประดิษฐ์นี้ไม่เคยยื่นขอรับสิทธิบัตร/อนุสิทธิบัตรมาก่อน <input type="checkbox"/> การประดิษฐ์นี้ได้พัฒนาปรับปรุงมาจาก				
16. ลายมือชื่อ (<input type="checkbox"/> ผู้ขอรับสิทธิบัตร/อนุสิทธิบัตร; <input checked="" type="checkbox"/> ตัวแทน)				

(นายรัชพงษ์ ทองตีแท้)

หมายเหตุ บุคคลใดยื่นขอรับสิทธิบัตรการประดิษฐ์หรือการออกแบบพลิตภัณฑ์ หรืออนุสิทธิบัตร โดยการแสดงข้อความอันเป็นเท็จแก่พนักงานเจ้าหน้าที่เพื่อให้ได้ไปรับสิทธิบัตรหรืออนุสิทธิบัตร ต้องระวังโทษจำคุกไม่เกินหกเดือน หรือปรับไม่เกินห้าพันบาท หรือทั้งจำทั้งปรับ

กรมทรัพย์สินทางปัญญา

กระทรวงพาณิชย์
ถนนนนทบุรี 1 จังหวัดนนทบุรี 11000

เลขที่คำขอ 1403001502



ปีงบประมาณ 2558

案號 25512 เลขที่ 019

ใบเสร็จรับเงิน

วันที่ 17 พฤษภาคม 2557

ได้รับเงินจาก รศ.ดร. ศิริพงษ์ เพ็ชรัตน์

ค่าธรรมเนียม อนุสิทธิบัตร

รายการ	จำนวนเงิน
ค่าขอจดทะเบียนใหม่ อนุสิทธิบัตร	250.00
	250.00

สองร้อยห้าสิบบาทถ้วน

ตัวอักษร () ไว้เป็นการถูกต้องแล้ว
เลขที่อ้างอิงการชำระเงิน 201411170030000219

เลขที่คำร้อง 2014111700134

ลงชื่อ _____ ผู้รับเงิน
นางสาวอ่าพร แสงศรีรัตน์

(นักวิชาการเงินและบัญชี)

ตำแหน่ง _____

(โปรดเก็บใบเสร็จรับเงินไว้เป็นหลักฐานแสดงต่อเจ้าหน้าที่เมื่อมาติดต่อ)